



2019.
GODINA
LXII

GRAĐEVINSKI MATERIJALI I KONSTRUKCIJE

4

BUILDING MATERIALS AND STRUCTURES

ČASOPIS ZA ISTRAŽIVANJA U OBLASTI MATERIJALA I KONSTRUKCIJA
JOURNAL FOR RESEARCH OF MATERIALS AND STRUCTURES



(a)



(b)



(c)



САВЕЗ ИНЖЕЊЕРА И ТЕХНИЧАРА СРБИЈЕ

ПОВЕЉА

Часопис

"Грађевински материјали
и конструкције"

издавач Друштво за грађевинске материјале
и конструкције Србије

за најбољу  ПУБЛИКАЦИЈУ
СРБИЈЕ

БЕОГРАД,

02. фебруар 2018.



ПРЕДСЕДНИК

Igor Maric
др Игор Марић

GRAĐEVINSKI MATERIJALI I KONSTRUKCIJE

BUILDING MATERIALS AND STRUCTURES

ČASOPIS ZA ISTRAŽIVANJA U OBLASTI MATERIJALA I KONSTRUKCIJA
JOURNAL FOR RESEARCH IN THE FIELD OF MATERIALS AND STRUCTURES

INTERNATIONAL EDITORIAL BOARD

Professor **Radomir Folić**, Editor in-Chief
Faculty of Technical Sciences, University of Novi Sad, Serbia
Fakultet tehničkih nauka, Univerzitet u Novom Sadu, Srbija
e-mail: folic@uns.ac.rs

Professor **Mirjana Malešev**, Deputy editor
Faculty of Technical Sciences, University of Novi Sad,
Serbia - Fakultet tehničkih nauka, Univerzitet u Novom
Sadu, Srbija, e-mail: miram@uns.ac.rs

Dr **Ksenija Janković**
Institute for Testing Materials, Belgrade, Serbia
Institut za ispitivanje materijala, Beograd, Srbija

Dr **Jose Adam, ICITECH**
Department of Construction Engineering, Valencia, Spain.

Professor **Radu Banchila**
Dep. of Civil Eng. „Politehnica“ University of Timisoara,
Romania

Professor **Dubravka Bjegović**
University of Zagreb, Faculty of Civil Engineering,
Department of Materials, Zagreb, Croatia

Professor **Meri Cvetkovska**
Faculty of Civil Eng. University "St Kiril and Metodij",
Skopje, Macedonia

Professor **Michael Forde**
University of Edinburgh, Dep. of Environmental Eng. UK

Dr **Vladimir Gocevski**
Hydro-Quebec, Montreal, Canada

Sekretar redakcije: **Slavica Živković**, mast.ekon.

Lektori za srpski jezik: Dr **Miloš Zubac**, profesor
Aleksandra Borojev, profesor

Proofreader: Prof. **Jelisaveta Šafranj**, Ph D

Technical editor: Stoja Todorovic, e-mail: saska@imk.grf.bg.ac.rs

Acad. Professor **Yachko Ivanov**
Bulgarian Academy of Sciences, Sofia, Bulgaria

Dr. Habil. **Miklos M. Ivanyi**
UVATERV, Budapest, Hungary

Professor **Asterios Liolios**
Democritus University of Thrace, Faculty of Civil Eng.,
Greece

Professor **Doncho Partov**
University of Construction and Architecture - VSU
"LJ.Karavelov" Sofia, Bulgaria

Predrag Popović
Wiss, Janney, Elstner Associates, Northbrook, Illinois,
USA.

Professor **Rüdiger Höffer**
Ruhr University of Bochum, Bochum, Germany

Professor **Valeriu Stoin**
Dep. of Civil Eng. „Poloitehnica“ University of
Timisoara, Romania

Acad. Professor **Miha Tomažević**, SNB and CEI,
Slovenian Academy of Sciences and Arts,

Professor **Mihailo Trifunac**, Civil Eng.
Department University of Southern California, Los
Angeles, USA

PUBLISHER

Society for Materials and Structures Testing of Serbia, 11000 Belgrade, Kneza Milosa 9
Telephone: 381 11/3242-589; e-mail: dimk@ptt.rs, veb sajt: www.dimk.rs

REVIEWERS: All papers were reviewed

KORICE: Most tokom građenja a) i b) i tokom eksploatacije c)

COVER: The bridge in construction period (a, b) and in service period (c)

Štampa/Print: Razvojno istraživački centar grafičkog inženjerstva, Beograd

Publikacija: tromesečno

Edition: quarterly

Financial supports: Ministry of Scientific and Technological Development of the Republic of Serbia

GRAĐEVINSKI MATERIJALI I KONSTRUKCIJE

BUILDING MATERIALS AND STRUCTURES

ČASOPIS ZA ISTRAŽIVANJA U OBLASTI MATERIJALA I KONSTRUKCIJA
JOURNAL FOR RESEARCH IN THE FIELD OF MATERIALS AND STRUCTURES

SADRŽAJ

Alexander ILIEV Dimitar DIMITROV Dimitar STEFANOV NLINEARNA ANALIZA OKVIRNOG AB MOSTA FUNDIRANOG NA PLITKIM TEMELJIMA I NA ŠIPOVIMA Originalni naučni rad	3
Konstantin KAZAKOV Lena MIHOVA Doncho PARTOV KOMPARATIVNA ANALIZA MODELA INTERAKCIJE TLA I LUČNOG MOSTA SA ZEMLJANOM ISPUNOM ZASNOVANIH NA MKE Originalni naučni rad	15
Aizada KALMAGAMBETOVA Tatyana BOGOYAVLENSKAYA JEDINJENJA ZA SPREČAVANJE KOROZIJE I ZA POVEĆANJE TRAJNOSTI PRETHODNO IZOLOVANIH CEVI Originalni naučni rad	29
Vladimir ŽIVALJEVIĆ Vlastimir RADONJANIN Ivan LUKIĆ Dušan KOVAČEVIĆ NUMERIČKA SIMULACIJA PONAŠANJA UZORAKA OD LAKOAGREGATNOG BETONA U SLUČAJEVIMA LABORATORIJSKOG ISPITIVANJA Originalni naučni rad	37
Uputstvo autorima	53

CONTENTS

Alexander ILIEV Dimitar DIMITROV Dimitar STEFANOV NON-LINEAR ANALYSIS OF FRAME REINFORCED CONCRETE BRIDGE- SHALLOW VS. PILE FOUNDATION Original scientific paper	3
Konstantin KAZAKOV Lena MIHOVA Doncho PARTOV COMPARATIVE ANALYSIS OF DIFFERENT FINITE ELEMENT MODELS OF THE SOIL-BURIED ARCH BRIDGE INTERACTION Original scientific paper	15
Aizada KALMAGAMBETOVA Tatyana BOGOYAVLENSKAYA CORROSION-PREVENTIVE COMPOUNDS FOR INCREASING THE DURABILITY OF PREINSULATED PIPES Original scientific paper	29
Vladimir ZIVALJEVIC Vlastimir RADONJANIN Ivan LUKIC Dusan KOVACEVIC NUMERICAL SIMULATION OF THE BEHAVIOUR OF THE LIGHTWEIGHT CONCRETE SPECIMEN IN THE LABORATORY TESTING Original scientific paper	37
Guidelines for authors	53

CIP - Каталогизacija u publikaciji
Narodna biblioteka Srbije, Beograd

620.1

GRAĐEVINSKI materijali i konstrukcije : časopis za
istraživanja u oblasti materijala i konstrukcija = Building materials and
structures : journal for research of materials and structures / editor-in-chief
Radomir Folić. - God. 54, br. 3 (2011)- . - Begrade : Društvo za
ispitivanje i istraživanje materijala i konstrukcija Srbije = Society for
Materials and Structures Testing of Serbia, 2011- (Beograd : Razvojno
istraživački centar grafičkog inženjerstva). - 30 cm

Dostupno i na:

http://www.dimk.rs/stg/website/filemanager/files/Casopis_1_2011.pdf -

Tromesečno. - Tekst na srp. i engl. jeziku. -

Je nastavak: Materijali i konstrukcije = ISSN 0543-0798. -

Drugo izdanje na drugom medijumu: Građevinski materijali i konstrukcije
(Online) = ISSN 2335-0229

ISSN 2217-8139 = Građevinski materijali i konstrukcije

COBISS.SR-ID 188695820



NON-LINEAR ANALYSIS OF FRAME REINFORCED CONCRETE BRIDGE- SHALLOW VS. PILE FOUNDATION

NELINEARNA ANALIZA OKVIRNOG AB MOSTA FUNDIRANOG NA PLITKIM TEMELJIMA I NA ŠIPOVIMA

Alexander ILIEV
Dimitar DIMITROV
Dimitar STEFANOV

ORIGINALNI NAUČNI RAD
ORIGINAL SCIENTIFIC PAPER
UDK:624.21.012.45
doi:10.5937/GRMK1904003I

1 INTRODUCTION

The bridge design includes the choice of the bridge structural system, materials, section dimensions, aesthetics and economic considerations. In EN 1998-2 [1] the main principle is that bridges behave in case of seismic action in a ductile or limited ductile/essentially elastic manner. In regions of moderate to high seismicity is preferable to design a bridge for ductile behaviour. The bridge deck shall remain within elastic range. The formation of the plastic hinges is allowed in the piers which are the energy dissipating bridge components.

The theoretical investigations and the experience from the past earthquakes show that the continuous bridge structures behave better than bridges with many expansion joints and bearings.

The frame bridges have advantageous "ductile behaviour of the structure" during the seismic event. In this case the seismic action is considerably reduced in comparison with the other bridges, for instance bridges with elastomeric bearings. According to EN 1998-2 [1], the structural behaviour of the last ones is ductile limited. This leads to significant difficulties in the satisfaction of the bearing checks, increased dimensions of the sub-structure elements and the reinforcement. Anchorage of the bearings is a common design solution for the bridges

in high risk seismic areas. The author's opinion is that the frame bridges application will be extended due to these reasons. Of course, the detailing rules for the ductile behaviour should be strictly followed.

The design of flexible piers reduces the seismic action but the displacements are increased. The second order effects might be significant.

According to EN 1998-2 [1] the maximum allowable seismic action reduction coefficients (behaviour factors q) are:

- $q \leq 3.5$ for vertical piers with ductile behaviour;
- $q \leq 2.1$ for inclined ones.

The coefficients q depend on the ratio $\alpha_s = L/h$, where L is the distance between the plastic hinge and the section with zero bending moment and h is the cross section dimension in the direction of the bending.

The influence of the normal force at the section with plastic hinge should be taken into account. The normalized force is $\eta_k = N_{Ed}/(A_c f_{cd})$. Piers with $L/h < 1$ and/or $\eta_k > 0.60$ should be avoided. In these cases the ductile behaviour is not ensured. The vertical seismic action increases the normal force N_{Ed} at the plastic hinge section, i.e. the q -coefficient is reduced. This influence is analyzed in the paper.

These values are used only for "linear analysis" and only in horizontal direction. It is allowed, based on the designer's and/or client's evaluation, to apply smaller q -values.

The best way for the determination of the ductility is the static non-linear (push-over) analysis. According to EN 1998-2 [1] this analysis could be applied for the whole bridge structure or for a single pier. At the paper a model of the whole structure is done and the ductility is determined from the results for a single pier. Using this

Alexander Iliev, National Institute of Geophysics, Geodesy and Geography- Bulgarian Academy of Sciences. Sofia, Bulgaria

Dimitar Dimitrov, National Institute of Geophysics, Geodesy and Geography- Bulgarian Academy of Sciences. Sofia, Bulgaria

Dimitar Stefanov, National Institute of Geophysics, Geodesy and Geography- Bulgarian Academy of Sciences. Sofia, Bulgaria

approach, a comparison between the design ductility and the nominal ductility based on [1] could be done.

The vertical seismic action application is different for the buildings [2] and for the bridges [1]. If a push-over analysis is performed for a building, then the vertical seismic component could be neglected. This component should be applied for bridges with pre-stressed reinforced concrete superstructure. The recommended basic period T_1 of the bridge structure is between 1 and 2 sec for balance between the internal forces and the displacements. The calculated periods in the analysis are within these limits – see below.

The aims of the presented analysis in the paper are:

- Determination of the “real” ductility in the case of seismic action separately in longitudinal and transversal bridge direction using non-linear analysis;
- Comparison between the structural ductility between a bridge with flat footing and one with piles;
- Comparison between the “real” ductility and the “nominal” one based on EN 1998-2 [1];
- Evaluation of the influence of the vertical seismic action component to the bridge structural ductility.

2 BRIDGE STRUCTURE MODEL

The static non-linear analysis is reliable and applicable for bridge structures, which behaviour is similar to ones that could be approximated with a “single degree of freedom” model. Such bridges are approximately straight bridges and ones with negligible pier height change. The selected case study bridge meets these requirements.

The bridge is a three span frame one and it is situated on a motorway. The spans are 33+41+33m and the total bridge length is 107m. The length is less than L_{lim} according to [1] and the spatial variability of the seismic action shall not be considered.

The superstructure is a cast-in-place pre-stressed post-tensioned reinforced concrete one. The cross section is a hollow one with three cells – see Fig.1. The constant height of the section is 2 m. The concrete class is C45/55.

The piers are reinforced concrete solid “wall” type ones with 14 m height. At the top of the pier the solid cross section is separated into 2 parts for better connection with the superstructure – see Fig.2. The pier concrete class is C35/45. The reinforcement class is B500C ($f_{yk}=500$ MPa).

The bearings at the abutments are movable in both directions.

Two options for the foundations are selected:

- flat single footing
- drilled shaft piles with pile cap – 2 piles with 1.8 m diameter and 20 m length.

The longitudinal bars are 36 Φ 25 mm+ 10 Φ 22 mm. The stirrups are with 14mm diameter.

The bridge is situated at a site with reference maximum soil acceleration $a_{gR}=0.32g=3.14$ m/sec². The importance coefficient is $\gamma_I=1.4$. Then the design soil acceleration is $a_g=1.4*0.32g=0.448g=4.40$ m/sec².

According to [2] the push-over analysis is carried out:

- applying constant vertical actions. The traffic action is a load model LM1. According to the Bulgarian NA (National Annex) for road bridges with reinforced concrete superstructure quasi-permanent value of the action is assumed, i.e. $\psi_2=0.20$ for bridges on the highway;
- applying permanently increasing horizontal seismic actions.

The bridge model consists of 52446 finite elements: 21292 solid elements (8 nodes) for the concrete structure, 30978 shell elements for the reinforcement (smeared approach) and 176 truss elements representing the pre-stressing system (Fig.3). Average size of the solid element of the bridge structure is around 0,5 m. The connection between the columns and the top structure is considered rigid (united nodes). The soil-structure interaction is represented with two concrete piles for each column with elastic springs in both horizontal directions. The two ends of the bridge are also supported with vertical elastic springs representing the polymer joint connecting the top-structure to the columns (pinned connection). The full model of the bridge is presented in Fig.2.

For the numerical analyses standard implicit Hilber-Hughes method was used. Nonlinear behaviour of concrete is modelled with Ottosen constitutive model [3][7]. Crack formation and propagation is based on the smeared crack approach. The iteration method is BFGS combined with energy convergence criteria [6]. Two nonlinear static (pushover) analyses are performed for the bridge, one in each horizontal direction. The analyses use monotonic mass proportional load vector in both directions.

The stiffness of the elements is updated with every step of the calculation based on the accumulated deformations and the work diagram (stress-deformations) of concrete constitutive material model. Fig.4 shows the working diagram of concrete for one dimensional stress state.

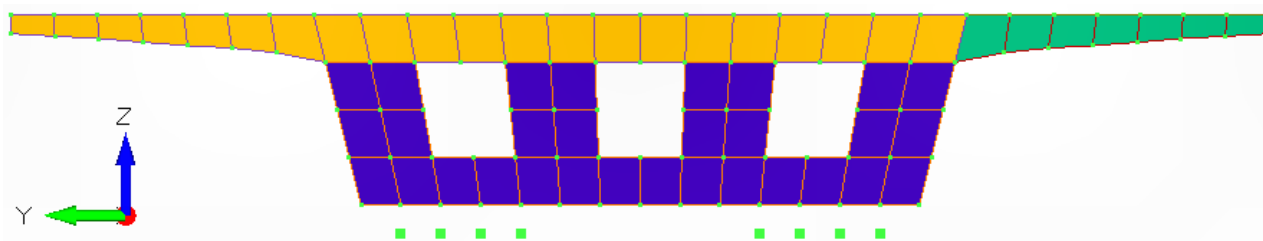


Fig. 1. Section cut of the top system

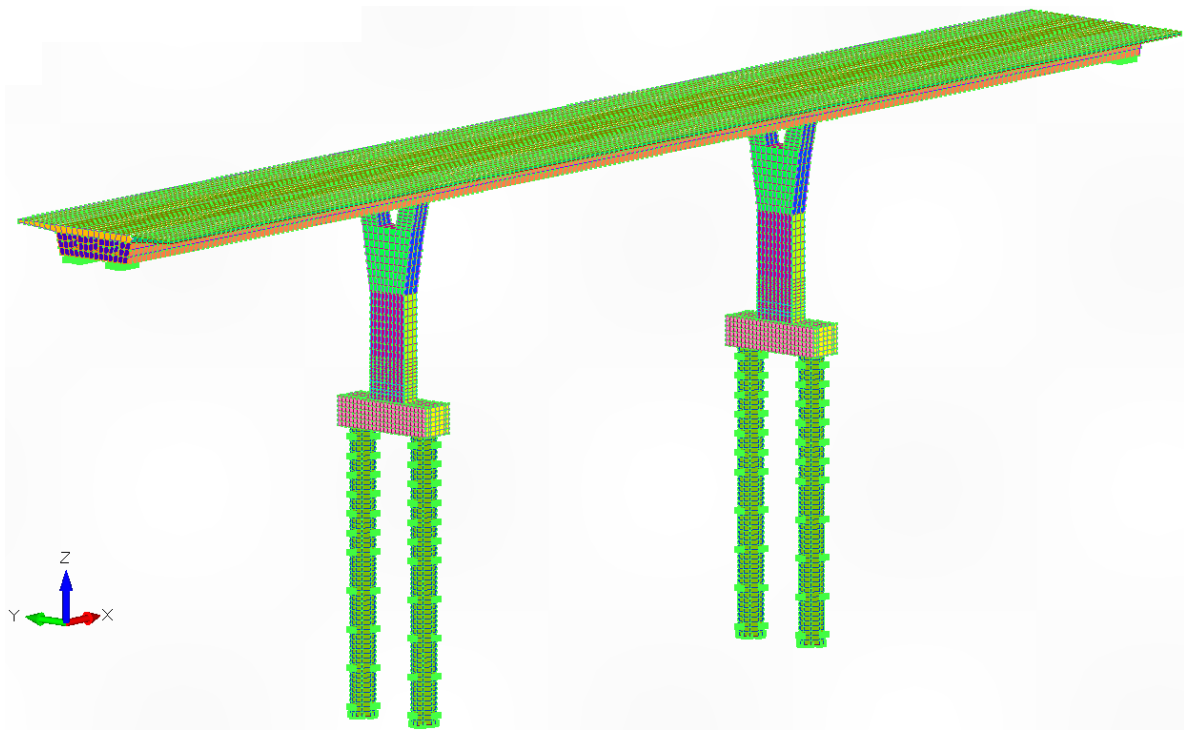


Fig. 2. Tree-dimensional view of the finite element model. Pile foundation case study

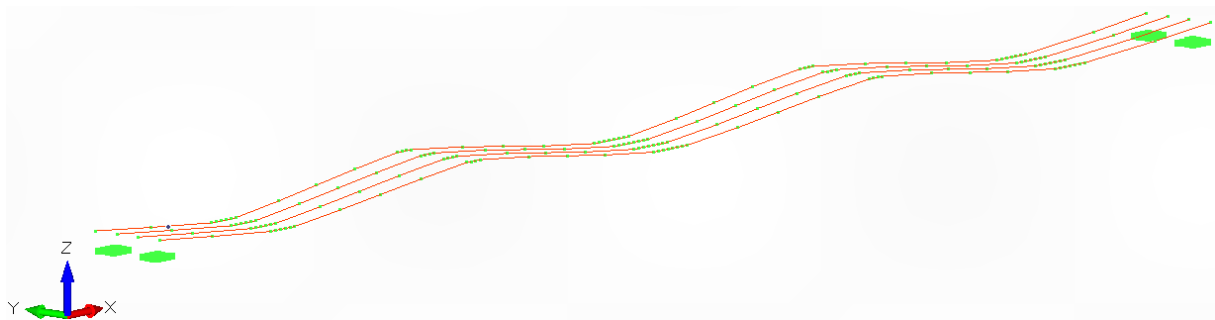


Fig. 3. Spatial geometry of the pre-stressing system

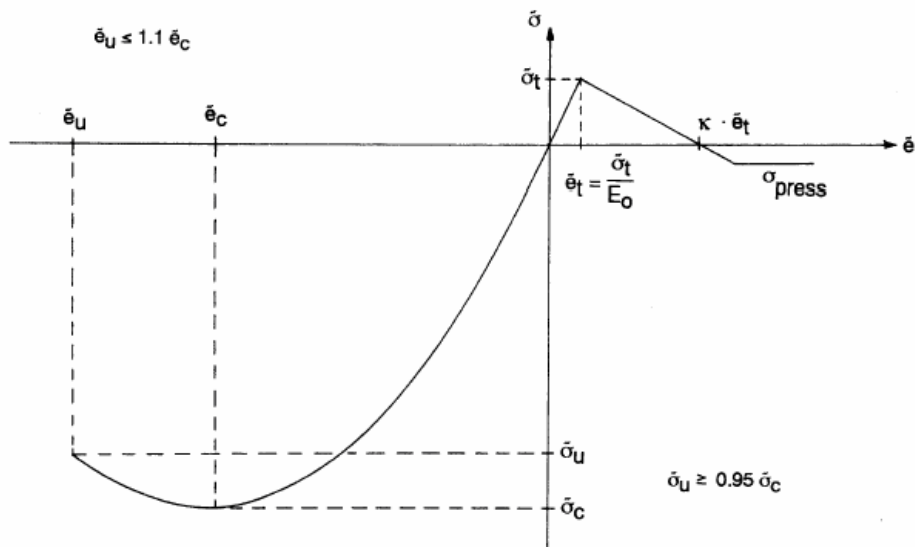


Fig. 4. One dimensional stress state of concrete material model

The type of the stress condition of the element influences significantly to the strength-deformation concrete characteristics. The damage criterions are based on comparison between the current stress condition and the limit (allowable) concrete stresses – see the envelope curve at Fig.5.

3 RESULTS

Behaviour coefficients according to EN 1998-2 [1]

The preliminary determination of the behaviour coefficients is based on the following assumptions:

- in longitudinal direction the length L is a half pier clear length;
- in transversal direction the length L is a full pier clear length plus the distance to the centre of the gravity of the superstructure, i.e. the plastic hinge is at the bottom of the pier and the behaviour is similar to cantilever.

The results are presented in the Table 1.

The distance from the top pier section to the centre of the gravity of the superstructure is $z_c=1130\text{ mm}$. Then in the transversal direction $L=14+1.13=15.13\text{ m}$.

Plastic hinge length

The plastic hinge length is according to Annex E from [1] using the formula (1).

$$L_p=0.10L+0.015f_{yk}d_{bl} \quad (1)$$

where:

$d_{bl}=25\text{ mm}$ is the maximum diameter of the pier longitudinal reinforcement

$$L_p=0.10L+0.015*500*25=0.10L+188$$

The relevant lengths are:

- in longitudinal direction the length $L_p=0.10*7000+188=888\text{ mm}$;
- in transversal direction the length $L_p=0.1*15\ 130+188=1701\text{ mm}$.

Procedure for the determination of the member displacement ductility factor μ_Δ and curvature ductility factor μ_ϕ

The displacement ductility factor μ_Δ could be determined using two possibilities:

A. Determination from the model and the push-over analysis of the displacement at yielding Δ_y and ultimate displacement Δ_u – see Fig.6. The displacement Δ_u is obtained when the strain at the concrete and/or steel reaches the maximum values – see below.

$$\mu_\Delta = \Delta_u / \Delta_y \quad (2)$$

B. Analytical calculation according to Annex B from EN 1998-2 [1]:

$$\mu_\phi = 1 + [\mu_d - 1] / [3\lambda(1 - 0.5\lambda)] \quad (3)$$

$$\mu_d = 1 + (\mu_\phi - 1)3\lambda(1 - 0.5\lambda) \quad (4)$$

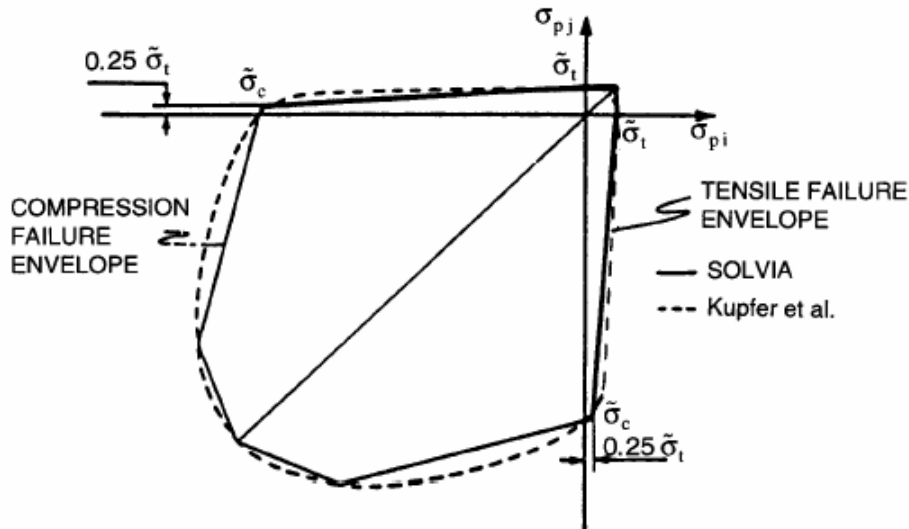


Fig. 5. Capacity (limit) envelope of concrete. Plane model

Table 1.

Direction	$L[m]$	$h[m]$	$\alpha_s=L/h$	$\lambda_s=(\alpha_s/3)^{1/2}$ or 1 if $\lambda_s>3$	$q=3.5\lambda_s$
Longitudinal - x	14/2=7	1.35	5.18	1	3.5
Transversal - y	15.13	3	5.04	1	3.5

where: $\lambda=L_p/L$

This formula is used for elements which behaviour is similar to the cantilever, i.e. for the piers in the transversal direction.

$$\mu\phi = \Phi_u / \Phi_y \quad (5)$$

The ultimate curvature Φ_u is determined according to Annex E from [1]:

$$\Phi_u = (\varepsilon_s - \varepsilon_c) / d \quad (6)$$

where:

- d is the effective depth;
- ε_s and ε_c are the steel and concrete strains respectively (concrete strain with sign "-").

They separately or both reach the following maximum strains:

a. maximum strain of the unconfined concrete ε_{cu1} according to EN 1992-1-1 [2]. For concrete class C35/45 $\varepsilon_{cu1}=3.5\%$

b. maximum strain of the confined concrete $\varepsilon_{cu,c}$ according to Annex E from [1] – see below.

c. maximum steel strain ε_{su} at maximum force. For steel B500C (ductility class C is required for structures at high seismic areas) $\varepsilon_{su}=75\%$.

In the paper the following maximum strains are assumed:

- for the confined concrete $\varepsilon_{cu,c}=14.36\%$ - see below
- for the steel $\varepsilon_{su}=75\%$

The calculation of the maximum strain of the confined concrete $\varepsilon_{cu,c}$ is according to:

- the transversal reinforcement ratio ρ_w in the two transverse directions 2 and 3 (direction 1 is along the pier axis)

- the coefficient of the effectiveness of the confinement $\alpha=\alpha_n\alpha_s$

- for the piers with minimum cross section dimension $b=1m$ could be assumed $\alpha=1$. In the presented paper $b>1m$ and then $\alpha<1$ – see below

- the effective confined stress σ_e at the concrete
- the ultimate strength of the confined concrete $f_{cm,c}$

The average concrete strength of the unconfined concrete f_{cm} according to [2] is:

$$f_{cm}=f_{ck}+8=35+8=43 \text{ MPa.}$$

The calculation for the effective confined stress σ_e is presented in the following Table 2.

Table 2.

ρ_{w2}	ρ_{w3}	α_n	α_s	$\alpha=\alpha_n\alpha_s$	$\sigma_{e2} \text{ [MPa]}$	$\sigma_{e3} \text{ [MPa]}$	$\sigma_e=(\sigma_{e2}\sigma_{e3})^{1/2}$
0.00567	0.00582	0.9327	0.9317	0.869	2.46	2.53	2.49

$$f_{cm,c}=f_{cm}*\lambda_c$$

$$\sigma_e/f_{cm}=2.49/43=0.0579$$

$$\begin{aligned} \lambda_c &= 2.254*(1+7.94*\sigma_e/f_{cm})^{1/2}-2*\sigma_e/f_{cm}-1.254= \\ &= 2.254*(1+7.94*0.0579)^{1/2}-2*0.0579- \\ &- 1.254=1.3535 \end{aligned}$$

$$f_{cm,c}=43*1.3535=58.2 \text{ MPa}$$

The confined concrete strain $\varepsilon_{c1,c}$ at $\sigma_c=f_{cm,c}$ is:

$$\varepsilon_{c1,c}=0.002[1+5(\lambda_c-1)]$$

$$\varepsilon_{c1,c}=0.002[1+5(1.3535-1)]=0.005535 \text{ (5.53\%)}$$

The maximum strain of the confined concrete $\varepsilon_{cu,c}$ is:

$$\varepsilon_{cu1,c}=0.004+(1.4*\rho_s*f_{ym}*\varepsilon_{su})/f_{cm,c}, \text{ where:}$$

$$\rho_s=2\rho_w \text{ in case of rectangular stirrups.}$$

It is ambiguously defined in [1] the determination of the ratio ρ_w in the case of different ratios in two directions - $\rho_{w2} \neq \rho_{w3}$. In the paper it is assumed $\rho_w=(\rho_{w2}\rho_{w3})^{1/2}$.

$$\rho_w=(0.00567*0.00582)^{1/2}=0.00574$$

$$\rho_s=2\rho_w=2*0.00574=0.01148$$

$$\begin{aligned} \varepsilon_{cu1,c} &= 0.004+(1.4*0.01148*500*75*10^{-3})/58.2= \\ &= 0.01436 \text{ (14.36\%)} \end{aligned}$$

The calculated values for $f_{cm,c}$, $\varepsilon_{c1,c}$ and $\varepsilon_{cu1,c}$ correspond well with the experimental results [4].

The following requirements according to [1] are checked and controlled:

- The analysis is based on Annex H. The "target displacement" of the "reference point" is controlled. The "reference point" is the centre of masses of the superstructure.

- The rotations $\theta_{p,E}$ at the plastic hinges are checked according to 4.2.4.4 of [1].

$\theta_{p,E} < \theta_{p,d}$, where $\theta_{p,d}$ is the design value of the plastic rotation capacity and it is calculated from the formula

$$\theta_{p,d} = \theta_{p,u} / \gamma_{R,p} \quad (7)$$

where:

- $\theta_{p,u}$ is determined according to Annex E from [1] – see formula (8)

- $\gamma_{R,p}=1.40$ in the case of missing data from experiments.

$$\theta_{p,u} = (\Phi_u - \Phi_y)L_p(1-L_p/2L) \quad (8)$$

Determination of the member displacement ductility factor μ_Δ and curvature ductility factor μ_ϕ at longitudinal direction and in the case of flat foundation

The distribution of deformations is presented at Fig.6. The compressive failure of concrete is labelled as "CRUSHED" and coloured in red. The tensile failure is coloured in different parts of green depending on the number of cracks in the cross section. The following results can be observed:

- maximum displacement of the reference point Δ_u =59.5 cm – see Fig.7;

- displacement of the reference point at yielding Δ_y =6.5 cm – see Fig.7;

- maximum strain at the tensile reinforcement $\varepsilon_{su}=75\%$ - see Fig.8;

- maximum stress at the tensile reinforcement – $\sigma_s=675 \text{ MPa}$ – see Fig.9;

- maximum strain at the concrete – $\epsilon_c = -9.3\%$. The strain is less than $\epsilon_{cu1,c} = 14.36\%$;
 - the fundamental response period – $1 \text{ sec} < T_1 = 1.21 \text{ sec} < 2 \text{ sec}$.
- The recommended value [5] for Δ_y is $\Delta_y = 0.005H$, where $H = 15.13 \text{ m}$ is the distance between the centre of gravity of the superstructure and the base of the pier.
- $\Delta_y = 0.005H = 0.005 * 15.13 = 0.076 \text{ m}$

The effective depth of the cross section is $d = 1273 = 1.273 \text{ m}$.

The displacement ductility factor is:
 $\mu_d = \Delta_u / \Delta_y = 59.5 / 6.5 = 9.15$

The ultimate curvature is:
 $\Phi_u = (\epsilon_s - \epsilon_c) / d = [75 - (-9.36) * 10^{-3}] / 1.273 = 0.0663 [1/m]$

The curvature at yielding is $\Phi_y = 0.0045 [1/m]$ - see Fig.10.



Fig. 6. Damage distribution in the bridge in longitudinal direction. Flat foundation case study.

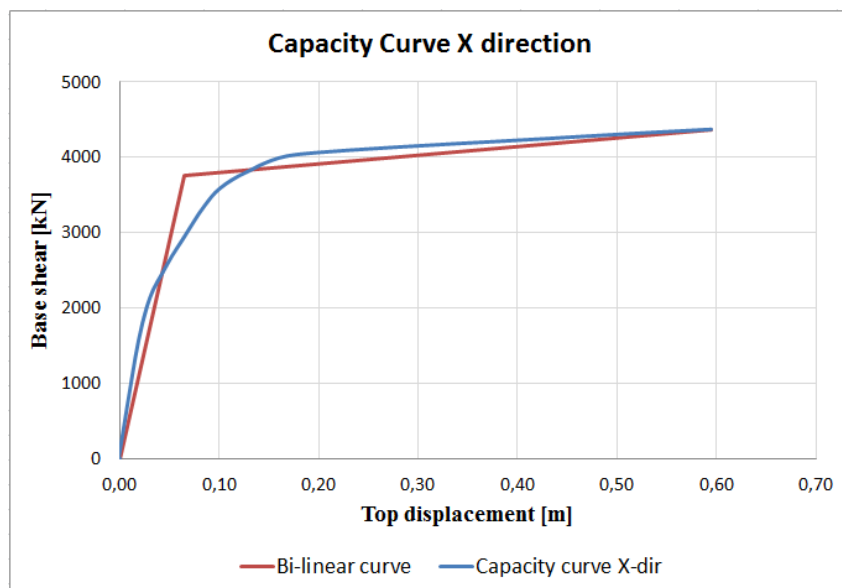


Fig. 7. Push-over (capacity) curve for the flat foundation case study

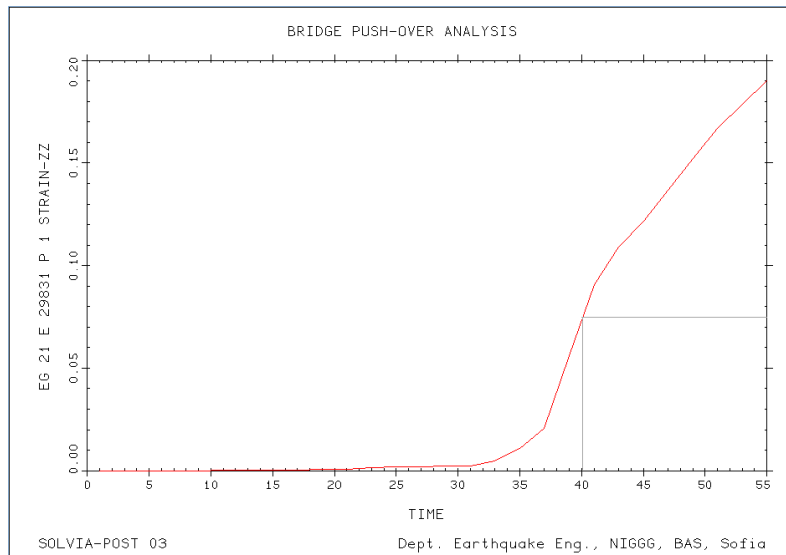


Fig. 8. Strain distribution in the tensile reinforcement at the base of the pier. Flat foundation.

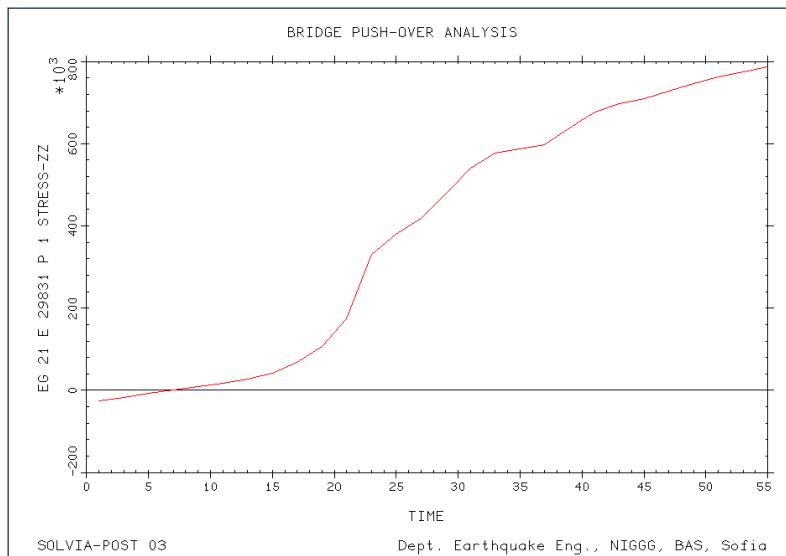


Fig. 9. Stress distribution in the tensile reinforcement at the base of the pier. Flat foundation,

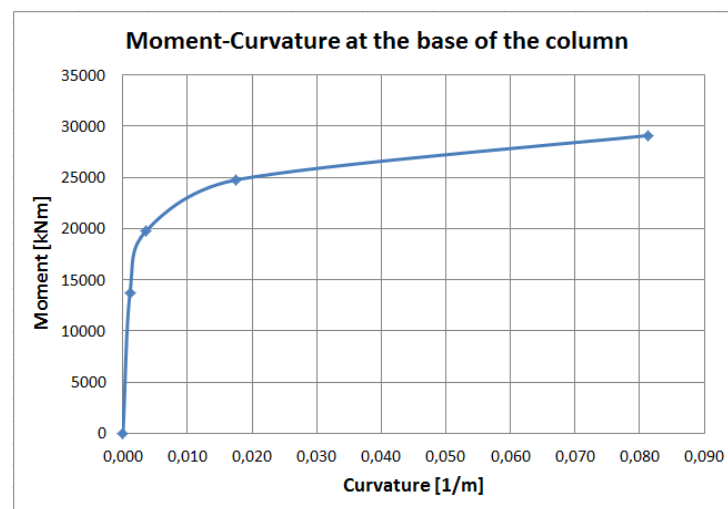


Fig. 10. Moment-curvature relationship at the base of the pier. Case study- flat foundation.

The curvature ductility factor μ_ϕ is:

$$\mu_\phi = \Phi_u / \Phi_y = 0.0663 / 0.0045 = 14.73$$

The length of the plastic hinge is $L_p = 0.888$ m and the distance to the zero moment is $L = 7$ m.

The plastic rotation capacity is:

$$\theta_{p,d} = \theta_{p,u} / \gamma_{R,p}$$

$$\begin{aligned} \theta_{p,u} &= (\Phi_u - \Phi_y) L_p (1 - L_p / 2L) = \\ &= (0.0663 - 0.0045) * 0.888 * (1 - 0.888 / 2 * 7) = \\ &= 0.0514 \text{ [rad]} \end{aligned}$$

$$\theta_{p,d} = \theta_{p,u} / \gamma_{R,p} = 0.0514 / 1.4 = 0.0367 \text{ [rad]}$$

The rotations $\theta_{p,E}$ at the plastic hinge is:

$$\begin{aligned} \theta_{p,E} &= \Delta p / (H - L_p) = (0.595 - 0.065) / (15.13 - 0.888) = \\ &= 0.0372 \text{ [rad]} \end{aligned}$$

Determination of the member displacement ductility factor μ_Δ and curvature ductility factor μ_ϕ in TRANSVERSAL direction and in the case of flat foundation

The presented approach is applied in the transversal bridge direction. Due to the higher stiffness the ultimate curvature is at maximum concrete strain $\epsilon_{cu1} = 3.5\text{‰}$. The steel strain $\epsilon_{su} = 46\text{‰} < 75\text{‰}$. The results are presented in the Table 3.

The length of the plastic hinge is $L_p = 1.701$ m and the distance to the zero moment is $L = 15.13$ m.

$$\lambda = L_p / L = 1.701 / 15.13 = 0.1124$$

The displacement ductility could be calculated using formula (4), because in the transversal direction the behaviour is similar as a cantilever – Fig.11.

$$\begin{aligned} \mu_d &= 1 + (\mu_\phi - 1) 3\lambda (1 - 0.5\lambda) = 1 + (13 - 1) 3 * 0.1124 (1 - 0. * 0.1124) = \\ &= 4.82 \end{aligned}$$

($\mu_d = 4.29$ from the push-over analysis – see Table 3)

The plastic rotation capacity is:

$$\begin{aligned} \theta_{p,u} &= (\Phi_u - \Phi_y) L_p (1 - L_p / 2L) = (0.0169 - 0.0013) * 1.701 * \\ & * (1 - 1.701 / 2 * 15.13) = 0.025 \text{ [rad]} \end{aligned}$$

$$\begin{aligned} \theta_{p,d} &= \theta_{p,u} / \gamma_{R,p} = 0.025 / 1.4 = 0.0179 \text{ [rad]} > \theta_{p,E} = \\ &= (0.193 - 0.045) / (15.13 - 1.701) = 0.011 \text{ [rad]} \end{aligned}$$

The distribution of deformations in transverse direction is presented in Fig.11.

Determination of the member displacement ductility factor μ_Δ and curvature ductility factor μ_ϕ in LONGITUDINAL direction and in the case of PILE foundation.

The results of the case study with pile foundation are as following:

- maximum displacement of the reference point $\Delta_u = 100$ cm – see Fig.13;
- displacement of the reference point at yielding $\Delta_y = 13.5$ cm – see Fig.13;
- maximum strain at the tensile reinforcement $\epsilon_{su} = 75\text{‰}$ - see Fig.14;
- maximum stress at the tensile reinforcement – $\sigma_s = 630$ MPa – see Fig.15

The displacement ductility factor is:

$$\mu_d = \Delta_u / \Delta_y = 100 / 13.5 = 7.41$$

This value is less than the one determined for the case with flat foundation.

Table 3.

Δ_u [cm]	Δ_y [cm]	$\mu_d = \Delta_u / \Delta_y$	$\Phi_u = (\epsilon_s - \epsilon_c) / d$ [1/m]	Φ_y [1/m]	$\mu_\phi = \Phi_u / \Phi_y$	T_1 [sec]
19.3	4.5	4.29	$[46 - (-3.5) * 10^{-3}] / 2.923 = 0.0169$	0.0013	13	$1 < 1.19 < 2$

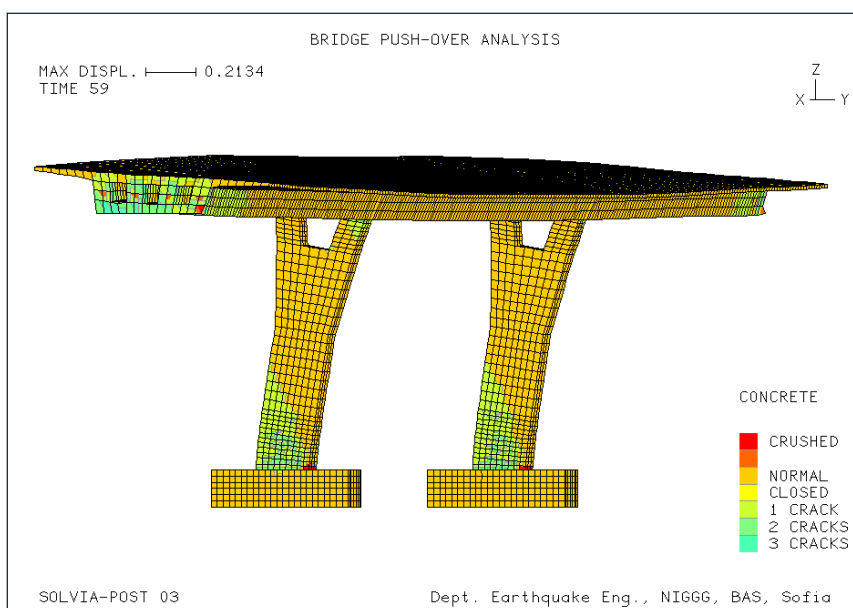


Fig. 11. Damage distribution in the bridge in transverse direction. Flat foundation case study.

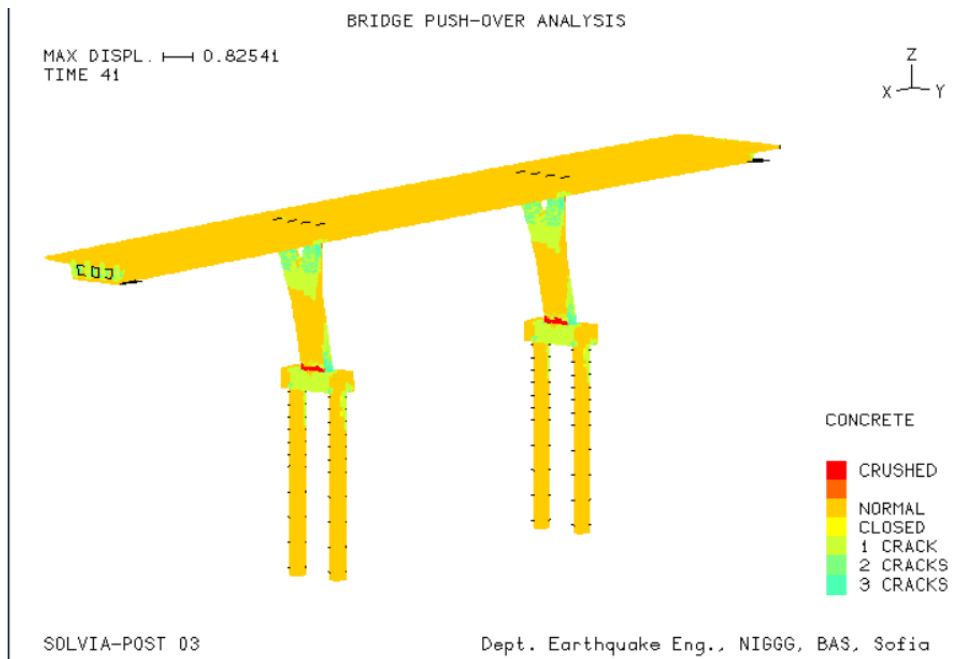


Fig. 12. Damage distribution in the bridge in longitudinal direction. Pile foundation case study.

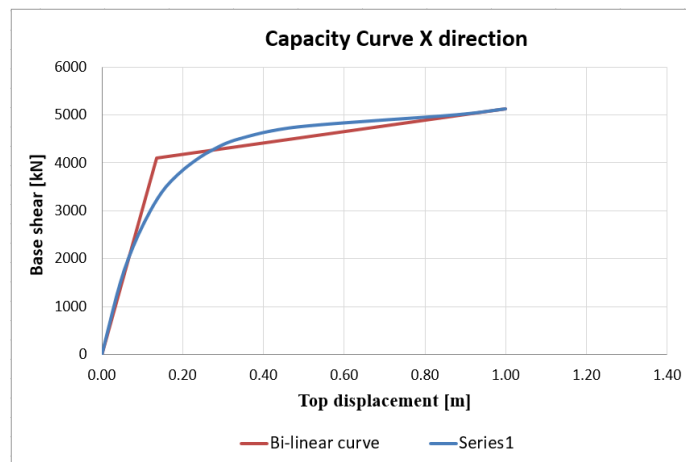


Fig. 13. Push-over (capacity) curve for the pile foundation case study

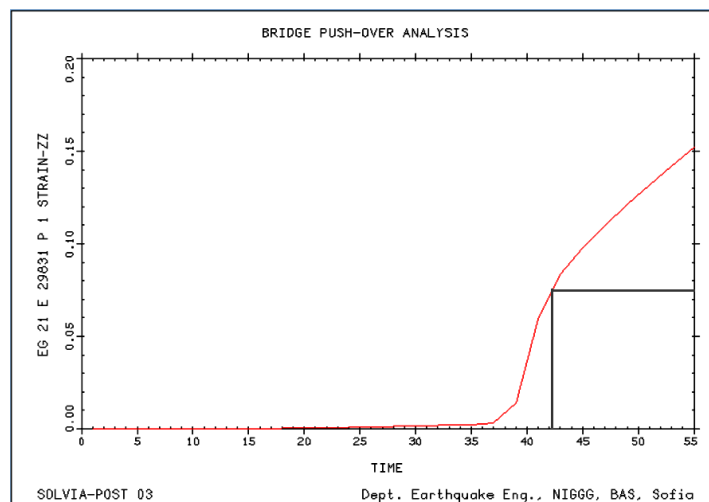


Fig. 14. Strain distribution in the tensile reinforcement at the base of the pier. Pile foundation.

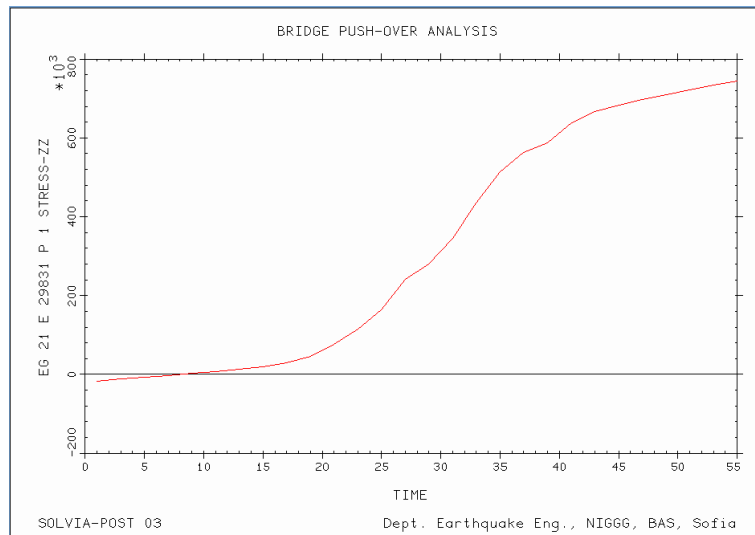


Fig. 15. Stress distribution in the tensile reinforcement at the base of the pier. Pile foundation.

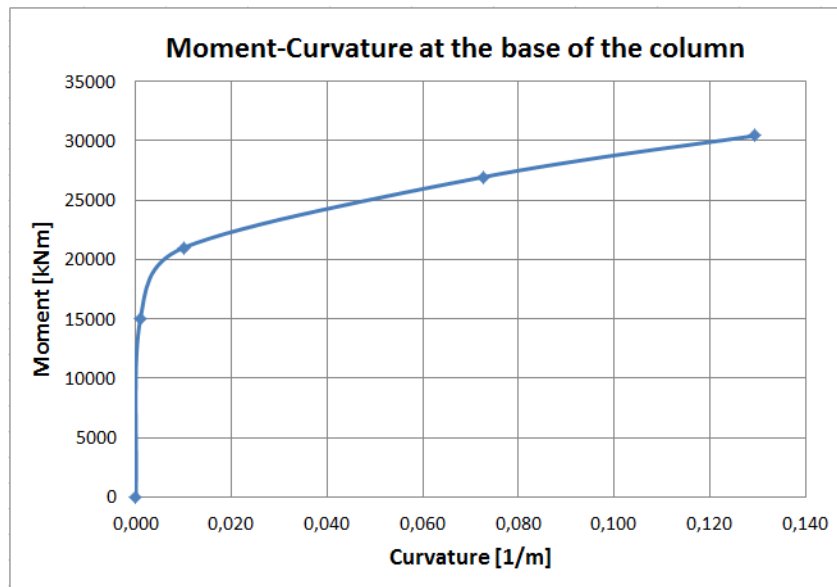


Fig. 16. Moment-curvature relationship at the base of the pier. Case study- pile foundation.

Determination of the curvature ductility factor μ_ϕ in LONGITUDINAL direction in the case of FLAT foundation TAKING THE VERTICAL COMPONENT OF THE SEISMIC ACTION INTO ACCOUNT.

The analysis is performed based on the following assumptions:

- The ratio between the vertical and horizontal acceleration $a_{vg}/a_g=0.90$;
- The analysis is only for the longitudinal direction and only for the option “flat foundation”;
- The design combination according to [2] is “ $E_x+0.30E_z$ ”

The results are presented in Fig.17. The curvature ductility is:

$$\mu_\phi = \Phi_u / \Phi_y = 0.025 / 0.0025 = 10$$

This value is less than the determined without taking the vertical seismic action into account - $\mu_\phi = 14.73$.

This result shows that the vertical seismic action reduces the ductility and should not be neglected.

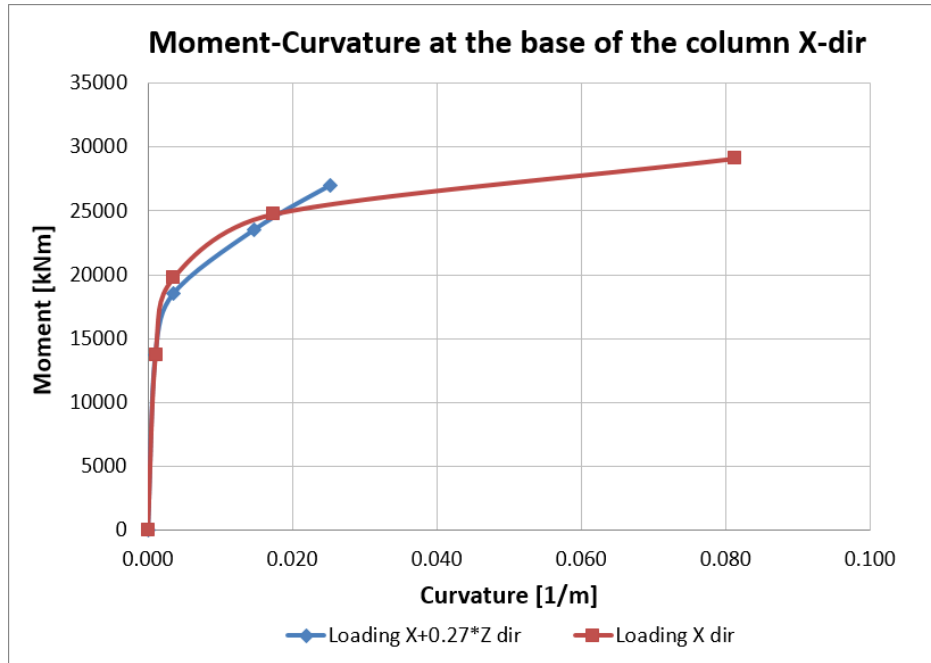


Fig. 17. Moment-curvature relationship at the base of the pier- comparison with/without VERTICAL seismic action

4 CONCLUSIONS

The ductility of the frame type bridges has been analyzed using nonlinear static analysis (push-over). The main results from the analysis of the presented bridge structure are:

- The ductility in the longitudinal direction in the case of flat foundation is higher than one in the transversal direction. The calculated displacement ductility factor $\mu_d=4.29$ in TRANSVERSAL direction is still higher than

the value of the behaviour coefficient from EN 1998-2 [1] – $q=3.5$.

- The calculated displacement ductility factor μ_d for the case “flat foundation” is higher than one for the case “pile foundation” – see Fig.18.

- The vertical seismic component should be always taken into account due to the reduced bridge member ductility

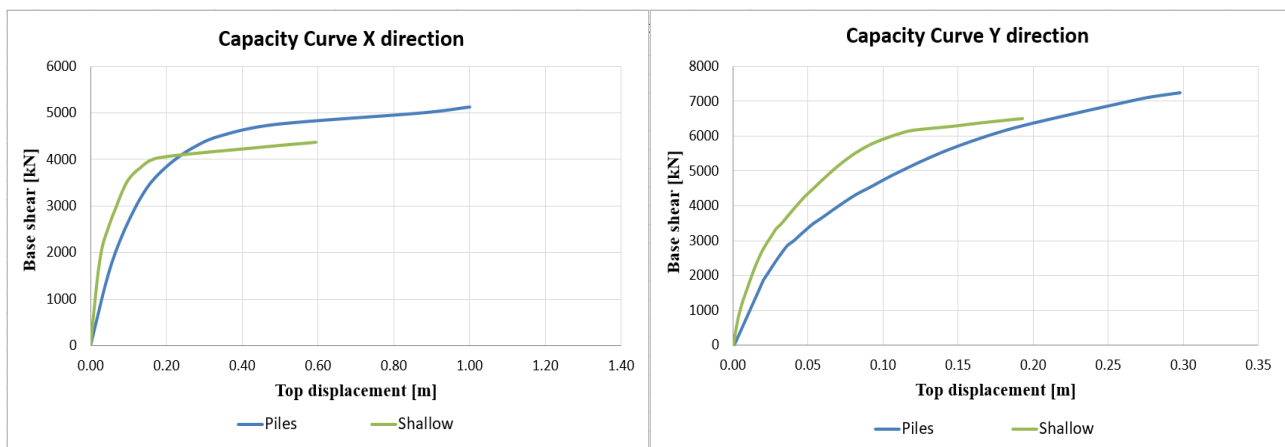


Fig. 18. Push-over (capacity) curve comparison

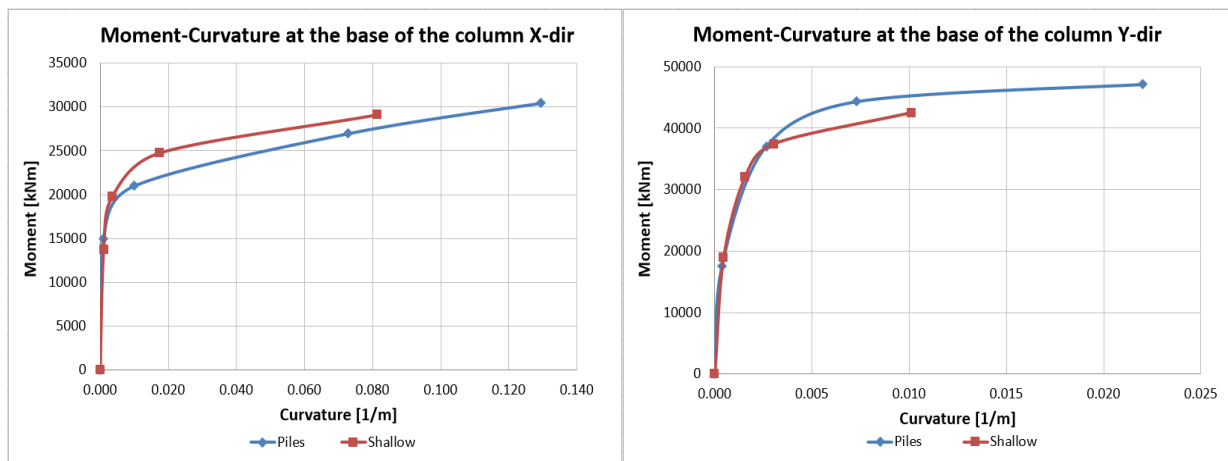


Fig. 19. Moment-curvature relationship at the base of the pier- comparison

ACKNOWLEDGEMENTS

This study is financially supported by „Program for the promotion of research in the field of environmental protection and reduction of the risk of adverse events and natural disasters“, WP.I.10. „Assessing the dangers of catastrophic earthquakes and their consequences“.

ABSTRACT

NON-LINEAR ANALYSIS OF FRAME REINFORCED CONCRETE BRIDGE- SHALLOW VS. PILE FOUNDATION

Alexander ILIEV
Dimitar DIMITROV
Dimitar STEFANOV

The paper presents the application of the non-linear (push-over) analysis for a selected frame reinforced concrete bridge which meets the requirements of [1]. Two options for the foundations are considered – flat and pile ones. Comparison between the structural ductility in longitudinal and transversal direction is made. The vertical component of the earthquake action is taken into account and the influence to the ductility is analyzed.

Key words: Bridges, Non-Linear Analysis, Eurocode, Ductility

5 REFERENCES

- [1] Eurocode 8 - Design of structures for earthquake resistance. Part 2: Bridges.
- [2] Eurocode 8 - Design of structures for earthquake resistance. Part 1: General rules, seismic actions and rules for buildings.
- [3] SOLVIA Finite Element System. User manual. SOLVIA Engineering AB, Vasteras, Sweden, 2003.
- [4] Sheikh, S.A., Uzimeri, M. Strength and Ductility of Tied Concrete C, Journal of the Structural Division, Vol.108, ST12, 1982.
- [5] Priestley, M.J.N, Seible, F., Calvi, G.M. Seismic Design and Retrofit of Bridges, JOHN WILEY & SONS, INC., New York, 1996.
- [6] Fletcher, Roger. Practical methods of optimization (2nd ed.), New York: John Wiley & Sons, 1987.
- [7] Len Schwer. The Winfrith Concrete Model: Beauty or Beast? Insights into the Winfrith Concrete Model, 8th European LS-DYNA Users Conference, Strasbourg, 2011.

REZIME

NELINEARNA ANALIZA OKVIRNOG AB MOSTA FUNDIRANOG NA PLITKIM TEMELJIMA I NA ŠIPOVIMA

Alexander ILIEV
Dimitar DIMITROV
Dimitar STEFANOV

U radu je prikazana primena nelinearne (push-over) analize za okvirni armirano-betonski most prema zahtevima izloženim u [1]. Razmatrane su dve opcije fundiranja - plitko fundiranje i fundiranje na šipovima. Upoređena je duktilnost konstrukcije u podužnom i poprečnom pravcu. Uzeta je u obzir i vertikalna komponenta zemljotresnog dejstva i analiziran je njen uticaj na duktilnost konstruktivnog sistema.

Ključne reči: Mostovi, Nelinearna analiza, Evrokod, Duktilnost

COMPARATIVE ANALYSIS OF DIFFERENT FINITE ELEMENT MODELS OF THE SOIL-BURIED ARCH BRIDGE INTERACTION

KOMPARATIVNA ANALIZA MODELA INTERAKCIJE TLA I LUČNOG MOSTA SA ZEMLJANOM ISPUNOM ZASNOVANIH NA MKE

Konstantin KAZAKOV
Lena MIHOVA
Doncho PARTOV

ORIGINALNI NAUČNI RAD
ORIGINAL SCIENTIFIC PAPER
UDK:624.6:624.131.5
doi:10.5937/GRMK1904015K

1 INTRODUCTION

Comparative analysis is made of different static schemes and finite element models of the buried arch bridge with span of 15.29 m which is built in a railway-road junction "Tri Voditsi" situated between the villages Tri Voditsi and Novo Selo in Bulgaria. The bridge is composed of 8 arches which consist of 24 prefabricated reinforced C50/60 concrete elements. The prefabricated elements are used for part of the foundations, for external retaining 0.60-0.35m thick walls and for a 0.35 m thick vault plate. The foundation is constructed of two strips with width of 4.0 m and average thickness of 0.60 m. The prefabricated strips are the half of the foundation

inside of the arch structure. The part of the foundation is done on site of concrete C35/45. Photos of the bridge in construction phase and in service phase are presented in Figure 1.

The following two static schemes of bridge structure are considered:

- A continuous static scheme i.e. the connection between all structure elements is rigid;
- A static scheme of hinged connection between the retaining walls and the vault plate. The hinged connection does not bear a bending moment.

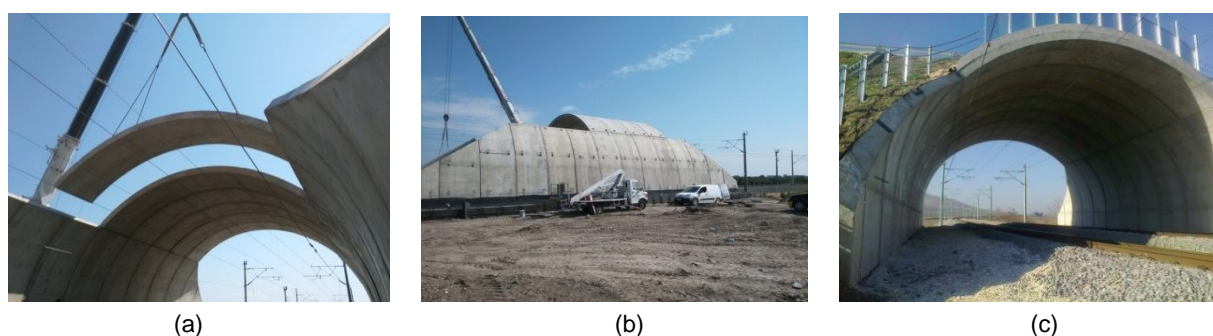


Figure 1. The bridge in construction period (a, b) and in service period (c)

Konstantin Kazakov, Prof. DSc, University of Structural Engineering and Architecture, Sofia, Bulgaria, kazakov@vsu.bg
Lena Mihova, Prof. PhD, University of Architecture, Civil Engineering and Geodesy, Sofia, Bulgaria, L_mihova@yahoo.com
Doncho Partov, Prof. PhD, University of Structural Engineering and Architecture, Sofia, Bulgaria.partov@vsu.bg

There are different approaches for modeling the soil-structure interaction in the finite element (FE) method [1]. The Winkler spring model is the most frequently applied in FE analyses. The main reason of this conclusion is the simplicity of this model and the fact that it is developed in most of the computer software products for structural analysis. The stiffness of the Winkler springs is determined using subgrade reaction moduli. This approach is applied in a previous analysis of the bridge structure using Autodesk Robot software [2] where the calculation of the subgrade reaction moduli is done according to the Menard theory [3]. Here are mentioned some Bulgarian researches based on the application of the Winkler spring model for the interaction of soil and different kinds of structures: shallow foundations [4], [5]; raft-pile foundation [6]; bridge support structures [7], [8]; retaining structures [9], [10].

The state-of-the-art approaches for modeling the soil-structure interaction consider the behavior both the structure and the soil body around the structure. For this purpose it is necessary to perform a finite element discretization of both the structure and the soil body and use appropriate constitutive models for the different materials and their contact. Advanced constitutive models are developed on the base of theoretical and experimental achievements in the soil mechanics. They take into account complex and highly varied mechanical behavior of the materials and use a lot of parameters. It is necessary to perform accurate experimental procedures and sensitivity analyses for identification of the constitutive parameters. A review of constitutive models for soil material is presented in reference [11]. Constitutive parameters of improved soil materials by advanced technologies are presented in [12], [13], [14], [15]. Features of the dynamic soil behavior and dynamic soil parameters are discussed in [16], [17], [18].

The stress-strain behaviour of the structure, the settlement and the bearing capacity of the soil ground

are evaluated in construction and service periods of the bridge. The self-weight loading of the backfill and traffic loading of the road above the bridge are taken into account in the FE analyses performed by the Plaxis 2D software. Considerations about requirements of Eurocodes are discussed.

2 FINITE ELEMENT MODELING

2.1 Finite element discretization, boundary and hydraulic conditions

Plane strain condition in finite element modeling of the bridge is assumed. It means that all used finite elements have dimension perpendicular to the cross section plane equal to 1. The cross section plane is denoted with xy .

Two alternative types of finite elements are used for the bridge structure (Figure 2): 15-node triangular plate elements (Figure 2 a, b) and 5-node linear beam elements with width of 1 (Figure 2 c). The plate elements are formulated in normal and shear stresses. The beam elements are formulated in bending moments, axial and shear forces. The latter approximation is suitable because the output data include forces which allow designing the structure easily according to codes. A rotation stiffness of zero is defined in the beam joints of hinges. The hinge connection is simulated by a short beam element.

The rectangular soil body with width of 50 m, height of 20 m and thickness of 1 m is discretized with triangular plate elements with two node parameters: displacements U_x and U_y in xy plane. Boundary conditions involve zero horizontal displacement, U_x , and zero vertical displacement, U_y (Figure 3). In the same figure the ground water level is denoted with WL.

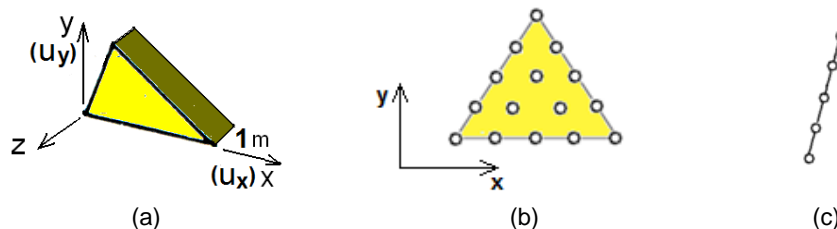


Figure 2. 15-node plane strain finite element (a, b) and 5-node beam element (c)

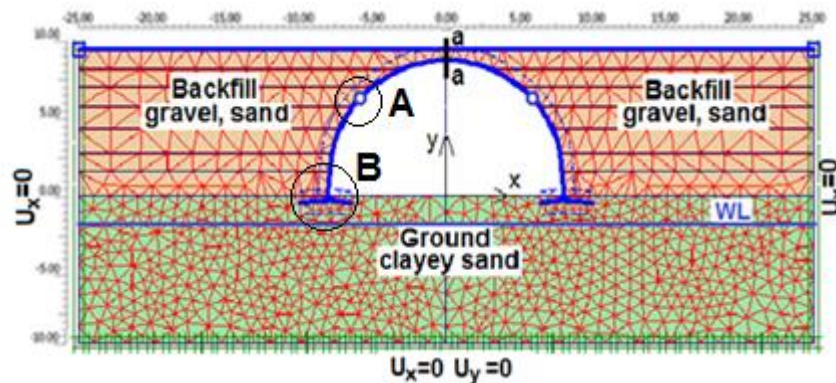


Figure 3. FE mesh of the plane strain model with boundary conditions (U_x , U_y) and hydraulic conditions (WL)

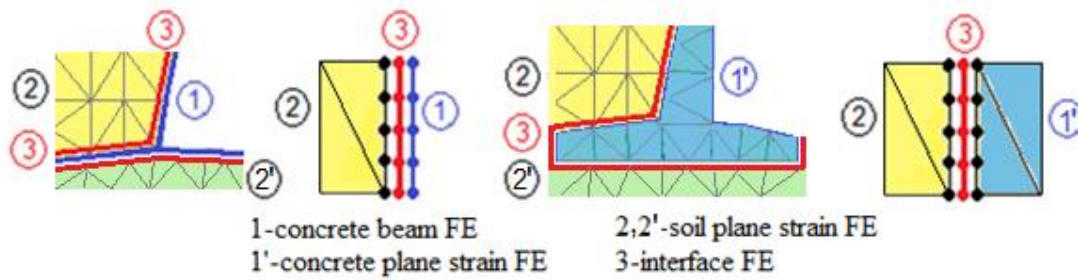


Figure 4. Detail B from Fig. 3: Two approaches for FE modeling of soil-structure interaction

The soil-structure contact is modeled by interface elements of thickness closed to zero (Figure 4). The role of the interfaces is to reduce the friction in soil-structure contact compared to the friction in the soil. In Plaxis software the parameter which relates the shear strength of the soil to the shear strength in the interfaces is R_{inter} . Here the value $R_{inter} = 0.5$ is assumed. Some alternative approximations of soil-structure interaction are suggested in references [19], [20].

Figure 5 presents FE modeling of rigid connection and hinged connection in bridge structure (see detail A in Figure 3). These two variants of static scheme are analyzed.

The bridge structure is undergone live traffic loads from the road which is built on the top of the backfill. The thickness of the backfill at the top of the bridge is only 0,50 m. The traffic loads are simulated by the model LM1 according to Eurocode 1[21] and its Bulgarian Annex. According to this model the carriageway is divided into notional lanes. The loading of each lane is composed of concentrated loads (*Tandem System TS*) and uniformly distributed load (*System UDL*). The most

unfavorable loading is located on the lane number 1 represented in Figure 6. For the study here the concentrated loads are approximated as a distributed load q_2 and the total distributed traffic load ($q_1 + q_2$) is applied pseudostatic. Different states of the total traffic load are taken into consideration.

2.2 Constitutive laws for the bridge and soil materials

The constitutive law is a mathematical description of stress-strain behaviour of the materials in response to the applied loads.

Hooke's law of linear, isotropic elasticity is used for modeling the concrete bridge structural elements. Input material parameters involved in equations of stress-strain relationship are only two – Young's modulus, E , and Poisson's ratio, ν . Here are used two alternative constitutive models for the soil materials: the linear elastic-perfectly plastic Mohr-Coulomb's model and the advanced elastic-plastic Hardening-Soil model.

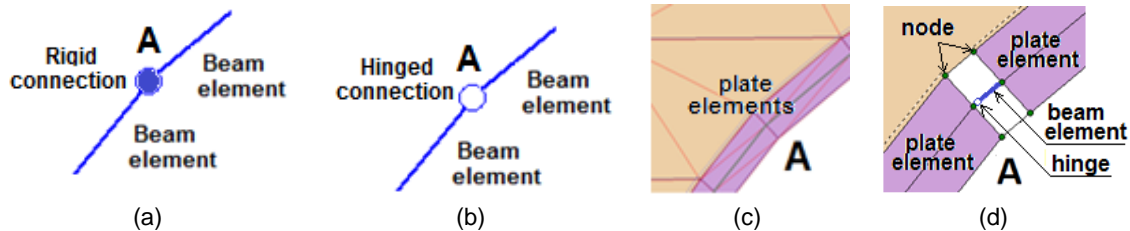


Figure 5. Detail A from Fig. 3 for connection between structural elements: (a) Rigid connection between beams; (b) Hinged connection between beams; (c) Rigid connection between plates; (d) Hinged connection between plates

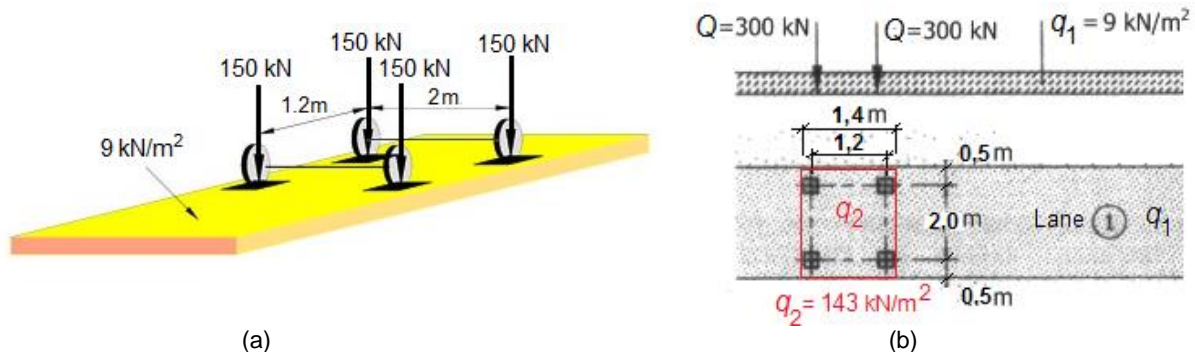


Figure 6. Model LM1 for road traffic loading: (a) TS and UDL systems; (b) Approximation of the TS system as a distributed load q_2

2.2.1 Mohr-Coulomb's soil model (M-C)

According to M-C model, the stresses are proportional to the strains until the yield point is reached. The stress state corresponding to the yield point is defined by Mohr-Coulomb's yield function, F . The latter is represented as a hexagonal cone and it is shown in Figure 7. The plastic strain increments are determined using the flow rule defined with a prescribed function of the effective stresses, known as plastic potential, Q . The flow rule is termed *associated flow rule* when the plastic potential is equal to the yield function, i.e. $F = Q$. This is the classical form of plasticity, introduced by Von Mises (1928), which postulates that the direction of the vector of the plastic strain increment is perpendicular to the yield surface.

The flow rule is connected to the volume increase caused by the shearing during the plastic flow, so called dilatancy. However, the theory of associated plasticity with the Mohr-Coulomb's yield criterion predicts a dilatancy rate of the soil materials far greater than the one observed in real soil. For remediation of this inaccuracy of the model, the function of the plastic

potential is chosen with the same form as the yield function, but the internal friction angle, φ , is replaced by the dilatancy angle, ψ . The dilatancy angle controls the volume change of the material undergoing plastic deformation. The dilatancy angle of the soil actually varies during the plastic deformation and it has values less than the value of the internal friction angle. The plastic volumetric strain increment is proportional to $\sin\psi$ and, consequently, is smaller than the ones predicted by the associative model. The flow rule corresponding to the case of $Q \neq F$ is known as a *non-associated flow rule*. The plastic deformation behavior of real soil obeys the non-associated flow rule. A constant rate of dilation and, respectively, a constant dilatancy angle of the soil, are often assumed in practice. In absence of laboratory or field data, the dilatancy angle, ψ , value can be selected in the range $0 \leq \psi \leq \varphi/3$ [22]. The M-C model involves five input material parameters: E and ν for the soil elasticity, φ and c for the soil plasticity and ψ – the angle of dilatancy.

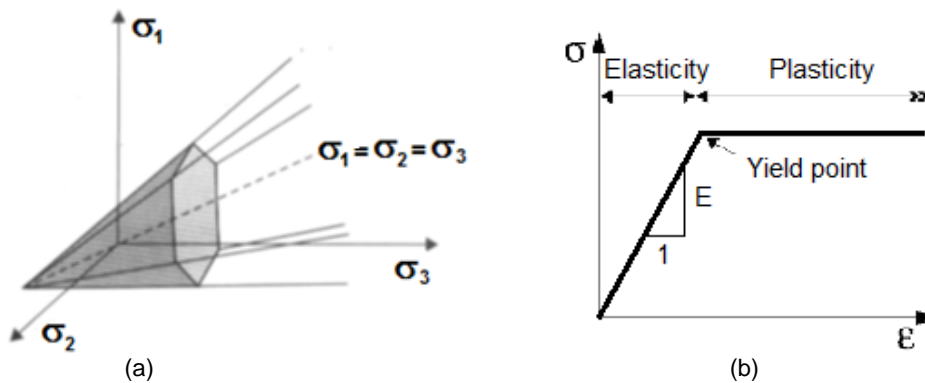


Figure 7. Mohr-Coulomb's model: (a) Yield surface in principal stress space; (b) Stress-strain curve and definition of E -modulus

Table 1. M-C model parameters of the backfill material and clayey sand ground

Parameter	Symbol	Dimension	Backfill	Clayey sand
Unit weight of unsaturated soil	γ_{unsat}	kN/m^3	18	18
Unit weight of saturated soil	γ_{sat}	kN/m^3	-	20
Young's modulus	E	kN/m^2	50 000	20 000
Poisson's ratio	ν	-	0,3	0,3
Friction angle	φ	$^\circ$	38	29
Dilatancy angle	ψ	$^\circ$	8	0

2.2.2 Hardening Soil model (HS)

HS model is an advanced constitutive conception simulating the behavior of different types of soil [23]. The description of the model presented here is according to the reference [24]. As for the Mohr-Coulomb's model, limiting states of stress are described by means of friction angle, φ , the cohesion, c , and the dilatancy angle, ψ . However, the soil stiffness is defined much more accurately by involving three different input stiffnesses: the triaxial loading stiffness, E_{50} , the triaxial unloading stiffness, E_{ur} , and the oedometer loading stiffness, E_{oed} . HS model also takes into account stress-dependency of the stiffness that means that all stiffnesses increase with pressure, i.e. the soil is hardening. The yield surface is not fixed in principal stress space, but it can expand due to plastic straining. The yield surface of the HS model in principal stress space is represented in Figure 8a. Two types of hardening are possible: shear hardening and compression hardening. The shear hardening is used to model irreversible plastic strains due to primary deviatoric

loading. Compression hardening is used to model irreversible plastic strains due to primary compression in oedometer loading and in isotropic loading. Hyperbolic Duncan-Chang's relationship is assumed between the axial strain and the deviatoric stress for the standard drained triaxial test [25] (Figure 8b).

The basic characteristics of the HS model can be generalized as follows:

- 1) Stress dependent stiffness;
- 2) Hyperbolic stress-strain relation in primary loading for triaxial standard drained test;
- 3) Plastic straining due to primary deviatoric loading;
- 4) Plastic straining due to primary compression;
- 5) Elastic unloading/reloading;
- 6) Failure according to the Mohr-Coulomb's failure criterion.

The HS model has 15 input parameters including already mentioned basic parameters. The additional parameters of the HS model for material of the bridge soil body are shown in Table 2.

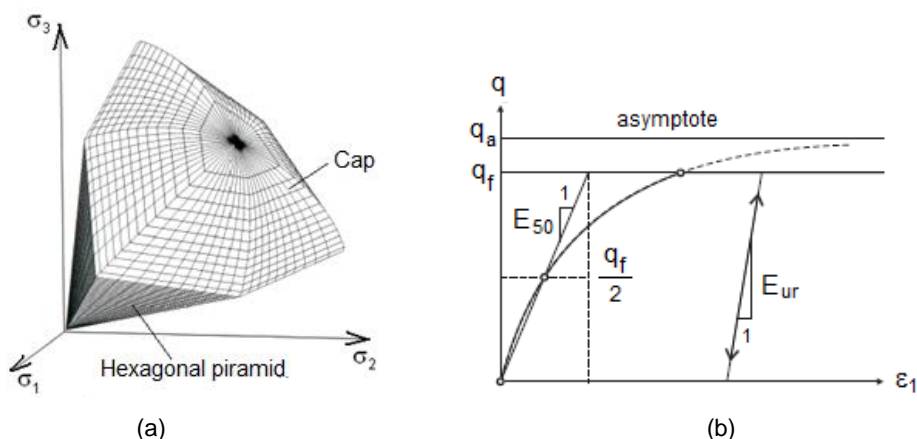


Figure 8. Hardening Soil model: (a) Yield surface in principal stress space; (b) Stress-strain curve for triaxial standard drained test and definition of E -moduli

Table 2. HS model parameters of the backfill material and clayey sand ground

Parameter	Symbol	Dimension	Backfill	Clayey sand
Reference stress for stiffnesses	p_{ref}	kN/m ²	100	100
Tangent stiffness for primary oedometer loading	$E_{oed,ref}$	kN/m ²	50 000	20 000
Secant stiffness in standard drained triaxial test	$E_{50,ref}$	kN/m ²	50 000	20 000
Unloading/reloading stiffness	$E_{ur,ref}$	kN/m ²	150 000	60 000
Poisson's ratio for unloading/reloading	ν_{ur}	-	0,2	0,2
Power for stress-level dependency of stiffness	m	-	0,5	0,6
Coefficient of lateral earth pressure	K_0	-	0,384	0,515
Failure ratio	R_f	-	0,9	0,9

2.3 Considerations of Eurocodes

The Eurocodes are the current design codes in Bulgaria. The Eurocodes are based on the limit state design approach using partial factors for actions/effects of actions, material parameters and resistances. Eurocode 7 for geotechnical design [26] includes only general concepts for analysis of the soil-structure interaction. There are some clarifying books about the design according to Eurocode 7 [27], [28]. Bearing capacity analysis of the soil is the most important geotechnical analysis because it considers many parameters of the foundations, loading and soil materials. The Eurocode's requirements of the soil bearing capacity analysis and results from commonly used formulae for shallow foundations are presented in references [29], [30], [31]. The determining of the bearing capacity in case of presence of structural elements in soil body are discussed in references [32], [33].

The purpose of the present paper is to accent on the advantages and disadvantages of the different static schemes and numerical models of the bridge structure and its interaction with soil ground and filling material. That is why the analyses are performed without using partial factors according to Eurocodes. Special attention is given to bearing capacity analysis of the soil using unfactored resistance parameters of the soil.

2.4 Finite element analyses

2.4.1 "In situ" stress analysis

"In situ" stress analysis defines the initial stress state of the ground while the initial displacements of the ground are equal to zero. The initial stress state of the ground involves values of normal vertical and horizontal

stresses due to self-weight of the soil and values of water pressure. In the present case the ground surface is horizontal. The initial vertical effective stresses are determined by the expression $\sigma_{y,0'} = \gamma \cdot h$, where γ is the soil unit weight, h is depth below the ground surface. The initial horizontal effective stresses are determined by the expression $\sigma_{x,0'} = K_0 \cdot \sigma_{y,0'}$, where K_0 is coefficient of lateral pressure at rest calculated by Jaky's empirical formula $K_0 = 1 - \sin\phi$. The water pressure is calculated by the formula $p_w = \gamma_w \cdot h_w$, where γ_w is unit weight of water, h_w is depth below the water level.

Diagrams of the initial stresses in the soil ground are shown in Figure 9.

2.4.2 Construction period of the bridge

The construction period of the transport junction, part of which is the building of the arch bridge structure, is simulated by the following sequence of states (Fig. 9):

- State 1: Construction of the arch bridge structure by precast elements;
- State 2 - State 8: Backfilling;
- State 9: Construction of the road above the bridge.

The asphalt road above the bridge is modelled in stage 9 by elastic beam finite elements with the following material parameters: unit weight $\gamma = 22 \text{ kN/m}^3$, Young's modulus $E = 150 \cdot 10^6 \text{ kN/m}^2$ and Poisson's ratio $\nu = 0.2$.

2.4.3 Service period of the bridge

The live loading of the bridge structure due to the road traffic is simulated by a consequence of states (State 10 – State 13). All states consist of continuous uniformly distributed load $q_1 = -9 \text{ kN/m}^2$ and partial distributed load $q_2 = -143 \text{ kN/m}^2$. Different locations of the load q_2 are accepted (Figure 11).

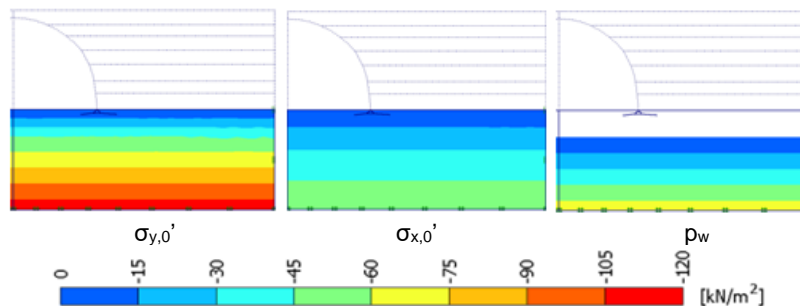


Figure 9. Diagrams of the initial stresses in the soil ground

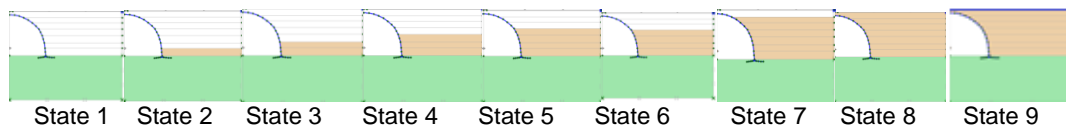


Figure 10. States in construction period

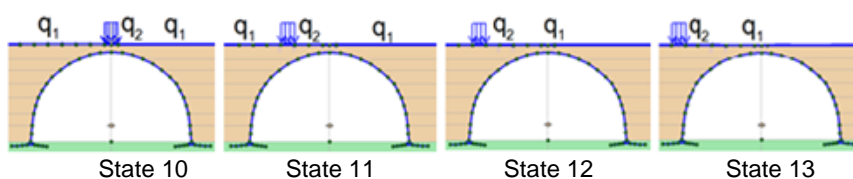


Figure 11. Simulation of the traffic live loading of the bridge structure

2.4.4 Bearing capacity analysis of the soil ground

The finite element method offers some advanced computer techniques for bearing capacity analysis. The main advantage is the ability to develop failure mechanism considering the deformation and the strength properties of the soil. Here is used the shear strength reduction technique (SSR) included in Plaxis 2D software. The soil Mohr-Coulomb's strength parameters (the friction angle, ϕ , and the cohesion, c) are reduced artificially and progressively until the state of soil failure is reached. The bearing capacity safety factor, F_s , is deemed the factor by which the soil strength parameters

are reduced so that failure is reached [34]. The SSR technique is very suitable for bearing capacity analysis at cases of complex geotechnical conditions and complex loading [35].

3 RESULTS FROM FINITE ELEMENT ANALYSES

3.1 Results from the models of continuous bridge

Table 3 presents results of bending moment, axial force and normal stresses in the bridge structure obtained from solutions of different FE models.

Table 3. Results from FE analyses of State 9 in cross section a-a (see Figure 3) of the bridge

Type of modeling	M_{a-a} (kNm)	N_{a-a} (kN)	$\sigma_{x,a-a}^{top}$ (kPa)	$\sigma_{x,a-a}^{down}$ (kPa)	$U_{y,a-a}$ (m)
Soils - HS model; Bridge - plate FE	71	-363	2419	-4497	-0.07
Soils - HS model; Bridge - beam FE	65	-338	2120	-4052	-0.08
Soils - MC model; Bridge - plate FE	27	-216	253	-1955	-0.06
Soils - MC model; Bridge - beam FE	20	-314	83	-1877	-0.07

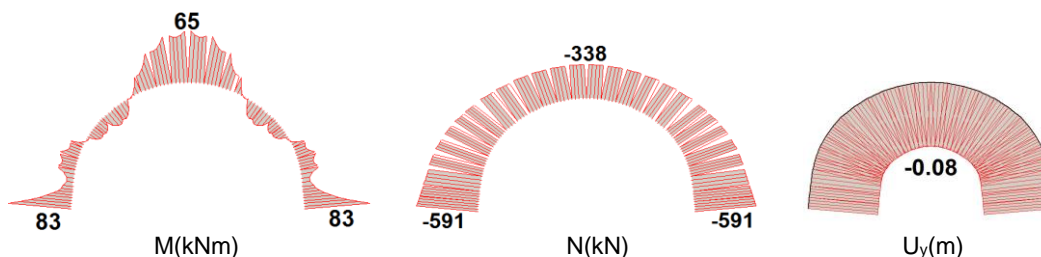


Figure 12. Type of modeling "Soils - HS model; Bridge - beam FE": Diagrams of bending moment M , axial force N and displacement $U_y(m)$ as a result from FE analysis of State 9

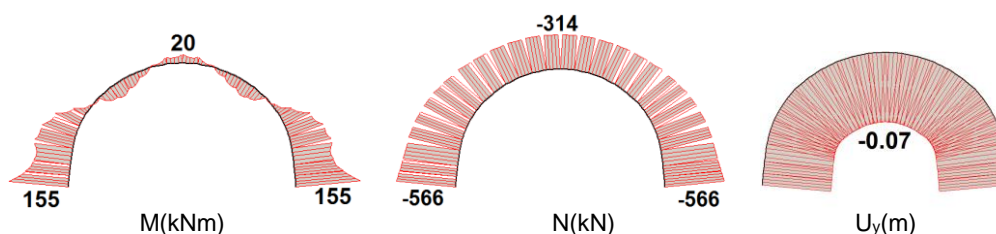


Figure 13. Type of modeling "Soils - MC model; Bridge - beam FE": Diagrams of bending moment M , axial force N and displacement U_y as a result from FE analysis of State 9

Table 4. Results of FE analyses of State 10 in cross section a-a (see Fig. 3) of the bridge

Type of FE modeling	M_{a-a} (kNm)	N_{a-a} (kN)	$\sigma_{x,a-a}^{top}$ (kPa)	$\sigma_{x,a-a}^{down}$ (kPa)	$U_{y,a-a}$ (m)
Soils - HS model; Bridge - plate FE	-30	-455	-2788	193	-0.08
Soils - HS model; Bridge - beam FE	-37	-507	-3265	369	-0.09
Soils - MC model; Bridge - plate FE	-92	-354	-5493	3469	-0.08
Soils - MC model; Bridge - beam FE	-94	-460	-5928	3300	-0.09

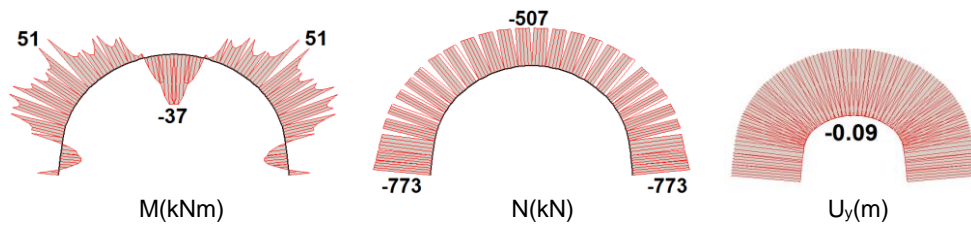


Figure 14. Type of modeling "Soils - HS model; Bridge - beam FE": Diagrams of bending moment M , axial force N and displacement U_y as a result from FE analysis of State 10

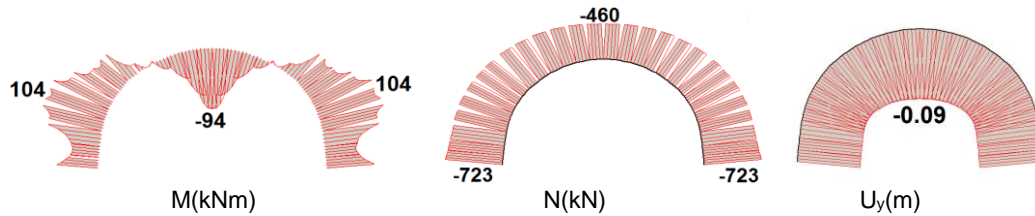


Figure 15. Type of modeling "Soils - MC model; Bridge - beam FE": Diagrams of bending moment M , axial force N and displacement U_y as a result from FE analysis of State 10

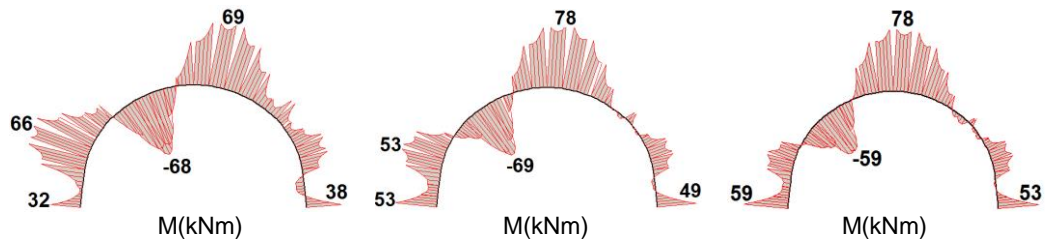


Figure 16. Type of modeling "Soils - HS model; Bridge - beam FE": Diagrams of bending moment M as a result from FE analysis of States 11, 12, 13

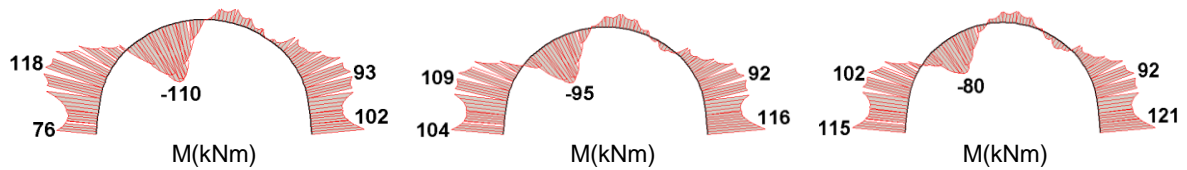


Figure 17. Type of modeling "Soils - MC model; Bridge - beam FE": Diagrams of bending moment M as a result from FE analysis of States 11, 12, 13

Results for the bearing capacity safety factor, F_s , obtained from solutions of the presented FE models are

summarized in Table 5 and typical failure modes are shown in Figure 18.

Table 5. Values of bearing capacity safety factor, F_s

Type of FE modeling	F_s		
	State 1	State 9	State 10
Soils - HS or MC model; Bridge - beam FE	4.0	2.4	2.4
Soils - HS or MC model; Bridge - plate FE	5.2	2.7	2.7

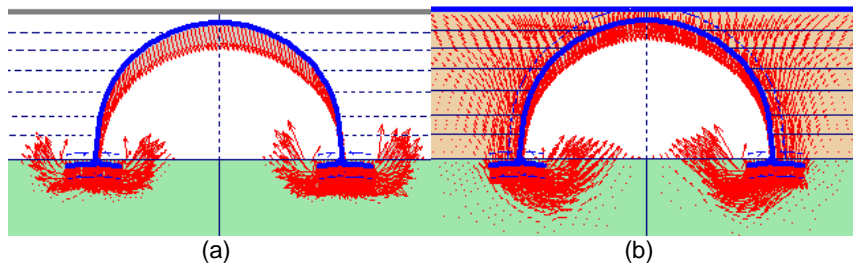


Figure 18. Failure modes presented by the vectors of deformation increments:
(a) State 1; (b) State 9 – State 13

3.2 Results from the models of hinged bridge

Table 6. Results from FE analyses of State 9 in cross section a-a (see Fig. 3) of the bridge

Type of modeling	M_{a-a} (kNm)	N_{a-a} (kN)	$\sigma_{x,a-a}^{top}$ (kPa)	$\sigma_{x,a-a}^{down}$ (kPa)	$U_{y,a-a}$ (m)
Soils - HS model; Bridge - plate FE	68	-355	2297	-4327	-0,066
Soils - HS model; Bridge - beam FE	71	-340	2506	-4449	-0,086
Soils - MC model; Bridge - plate FE	-2	-267	-859	-667	-0,063
Soils - MC model; Bridge - beam FE	6	-311	-595	-1183	-0,071

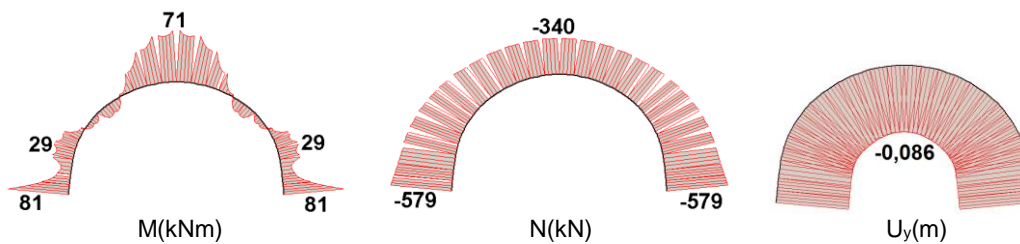


Figure 19. Type of modeling "Soils - HS model; Bridge - beam FE": Diagrams of bending moment M , axial force N and displacement $U_y(m)$ as a result from FE analysis of State 9

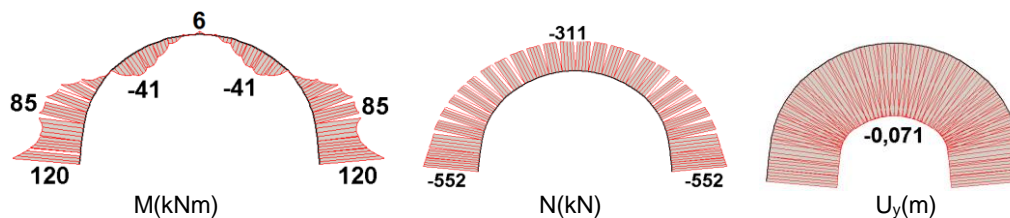


Figure 20. Type of modeling "Soils - MC model; Bridge - beam FE": Diagrams of bending moment M , axial force N and displacement U_y as a result from FE analysis of State 9

Table 7. Results from FE analyses of State 10 in cross section a-a (see Fig. 3) of the bridge

Type of FE modeling	M_{a-a} (kNm)	N_{a-a} (kN)	$\sigma_{x,a-a}^{top}$ (kPa)	$\sigma_{x,a-a}^{down}$ (kPa)	$U_{y,a-a}$ (m)
Soils - HS model; Bridge - plate FE	-37	-452	-3119	534	-0,083
Soils - HS model; Bridge - beam FE	-43	-519	-3589	623	-0,095
Soils - MC model; Bridge - plate FE	-119	-331	-6790	4903	-0,083
Soils - MC model; Bridge - beam FE	-121	-465	-7256	4598	-0,091

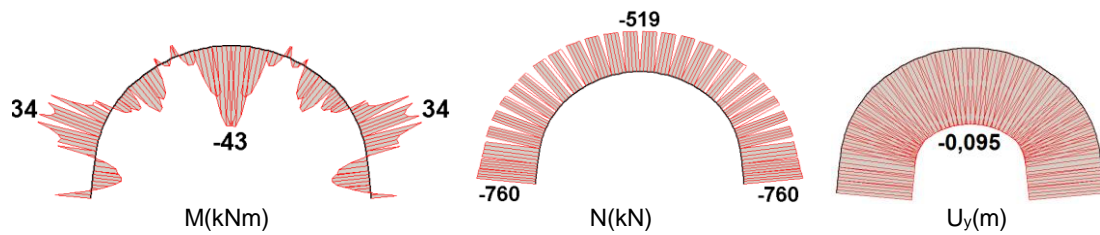


Figure 21. Type of modeling "Soils - HS model; Bridge - beam FE": Diagrams of bending moment M , axial force N and displacement U_y as a result from FE analysis of State 10

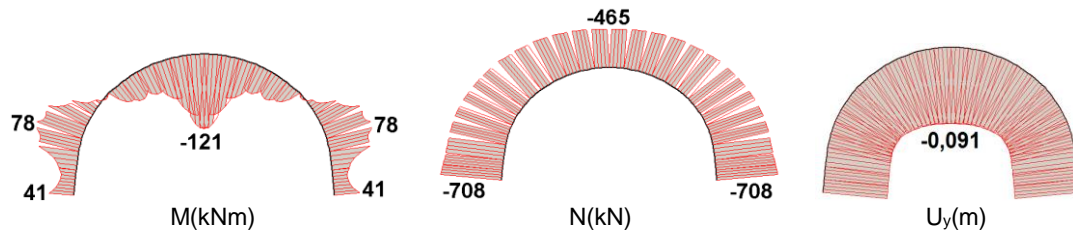


Figure 22. Type of modeling "Soils - MC model; Bridge - beam FE": Diagrams of bending moment M , axial force N and displacement U_y as a result from FE analysis of State 10

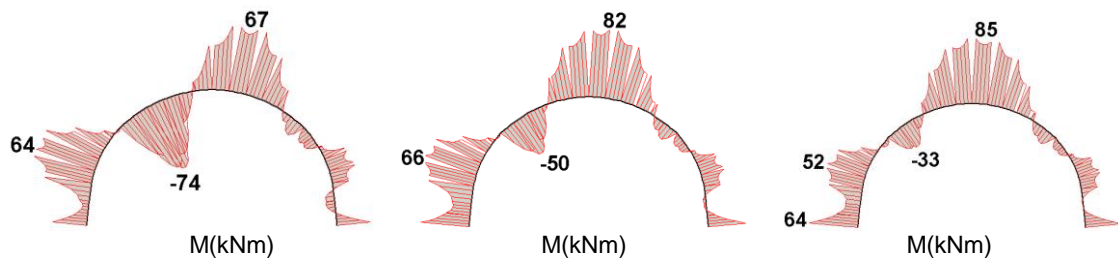


Figure 23. Type of modeling "Soils - HS model; Bridge - beam FE": Diagrams of bending moment M as a result from FE analysis of States 11, 12, 13

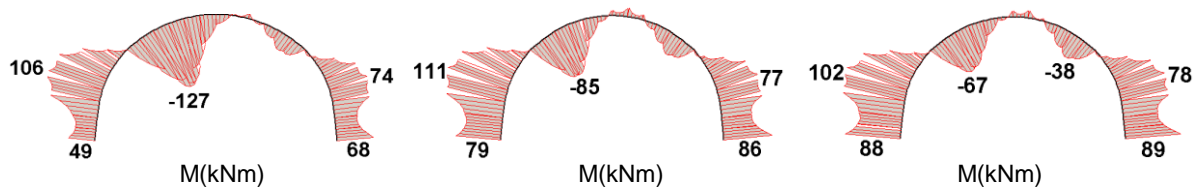


Figure 24. Type of modeling "Soils - MC model; Bridge - beam FE": Diagrams of bending moment M as a result from FE analysis of States 11, 12, 13

Results for the bearing capacity safety factor, F_s , obtained from solutions of the presented FE models are

summarized in Table 8 and typical failure modes are shown in Figure 25.

Table 8. Values of bearing capacity safety factor, F_s

Type of FE modeling	F_s		
	State 1	State 9	State 10
Soils - HS or MC model; Bridge - beam FE	3,5	1,8	1,8
Soils - HS or MC model; Bridge - plate FE	4,2	1,9	1,9

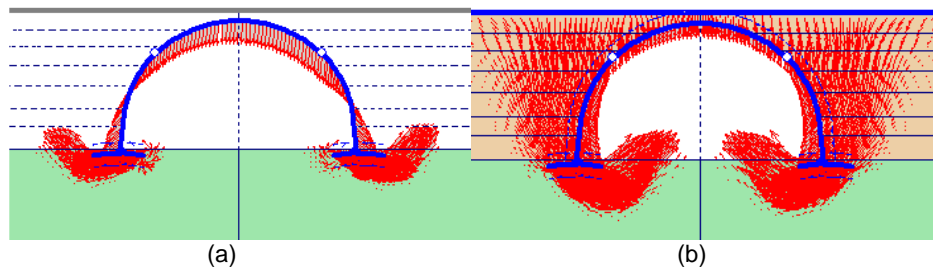


Figure 25. Failure modes presented by the vectors of deformation increments:
(a) State 1; (b) State 9– State 13

4 ANALYSIS OF THE RESULTS FROM FE MODELS

4.1 Analysis of the results from models of continuous bridge

- The solutions which use models with beam elements for the bridge structure give from 1.1 to 1.35 times larger values of the bending moment than those obtained from the solutions with plate elements for the bridge structure.

- There are differences in the values of the axial force in the bridge structure obtained from different models. The solutions of the State 9 (the end of construction period) and State 10 (the first service state) which use models with beam elements for the bridge structure gives from 1.2 to 1.5 times larger values of the axial forces than those obtained with the solutions which use models with Plate elements for the bridge structure.

- The solutions which use models with beam elements for the bridge structure give from 1.1 to 1.2 times larger values of the vertical displacement of the bridge than those obtained with the solutions with Plate elements for the bridge structure.

- Hardening Soil (HS) constitutive model is an advanced conception in the soil mechanics. It uses more than 15 material parameters. Mohr-Coulomb (M-C) constitutive model is the most applicable classical theoretical model for the mechanical behavior of the soils.

- The differences between the values of bending moment in bridge structure obtained from the solution according to HS and M-C constitutive models are about 2-3 times.

- HS constitutive model gives 1.1 times larger values of axial forces in bridge structure in comparison to M-C constitutive model.

- M-C constitutive model gives from 1.1 to 1.2 times larger values of vertical displacement in bridge structure in comparison to HS constitutive model.

- The values of the vertical displacements in the bridge structure are 8.3– 9.5 cm due to mainly the settlements of the ground.

- The lowest value of bearing capacity safety factor is $F_s = 2.4$ which means that there is not a risk of failure of the bridge.

4.2 Analysis of the results from models of hinged bridge

- The finite element solutions which use plate elements or beam elements for the bridge structure modeling obtain approximately same values of bending moments.

- There are differences in the values of the axial force in the bridge structure obtained from different models. The solutions of the State 9 (the end of construction period) and State 10 (the first service state) which use models with beam elements for the bridge structure give from 1.2 to 1.4 times larger values of the axial forces than those obtained with the solutions which use models with Plate elements for the bridge structure.

- The solutions which use models with beam elements for the bridge structure give from 1.1 to 1.3 times larger values of the vertical displacement of the bridge than those obtained from the solutions with plate elements for the bridge structure.

- There are significant differences between the values of bending moment in the bridge structure obtained from the solution according to HS and M-C constitutive models for soil ground and filling material. The differences of bending moment increase from 2 to 10 times.

- HS constitutive model gives from 1.1 to 1.4 times larger values of axial forces in bridge structure in comparison to MC constitutive model.

- HS and MC constitutive models give similar results for the vertical displacements of the bridge structure.

- The bridge structure has high values of vertical displacements (8– 9cm) due to mainly the settlements of the ground.

- The lowest value of the bearing capacity safety factor is $F_s = 1.8$ which means that there is not a risk of failure of the bridge.

4.3 Comparative analysis of the results

Comparative analysis between the model of the bridge with two hinges developed here and the model of continuous bridge gives the following conclusions:

- The differences between the two models of the bridge are larger when the M-C constitutive law is used: the model with two hinges gives about 30% larger bending moments and axial forces than the model of continuous bridge.

- The values of the vertical displacements of the bridge structure obtained from all solutions are too high and do not satisfy the serviceable limit state requirements. It is necessary to improve the soil ground or to build deep foundations of the structure.

- The model with two hinges gives 30% lower values of the bearing capacity safety factor.

- The failure mechanism in the State 1 (the state of the bridge construction before the backfilling) is two-sided in the case of continuous bridge and one-sided in the case of hinged bridge.

5 CONCLUSIONS

A new approach is applied for numerical modeling of the mechanical behavior of an arch bridged structure. The approach consists in using plane strain finite elements for the soil body and interface elements for the soil-structure contact. The numerical modeling is developed on the basis of two non-linear constitutive laws of the soil materials – the linear elastic-perfectly plastic Mohr-Coulomb's model and the advanced elastic-plastic Hardening Soil model. They both are adapted in Plaxis software which is used for the accomplishment of the present research. The Hardening-Soil model is state-of-the-art scientific achievement which interprets the mechanical behavior of the soil materials with high accuracy using 15 material parameters.

Comparative analysis of the FE models shows that the numerical solutions based on the old classical concepts of the soil mechanics obtain considerably conservative results.

It is important to mention that the advanced soil constitutive models describe more precisely mechanical behavior of the soil because they use a lot of material parameters. But the correct application of the advanced models requires performing accurate experimental procedures and sensitivity analyses for identification of constitutive parameters.

6 REFERENCES

- [1] Milev, N., (2014). Approaches for Consideration of the Soil-Foundation-Structure Interaction. Annual of the University of Architecture, Civil Engineering and Geodesy, Fascicule IV, Geotechnical Engineering, Vol. XLVI, Sofia.
- [2] Summary of Design & Analysis for Structure of the project "Tri Voditsi", RS, (2014). Sofia.
- [3] Menard, L., (1975). The Menard Pressuremeter: Interpretation and Application of the Pressuremeter Test Results to Foundation Design, Sols-Soils, No. 26, Paris.
- [4] Milev, N., (2013). A Simplified Soil-Single Footing Interaction Based on Winkler Foundation Model. International Conference on Earthquake Geotechnical Engineering (ICEGE2013), Istanbul.
- [5] Tsvetanov, T., Mihov, Y., Mihova, L., (2003-2004). Structural analysis and calculation model of multi-storey RC building. Annual of the University of Architecture, Civil Engineering and Geodesy, Fascicule IV, Geotechnical Engineering, Vol. XLI, Sofia.
- [6] Tanev, T., Kerenchev, N., Manolov, A., Dimitrov, H., (2012). Analyzing the displacements of a pile frame to determine its transverse load-bearing capacity. Proc. of the 22-nd European Young Geotechnical Engineering Conference, EYGEC2012.Göteborg, Sweden.
- [7] Mihova, L., (2014). Computing models for design of a road bridge over the Litani River in Lebanon at partially existence of soil ground under the bridge slab. Proc. 14th International Scientific Conference VSU'2014, Sofia.
- [8] Mihov, Y., Mihova, L., (2012). Behavior of pile retaining walls as abutments of temporary bridges during the construction of the Sofia metropolitan. Proc. of the Vth International Geomechanics Conference, Varna.
- [9] Mihova, L., Mihov, Y., (2012). Design considerations and computing models of the zero cycle construction of the Mladost trade center. Proc. 70th Anniversary UACEG Int. Jubilee Conference UACEG2012: Science & Practice, Vol. 3. Sofia.
- [10] Mihova, L., Zayakova, H., (2015). Landslide supporting pile structures realized in Bulgarian road network. First Scientific-Applied Conference with International Participation "Reinforced concrete and masonry structures theory and practice", Sofia.
- [11] Mihova, L., Tanev, T., (2015). Elastic and elastoplastic constitutive models in soil mechanics. Annual of the University of Architecture, Civil Engineering and Geodesy, Fascicule IV, Vol. XLVII, Sofia.
- [12] Kalcheva, I., Totsev, A., (2014). Rapid Impact Compaction for Civil Engineering Applications – Compaction and Improving the Ground for High Embankments, VIII Regionalen Kongres Georeks, Skopje, Macedonia.
- [13] Totsev, A., (2014). Application of Impact Compaction Method for Reduction of the Ground Settlement. VII National Conference on Roads with International Participation, Sunny Beach, Bulgaria.

- [14] Totsev, A., Kerenchev, N., Parvanov, B., (2019). Foundation and Soil Improvements of the Subsoil under St. Ivan Rilski University Hospital Building or the Construction of a Cyberknife System Bunker. XVII ECSMGE, Reykjavik.
- [15] Milev, N., (2019). Strengthening of the Raft Foundation of an Existing RC Building by Application of Jet-Grouting as Structural and Ground Improvement Technique. Eight Geotechnics in Civil Engineering Conference, Vrnjačka Banja, Serbia.
- [16] Ivanov, I., (2008). Regarding some dynamic characteristics of the soils and the liquefaction potential of sands in Sofia. Proceedings 8th International Scientific Conference SGEM, Vol. II, Varna, Bulgaria.
- [17] Milev, N., (2017). Small-Strain Behavior of Cohesionless Soils by Triaxial Tests and Dynamic Measurement Methods. Seventh Conf. Geotechnics in Civil Engineering Conference, Šabac.
- [18] Milev, N., (2018). Static and Dynamic Evaluation of Elastic Properties of Sofia Sand and Toyoura Sand by Sophisticated Triaxial Tests – Journal for Research of Material sand Structures (ISSN 2217-8139), Belgrade, Serbia.
- [19] Kostova, S., (2017). Improvement of methods for determining of soil parameters used in soil-structure interaction models – study of anchor foundations behavior. Dissertation for the degree of PhD, Todor Kableshkov University of Transport, Sofia.
- [20] Milev, N., (2016). A Macroelement for Consideration of the Soil-Shallow Foundation-Superstructure Interaction Effect in Nonlinear Seismic Analysis. Fifth International Conference on Earthquake Engineering and Engineering Seismology, Novi Sad, Serbia.
- [21] Eurocode 1: Actions on structures, Part 2: Traffic loads on bridges - EN 1991-2, (2003).
- [22] Sloan, S. W., (2013). Geotechnical Stability Analysis. *Geotechnique*, Vol. 63, No. 7.
- [23] Schanz, T., Vermeer, P. A., Bonnier, P. G., (1999). The hardening-soil model: Formulation and verification. In R. B. J. Brinkgreve, *Beyond 2000 in Computational Geotechnics*, Balkema, Rotterdam.
- [24] Plaxis, *Material Model Manual*, (2015).
- [25] Duncan, J. M., Chang, C. Y., (1970). Nonlinear analysis of stress and strain in soil. *Journal of the Soil Mechanics and Foundations Division, ASCE*, Vol. 96.
- [26] Eurocode 7: Geotechnical design, Part 1: Basic rules - EN 1997-1: 2005.
- [27] Frank, R. et al., (2004). *Designer's guide to Eurocode 7 EN 1997-1: Geotechnical Design – General Rules*. ICE Publishing.
- [28] Bond, A., Harris, H., (2008). *Decoding Eurocode 7*, Taylor & Francis, London.
- [29] Kostova, St., (2011). Principles for determining of the soil ground bearing capacity according to Eurocode 7. *Academic Journal Mechanics, Transport, Communications*, Issue 2, No./Article ID: 00494, <http://www.mtc-aj.com>.
- [30] Kostova, St., (2011). Designing methods of the soil bearing capacity according to Eurocode 7 and Bulgarian norms, *Academic Journal Mechanics, Transport, Communications*, Issue 3, No./ Article ID: 00550, <http://www.mtc-aj.com>.
- [31] Kostova, St., (2018). Analysis of the procedure for calculation of the soil ground bearing capacity according to Eurocode 7, *Academic Journal Mechanics, Transport, Communications*, Vol. 16, No.1.
- [32] Markov, I., Totsev, A., (2014). Influence of Dynamic Load on the Ground Anchors Bearing Capacity, 24 European Young Geotechnical Engineers conference EYGEC, UK.
- [33] Kerenchev N., Markov I., (2016). Determining the axial bearing capacity of pile based on common methods and comparison with pile load test. Proc. of the 3th International Conference VITGEO2016, Hanoi.
- [34] Duncan, J. M., (1996). State of the Art: Limit Equilibrium and Finite-Element Analysis of Slopes. *Journal of Geotechnical Engineering*, Vol. 122, No. 7.
- [35] Kerenchev, N., (2015). Analysis of seismic slope stability and deformations. Dissertation for the degree of PhD, University of Architecture, Civil Engineering and Geodesy, Sofia.

ABSTRACT

COMPARATIVE ANALYSIS OF DIFFERENT FINITE ELEMENT MODELS OF THE SOIL-BURIED ARCH BRIDGE INTERACTION

Konstantin KAZAKOV
Lena MIHOVA
Doncho PARTOV

Comparative analysis is made of different finite element models of a buried arch bridge which is constructed from precast concrete elements. Two static schemes of the bridge structure are considered – a static scheme of rigid connection between all structure elements and a static scheme of hinged connection between the lateral retaining walls and the vault plate. The modeling is carried out by the Plaxis 2D software. Two nonlinear constitutive models for soil materials are used – linear elastic-perfectly plastic Mohr-Coulomb's model and advanced elastic-plastic Hardening-Soil model. The Hardening-Soil model is a state-of-the-art scientific achievement which approximates the mechanical behavior of the soil materials with high accuracy using 15 material parameters. Two types of finite elements are used for modeling of the bridge structure: beam and plate elements. The soil-structure contacts are modeled by interface elements of thickness closed to zero. Traffic loads on a road situated above the bridge are assumed according to the model LM1 of Eurocode 1. Mechanical behavior of the bridge is studied by analyses of states in construction and service periods. Analysis of the ground bearing capacity is performed using the shear strength reduction technique.

Key words: arch bridge, soil-structure interaction, hinge connection, rigid connection, plane strain, finite element modeling, constitutive model, traffic loading, Eurocode

SAŽETAK

KOMPARATIVNA ANALIZA MODELA INTERAKCIJE TLA I LUČNOG MOSTA SA ZEMLJANOM ISPUNOM ZASNOVANIH NA MKE

Konstantin KAZAKOV
Lena MIHOVA
Doncho PARTOV

U radu su uporedno analizirani različiti modeli ukopanog lučnog mosta izrađenog od montažnih betonskih elemenata, koji su zasnovani na MKE. Razmatrane su dve statičke šeme konstrukcije mosta - krute veze između svih elemenata konstrukcije i zglobne veze između bočnih potpornih zidova i zasvedena ljuska. Modeliranje je izvedeno primenom softvera Plaxis 2D. Dva nelinearna konstitutivna modela su korišćena za materijale tla - linearni elasto-plastični Mohr-Coulombov model i unapređeni elasto-plastični model očvršćavanja tla. Model očvršćavanja tla predstavlja visoki stepen naučnog dostignuća kojim se aproksimira mehaničko ponašanje tla sa visokom tačnošću, primenom 15 parametara materijala. Korišćene su dve vrste konačnih elemenata za modeliranje konstrukcije mosta: elementi greda i ploča. Kontakt tla i konstrukcije je modeliran pomoću veoma tankih kontaktnih elemenata. Pretpostavlja se saobraćajno opterećenje na mostu prema modelu LM1 iz EN1991. Mehaničko ponašanje mosta proučeno je analizom stanja konstrukcije i perioda korišćenja. Analiza nosivosti tla izvedena je korišćenjem tehnikom redukcije smičuće čvrstoće tla.

Ključne reči: lučni most, interakcija tla i konstrukcije, zglobna veza, kruta veza, ravne dilatacije, MKE modeliranje, konstitutivni modeli, saobraćajno opterećenje, Evrokod

CORROSION-PREVENTIVE COMPOUNDS FOR INCREASING THE DURABILITY OF PREINSULATED PIPES

JEDINJENJA ZA SPREČAVANJE KOROZIJE I ZA POVEĆANJE TRAJNOSTI PRETHODNO IZOLOVANIH CEVI

Aizada KALMAGAMBETOVA
Tatyana BOGOYAVLENSKAYA

ORIGINALNI NAUČNI RAD
ORIGINAL SCIENTIFIC PAPER
UDK:697.433:621.643.2]:620.193.5
doi:10.5937/GRMK1904029K

1 INTRODUCTION

In the construction of directly buried hot water networks laying, pipes in thermal insulation made of polyurethane foam with a waterproof outer casing of polyethylene currently occupy a leading place. The most significant advantages of pipes in polyurethane foam (PUR) insulation include: the tightness of the outer waterproof casing that prevents water from entering the thermal insulation layer; equipping pipelines with a measuring wires for surveillance systems; manufacturability in the factory, and, consequently, product quality - as a guarantee of durability and service life of the heating network. From the experience in the use of preinsulated bonded pipe systems in Europe, in particular in Germany and Denmark, it is known that the service life of such pipelines can reach up to 50 years. This is stated in most scientific papers on the study of pipes in polyurethane foam insulation (PUR) [1-7].

One of the key parameters affecting the durability and performance of the pipeline in polyurethane foam insulation (PUR) is the adhesion of polyurethane thermal insulation to a steel service pipe and to a waterproof outer casing of polyethylene. This is explained by the fact that the pipeline of the heat network under operating conditions (for example, operation pressure 1.6 MPa, operation temperature 130⁰C) experiences thermal

movements as a result of thermal expansion of materials. In this case, the steel service pipe, polyurethane thermal insulation and waterproof outer casing of polyethylene should work as a unit and form a rigid structure.

In the majority of works on the study of adhesion at the edge "Service steel pipe- Polyurethane thermal insulation", as well as "Waterproof outer casing of polyethylene - Polyurethane thermal insulation", for example, the problems of creating a test centre with the aim of testing pipe specimens for axial and tangential shear, allowing to determine the amount of adhesion of PUR, are reviewed in work [8]; the authors proposed the usage of plasma jets of polyethylene processing to improve the adhesive properties in reference to polyurethane foam in work [9].

The importance of the PUR adhesion indicator in terms of shear strength in the tangential direction is that it characterizes the ability of a rigid structure to transmit the force of thermal expansion of a steel service pipe to the outer casing of polyethylene. With sufficient structural strength, sliding occurs along "Outer casing of polyethylene – Ground" edge, and the pipe with insulation moves as a unit [10, 11].

It should be noted that the violation of the integrity of the insulation design at the edge «Waterproof outer casing of polyethylene - Polyurethane thermal insulation» leads to delamination of the waterproof casing of polyethylene from the thermal insulation layer, which, in turn, leads to damage to the insulation as a whole. In the case when the waterproof outer casing of polyethylene separated, when installing the pipe joints at the stage of checking the muff joints, it is not able to withstand the standard pressure of 0.5 bar for 5 minutes [11]. The result of damage to the muff joints is loss of tightness and wetting of thermal insulation, resulting in

Aizada Kalmagambetova, candidate of technical sciences, docent of Karaganda State Technical University, Karaganda, N. Nazarbayeva 56, Kazakhstan
Tatyana Bogoyavlenskaya, PhD Student of Karaganda State Technical University, Karaganda, N. Nazarbayeva 56, Kazakhstan
e-mail: t.bogoyavlenskaya88@gmail.com

an increase in heat loss, corrosion of the steel service pipe and a decrease in the insulation resistance of the measuring wires for surveillance systems.

With this approach, first of all, difficulties arise with pipeline waterproofing of the heating network. Currently, outer casing made of high density polyethylene (HDPE) are used as waterproofing of polyurethane foam thermal insulation of pipes manufactured in the factory, since their advantages are sufficient resistance to cracking and mechanical stress; resistance to ultraviolet radiation, high density, high strength, easy processability [12, 13].

Despite the advantages of a waterproof outer casing of polyethylene, depending on the diameter of the pipes, the adhesion rate at the "Waterproof outer casing of polyethylene - Polyurethane thermal insulation" edge decreases. This is due to the complexity of pipes manufacture using the "pipe-in-pipe" technology. Thermal insulation and waterproofing, polyurethane foam and waterproof outer casing of polyethylene are different in their resistance to materials and chemical composition. In this regard, corona effect technology is usually applied, i.e. surface processing of the outer casing of polyethylene by corona discharge; the formulation of foam components according to the chemical composition and ratio is selected; mechanical processing of the surface of the steel service pipe is made; temperature conditions in the factory is withstood; air-tight insulation plugs and other nuances of the technology for the production of preinsulated bonded pipe systems are used to improve the adhesion at the factory.

In order to extend the life of preinsulated bonded pipe systems used as a building material for directly buried hot water networks from standard 30 years to 50 years or more, in this work it is proposed to use corrosion-preventive compound from polyurea as a waterproof coating. Polyurea is used in construction as waterproofing of foundations, wells, structural elements of bridges, industrial floor coating [14-19].

2 METHODS

We investigated polyurea as a pipe waterproof in polyurethane thermal insulation. The following materials were used as waterproof materials during the tests: high density polyethylene, recommended for use for protecting pipelines of heating networks and polyurea.

To conduct tests for strength at tangential shear at a temperature of $(23 \pm 2)^\circ\text{C}$, an installation at the pipe insulation plant has been developed that allows testing pipes with a diameter of up to 219 mm inclusive, shown in the photo, Figure 1.

The principle of operation of the installation is to measure the tangential shear of the insulation relative to the steel service pipe, or waterproof coating relative to the layer of polyurethane foam. A specimen of a pipe fragment is motionlessly welded to a metal frame. A tangential load was applied to the waterproof of the pipe using two levers 1000 mm long, located coaxially horizontally on both sides of the sheath. The speed of the load application to the ends of the levers was 25 mm/min. The unwinding in the tangential direction occurs until the first signs of delamination appear along the boundaries of "Service steel pipe- Polyurethane

thermal insulation" or "Waterproof outer casing of polyethylene - Polyurethane thermal insulation".

At this installation, tests of specimens of steel service pipe fragments were carried out. Fragments of a pipe with an outer diameter of 57 mm, a wall thickness of 4.5 mm, in polyurethane thermal insulation, waterproof outer casing of polyethylene vs. with polyurea coating with a length equal to 0.75 of the diameter of the steel pipe were taken as specimens, the Photos are shown in Figure 2.



Figure 1 - Installation for determining the shear strength in the tangential direction



Figure 2 - Specimens of the pipe. On the left: in outer casing of polyethylene. On the right: with polyurea coating

In the manufacture of specimens in the factory, steel service pipes were preliminarily cleaned from corrosion products in a sandblasting installation; PUR components were poured into the space between the steel service pipe and the outer casing of polyethylene on a high-pressure filling machine. The thickness of the thermal

insulating layer was 31.5 mm. The thickness of the outer casing of polyethylene was 2.5 mm. The thickness of the polyurea coatings was 1 mm; 1.5 mm and 2.5 mm, respectively.

The shear strength in the tangential direction τ_{tan} , MPa, is calculated from the following formula:

$$\tau_{\text{tan}} = \frac{2 \cdot l \cdot F_{\text{tan}}}{\pi \cdot d^2 \cdot L} \quad (1)$$

where F_{tan} - the tangential force, in N;

L - length of specimen, in mm;

d - outside diameter of the service pipe, in mm;

l - length of each lever, in mm

In the process of testing, the effect of corrosion-preventive compounds of polyurea on the adhesion strength of polyurethane foam thermal insulation with corrosion-preventive compound was determined. Determination of the adhesion strength of polyurethane foam thermal insulation with corrosion-preventive compound was carried out 10 days after the manufacture of the specimens and 180 days after their storage in an unheated room.

The influence of an aggressive environment was determined, as well as the behaviour of the waterproof

composition of polyurea in the ground according to the procedure described in [20]. For the test, a simulated environment of the actual conditions for directly buried hot water networks was created. The basis is pure sand with a moisture content of over 0.5% and a grain size of 4 mm. A specimen pipe fragment was installed in a sandbox. Installation diagram in Figure 3.

Hot water circulated through the fragment of a steel pipe in insulation (specimen) for 24 hours with parameters $120 \pm 20\text{C}$. The box was filled with sand 1 meter high (imitation of ground pressure 18 kN/ m^2). The axial movement of the pipe fragment in insulation by 75 mm was performed at a speed of 10 mm / min. Thus, 100 cycles were performed, where one cycle is considered to be moving forward and backward.

The thermal conductivity of the pipe fragment was determined according to the procedure presented in [11]. For this purpose, an experimental setup was made, shown in Figure 4. It is a steel service pipe with the outer diameter of 57 mm and the length of 1 meter. A heating element mounted on a fire-resisting material was placed inside the pipe. The steel pipe was heated to a temperature of 50°C . Indications of thermal conductivity were measured by a wattmeter and thermocouples.

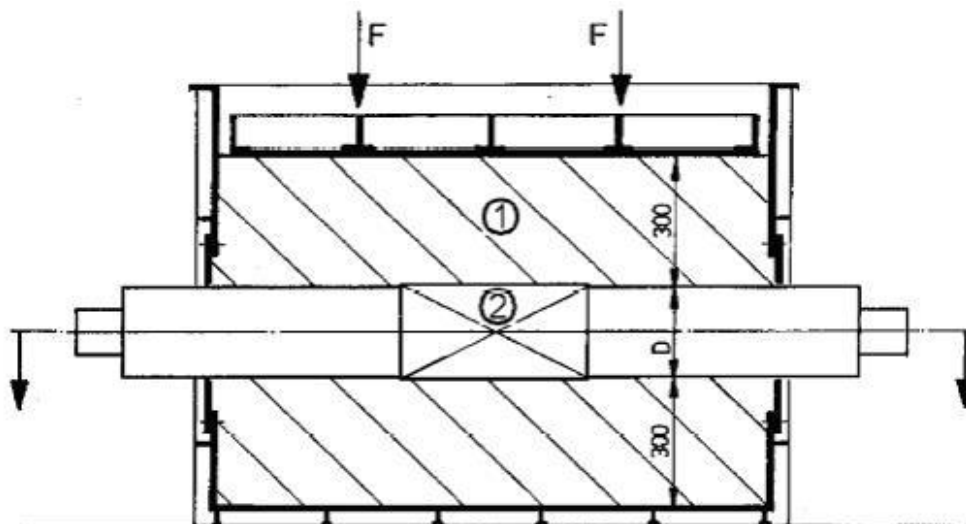


Figure 3 - Diagram of a test box with sand. 1 - sand; 2 - steel service pipe fragment in insulation



Figure 4 - Experimental setup for thermal conductivity measuring

3 RESULTS AND DISCUSSION

The test results of determining the specimens shear strength are presented in table 1.

A comparative analysis of the fracture pattern of the specimens showed that there is fracture along the edge "Waterproof outer casing of polyethylene - Polyurethane thermal insulation", adhesion of polyurea and polyurethane thermal insulation has better performance than that of outer casing of polyethylene and polyurethane thermal insulation. The test results further confirm that much attention needs to be paid to the strength of the joint between structure components.

The fracture along the edge "Waterproof outer casing of polyethylene - Polyurethane thermal insulation" is the result of insufficient adhesion of polyurethane foam to the outer casing material - polyethylene. This is due to differences in the chemical structure of the adhesion of polyurethane foam and polyethylene, and the adhesion of polyurethane foam to unprocessed polyethylene is practically absent. The adhesion is also negatively affected by the long filling time of the structure (the so-called late filling), as far as in this case a foam with a low content of functional groups that are capable of forming adhesive bonds comes into contact with polyethylene.

Polyurea coatings with a thickness of 1 mm have the best bonding. Figure 5 shows a graph of the dependence of the tangential shear strength on the wall thickness of the coating.

The test results of the specimens for behaviour in an aggressive environment are presented in table 2.

Test results show that specimens with a waterproofing polyurea coating also sustain 100 cycles. This means that polyurea, according to its technical characteristics, can be used in an aggressive environment, such as sand, and does not wear out. This indicator is important because of the real movements of the pipeline in the ground for directly buried hot water networks during thermal expansion.

To compare the heat loss through the structure, a calculation was carried out, taking into account the results of measuring the thermal conductivity of the pipe structure with insulation, determined at the experimental installation.

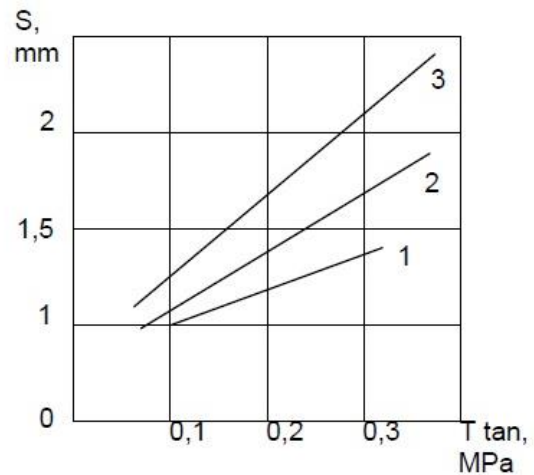


Figure 5 - Dependence of the tangential shear strength indicator on the coating wall thickness (for polyurea): 1 - for a specimen with a wall thickness of 1 mm; 2 - for a specimen with a wall thickness of 1.5 mm; 3 - for a specimen with a wall thickness of 2 mm

The calculations of the energy characteristics of water heating networks by the "heat loss" indicator for pipelines for directly buried hot water networks are presented below. For the initial data for the calculation, the following indicators are taken in table 3.

Table 1. Test results for determining the adhesion of polyurethane foam thermal insulation with waterproof material

specimen party a	Shear strength in the tangential direction τ_{tan} , MPa, (average) after 10 days of storage after pouring the specimen in outer casing of polyethylene	Shear strength in the tangential direction τ_{tan} , MPa, (average) after 10 days of storage after coating the specimen with a polyurea
1	0,2	0,3
2	0,23	0,35
3	0,25	0,4

Table 2. Test results of specimens for behaviour in an aggressive environment

specimen party a	Indicator	A specimen of a steel service pipe with outer diameter of 57 mm in polyurethane foam insulation and outer casing of polyethylene	A specimen of a steel service pipe with outer diameter of 57 mm in polyurethane foam insulation with a waterproof coating of polyurea
1	Sustain of 100 cycles	Sustained	sustained

Table 3. Characteristic Values

Indicator	Specimen of a pipe in polyethylene sheath	Specimen of a pipe in a polyurea sheath
Steel service pipe outer diameter, in mm	57	57
Wall thickness of steel service pipe, mm	4,5	4,5
Insulation thickness on the supply and return pipes, mm	78,9	78,9
The outer diameter of the casing, mm	125	122
Thermal conductivity of insulation material λ_i , W/m \cdot K	0,033	0,022
Thermal conductivity of casing λ_{HDPE} , W/m \cdot K	0,43	0,21
Thermal conductivity of ground λ_{ground} , W/m \cdot K	1,2	1,2
The distance between the pipelines, mm	250	250
Depth of laying to the axis of the pipeline (directly buried) H_m , mm	862,5	861
The distance between the axes of the pipelines, a , m	375	372
Annual average temperature of the supply pipeline, V_s , $^{\circ}$ N	120	120
Annual average temperature of return pipeline V_r , $^{\circ}$ N	60	60
Annual average temperature of ground, V_g , $^{\circ}$ N	10	10

The thermal resistance of the pipe [1 / KR] was calculated in accordance with the equation for multilayer pipes according to the formulas presented in [11] as follows:

$$\frac{1}{KR} = \frac{1}{2 \cdot \pi \cdot \lambda_i} \cdot \ln\left(\frac{Di}{da}\right) + \frac{1}{2 \cdot \pi \cdot \lambda_{HDPE}} \cdot \ln\left(\frac{Da}{Di}\right) + \frac{1}{2 \cdot \pi \cdot \lambda_{ground}} \cdot \ln\left(\frac{4 \cdot Hm}{Da}\right) + \frac{1}{2 \cdot \pi \cdot \lambda_{ground}} \cdot \ln\left(1 + \frac{2 \cdot Hm}{a^2}\right) \quad (2)$$

Here, \ln is the natural logarithm, Da is the outer diameter of the casing, mm; Di is the inner diameter of the casing, mm; da is the outer diameter of the steel service pipe, mm; di is the inner diameter of the steel service pipe, mm.

Heat loss per 1 meter of pipe was calculated:

$$QRT = 2 \cdot KR \cdot VM \quad (3)$$

Here, QRT is the heat loss, W/m; KR - heat flux, W; VM - annual average temperature of the pipeline, $^{\circ}$ C.

The annual average temperature of the pipeline was calculated by the formula:

$$VM = \frac{V_s + V_r}{2} - V_{ground} \quad (4)$$

Here, V_s - is the annual average temperature of the supply pipeline, $^{\circ}$ C; V_r - annual average return pipeline temperature, $^{\circ}$ C; V_g - annual average ground temperature, $^{\circ}$ C.

The calculation was made for the specimen pipe in polyurethane foam insulation and outer casing of polyethylene:

$$\frac{1}{KR} = \frac{1}{2 \cdot 3,14 \cdot 0,033} \cdot \ln\left(\frac{125}{57}\right) + \frac{1}{2 \cdot 3,14 \cdot 0,43} \cdot \ln\left(\frac{125}{120}\right) + \frac{1}{2 \cdot 3,14 \cdot 1,2} \cdot \ln\left(\frac{4 \cdot 862,5}{125}\right) + \frac{1}{2 \cdot 3,14 \cdot 1,2} \cdot \ln\left(1 + \frac{2 \cdot 862,5}{375^2}\right) = 4,03$$

$$\frac{1}{KR} = 4,03$$

$$QRT = 2 \cdot 0,248 \cdot 80 = 39,68W / m$$

$$VM = \frac{120 + 60}{2} - 10 = 80^{\circ}C$$

The similar calculation was made for a pipe specimen with waterproof coating of polyurea:

$$\frac{1}{KR} = \frac{1}{2 \cdot 3,14 \cdot 0,022} \cdot \ln\left(\frac{122}{57}\right) + \frac{1}{2 \cdot 3,14 \cdot 0,21} \cdot \ln\left(\frac{122}{120}\right) + \frac{1}{2 \cdot 3,14 \cdot 1,2} \cdot \ln\left(\frac{4 \cdot 861}{122}\right) + \frac{1}{2 \cdot 3,14 \cdot 1,2} \cdot \ln\left(1 + \frac{2 \cdot 861}{372^2}\right) = 5,95$$

$$\frac{1}{KR} = 5,95$$

$$QRT = 2 \cdot 0,168 \cdot 80 = 26,88W / m$$

As a result of numerical experiments with varying the thickness of waterproofing, it was found that the waterproofing thickness of 1 mm polyurea is optimal, providing a low amount of heat loss, as in the case of a 2.5 mm thick casing of polyethylene for a test specimen

of a 57 mm outer diameter steel service pipe. This is evidenced by a comparative analysis of the results of calculations on the indicator of "heat loss" of pipes with waterproofing from polyurea and polyethylene, presented in table 4.

Table 4. A comparative analysis of pipe specimens on "Heat loss" indicator

specimen party a	Indicator	A specimen of a steel service pipe with outer diameter of 57 mm in polyurethane foam insulation and outer casing of polyethylene	A specimen of a steel service pipe with outer diameter of 57 mm in polyurethane foam insulation with a waterproof coating of polyurea
1	The coefficient of thermal conductivity, W/m*K	0,033	0,022
2	Heatloss, W/m	39,68	26,88
3	Assessment of efficiency		30% less of heat loss per meter of a pipe

4 CONCLUSIONS

1. A comparative analysis of the nature of the demolition of the specimens showed that there is demolition along the edge "Waterproof outer casing of polyethylene - Polyurethane thermal insulation".

2. The strength properties of individual elements fail to give a complete picture of the strength and performance of the structure of pre-insulated pipes as a whole.

3. Extending the life of pipes for hot water networks from standard 30 years to 50 years or more is possible when corrosion-preventive compounds made of polyurea are used as a waterproof coating.

4. It is possible to reduce the wall thickness of a waterproofing coating based on polyurea from a standard of 2.5 mm to 1 mm.

5. The use of polyurea as waterproof coating for pipes with thermal insulation from polyurethane foam is possible.

6. The use of polyurea as waterproof coating for pipes with thermal insulation from polyurethane foam can reduce heat loss per meter by 30%.

5 REFERENCES

[36] Slepchenok V.S., Petrakov G.P. Increasing the energy efficiency of thermal insulation of heat network pipelines in Northern and Northeastern regions of Russia // Magazine of Civil Engineering. 2011. 4(22). Pp. 26-32. DOI: 10.5862/MCE.22.4.

[37] Turski, Michał, Sekret, Robert. Buildings and a district heating network as thermal energy storages in the district heating system. Energy and Buildings. 2018. Vol.179. Pp. 49-56. DOI: 10.1016/J.ENBUILD.2018.09.015

[38] Kayfeci, Muhammet. Determination of energy saving and optimum insulation thicknesses of the heating piping systems for different insulation materials. Energy and Buildings. 2014. Vol.69. Pp. 278-284. DOI: 10.1016/J.ENBUILD.2013.11.017

[39] Petrakov G.P. The service life of plastic pipes in polyurethane foam insulation used for heating systems // Magazine of Civil Engineering. 2012. No 3 (29). Pp. 54-62. 10.5862 / MCE.29.7.

[40] Wang, Hai, Meng, Hua, Zhu, Tong. New model for onsite heat loss state estimation of general district heating network with hourly measurements. Energy Conversion and Management. 2018. Vol.157. Pp. 71-85. DOI: 10.1016/J.ENCONMAN.2017.11.062

[41] Chopra, K., Tyagi, V.V., Pandey, A.K., Sari, Ahmet. Global advancement on experimental and thermal analysis of evacuated tube collector with and without heat pipe systems and possible applications. Applied Energy. 2018. Vol.228. Pp. 351-389. DOI: 10.1016/J.APENERGY.2018.06.067

[42] Danielewicz, J., Śniechowska, B., Sayegh, M.A., Fidorów, N., Jouhara, H. Three-dimensional numerical model of heat losses from district heating network pre-insulated pipes buried in the ground. Energy. 2016. Vol.108. Pp. 172-184. DOI:10.1016/J.ENERGY.2015.07.012

[43] Korolev I.A., Petrakov G.P. Creation of a testing center for checking the quality of polyurethane foam insulation of pre-insulated pipelines used in heat supply systems // Magazine of Civil Engineering. 2010. No. 1 (11). Pp. 23-25. DOI: 10.18720 / MCE.11.6.

[44] Yu. S. Akishev, A. V. Petryakov, N. I. Trushkin, V. A. Ustyugov. Improving of the adhesion of polyurethane foam to the low-pressure polyethylene processed by a plasma jet at the atmospheric pressure // Applied Physics. 2017. No. 5. Pp. 20-24.

[45] JörgKauschat. Patent EP2166269B2. Method for connecting clad pipes. Patent EP2166269B2 // EuropeanPatentOffice. Germany. isoplusFernwärmetechnik GmbH. 2017

[46] DIN EN 253-2013. District heating pipes – Preinsulated bonded pipe systems for directly buried hot water networks – Pipe assembly of steel service pipe, polyurethane thermal insulation and outer casing of polyethylene.

- [47] DIN EN 448-2009. District heating pipes – Preinsulated bonded pipe systems for directly buried hot water networks – Fitting assemblies of steel service pipes, polyurethane thermal insulation and outer casing of polyethylene.
- [48] Sadr-Al-Sadati, Syed Ali, JaliliGhazizadeh, Mohammadreza. The experimental and numerical study of waterleakage from High-Density Polyethylene pipes at elevated temperatures. *Polymer Testing*. 2019. Vol.74. Pp. 274-280. DOI: 10.1016/J.POLYMERTESTING.2019.01.014
- [49] Iqbal N, Sharma P, Kumar D, Roy P. Protective polyurea coatings for enhanced blast survivability of concrete. *Construction and Building Materials*. 2018. Vol. 175. Pp: 682-690. DOI: 10.1016/J.CONBUILDMAT.2018.04.204
- [50] Elnaggar E, Elsokkary T, Shohide M, El-Sabbagh B, Abdel-Gawwad H. Surface protection of concrete by new protective coating. *Construction and Building Materials*. 2019. Vol. 220. Pp: 245-252. DOI: 10.1016/J.CONBUILDMAT.2019.06.026
- [51] Hou H, Chen C, Cheng Y, Zhang P, Tian X, et. al. Effect of structural configuration on air blast resistance of polyurea-coated composite steel plates: Experimental studies. *Materials & Design*. 2019. Vol. 182. Pp: 108049. DOI: 10.1016/J.MATDES.2019.108049
- [52] He L, Attard T, Zhou H, Brooks A. Integrating energy transferability into the connection-detail of coastal bridges using reinforced interfacial epoxy-polyurea reaction matrix composite. *Composite Structures*. 2019. Vol. 216. Pp: 89-103. DOI: 10.1016/J.COMPSTRUCT.2019.02.094
- [53] GairJ, Lambeth R, Cole D, Lidston D, Stein I, et. al. Strong process-structure interaction in stoveable poly(urethane-urea) aligned carbon nanotube nanocomposites. *Composites Science and Technology*. 2018. Vol. 166. Pp: 115-124. DOI: 10.1016/J.COMPSCITECH.2018.02.011
- [54] Zhang F, Ju P, Pan M, Zhang D, Huang Y, et. al. Self-healing mechanisms in smart protective coatings: A review. *Corrosion Science*. 2018. Vol. 144. Pp: 74-88. DOI: 10.1016/J.CORSCI.2018.08.005
- [55] DIN EN 489-2009. District heating pipes - Preinsulated bonded pipe systems for directly buried hot water networks - Joint assembly for steel service pipes, polyurethane thermal insulation and outer casing of polyethylene.

ABSTRACT

CORROSION-PREVENTIVE COMPOUNDS FOR INCREASING THE DURABILITY OF PREINSULATED PIPES

Aizada KALMAGAMBETOVA
Tatyana BOGOYAVLENSKAYA

The adhesion of polyurethane thermal insulation to a waterproof outer casing of polyethylene in the construction of preinsulated bonded pipe systems used as a building material for directly buried hot water networks is investigated. In order to extend the life of pipes for hot water networks from standard 30 years to 50 years or more, it is proposed to use polyurea as a waterproof coating. It is proposed to determine the adhesion strength of thermal insulation with a waterproof outer casing for shear in the tangential direction at the edge "Waterproof outer casing of polyethylene - Polyurethane thermal insulation". Test results are presented. The results of calculations of the heat losses of the preinsulated pipe construction are presented. The testing results of the behaviour of polyurea coating in the ground are presented. Conclusions are drawn about the possibility of using polyurea as a waterproof coating for preinsulated bonded pipe systems for directly buried hot water networks.

Keywords: Building Materials, Durability, Mechanical Properties, Energy Efficiency, Energy Conservation, Heating, Heat Storage, Corrosion, Thermal Insulation, Polymers

САЖЕТАК

ЈЕДИЊЕЊА ЗА СПРЕЧАВАЊЕ КОРОЗИЈЕ И ЗА ПОВЕЋАЊЕ ТРАЈНОСТИ ПРЕТХОДНО ИЗОЛОВАНИХ ЦЕВИ

Аизада КАЛМАГАМБЕТОВА
Татуана БОГОУАВЛЕНСКАЈА

Испитује се пријањање полиуретанске топлотне изолације на водоотпорно спољно кућиште од полиетилена у конструкцији преинизолираних цевних система који се користе као грађевински материјал за директно закопане топоводне мреже. Да би се продужио век цеви за вреловодне мреже са стандардних 30 на 50 или више година, предлаже се употреба полиурее као водоотпорног премаза. Предлаже се утврђивање чврстоће лепљења топлотне изолације водонепропусним спољним кућиштем за смицање у тангенцијалном смеру на ивици „Водоотпорно спољно кућиште од полиетилена - полиуретанска топлотна изолација“. Представљени су резултати испитивања. Приказани су резултати израчуна топлотних губитака предизоловане цеви. Представљени су резултати испитивања понашања полиуреепремаза у земљи. Извучени су закључци о могућности употребе полиурее као водоотпорног премаза за преизолиране цеви за цевоводе за директно закопане топоводне мреже.

Кључне речи: грађевински материјали, издржљивост, механичка својства, енергетска ефикасност, уштеда енергије, грејање, складиштење топлоте, корозија, топлотна изолација, полимери

NUMERIČKA SIMULACIJA PONAŠANJA UZORAKA OD LAKOAGREGATNOG BETONA U SLUČAJEVIMA LABORATORIJSKOG ISPITIVANJA

NUMERICAL SIMULATION OF THE BEHAVIOUR OF THE LIGHTWEIGHT CONCRETE SPECIMEN IN THE LABORATORY TESTING

Vladimir ŽIVALJEVIĆ
Dušan KOVAČEVIĆ
Ivan LUKIĆ
Vlastimir RADONJANIN

ORIGINALNI NAUČNI RAD
ORIGINAL SCIENTIFIC PAPER
UDK:691.32:620.178.1
doi:10.5937/GRMK1904037Z

1 UVOD

Beton je veštački kompozitni građevinski materijal dobijen očvršćavanjem mešavine veziva, vode, agregata (i u mnogim slučajevima različitih dodataka) i već duže od jednog veka predstavlja najčešće korišćen građevinski materijal. Budući da godišnja proizvodnja betona premašuje količinu od deset milijardi tona, sve je značajnija upotreba alternativnih materijala. Jedna od mogućnosti upotrebe alternativnih komponenata jeste upotreba lakog agregata, umesto dela ili celokupne količine običnog agregata, kao punioca u betonskoj smeši. Iako je heterogen, za svakodnevne potrebe projektovanja građevinskih konstrukcija, beton se smatra homogenim materijalom. Tretiranje betona kao homogenog kontinuuma opravdano je kada se beton nalazi u elastičnoj fazi rada, što u najvećem broju situacija i jeste slučaj budući da su konstrukcije u izuzetno retkim slučajevima opterećene graničnim opterećenjima [8]. Napregnute graničnim opterećenjem, armiranobetonske konstrukcije

1 INTRODUCTION

Concrete is an artificial composite building material obtained by curing the mixture of the binders, water, aggregates (and in many cases various additives) and has been the most commonly used building material for over a century. Since the annual production of the concrete exceeds ten billion tonnes, the use of the alternative materials is of increasing importance. One possibility of using alternative components would be to use a lightweight aggregate instead of a part or the whole amount of a conventional aggregate as a filler in a concrete mixture. Although considered as heterogeneous, for everyday design purposes, concrete is considered to be a homogeneous material. The treatment of concrete as a homogeneous continuum is justified when the concrete is in an elastic phase of operation, which in the most situations is the case, since structures are loaded by the ultimate loads in extremely rare cases [8]. Loaded by the ultimate load reinforce

Vladimir Živaljević, mast. inž. građ. – asistent, Fakultet tehničkih nauka Univerziteta u Novom Sadu, Trg Dositeja Obradovića 6, 21000 Novi Sad, e-mail: zivaljevic.vladimir@uns.ac.rs
Profesor dr Vlastimir Radonjanin, dipl. inž. građ. Fakultet tehničkih nauka Univerziteta u Novom Sadu, Trg Dositeja Obradovića 6, 21000 Novi Sad, e-mail: radonv@uns.ac.rs
Docent dr Ivan Lukić, dipl. inž. građ. Fakultet tehničkih nauka Univerziteta u Novom Sadu, Trg Dositeja Obradovića 6, 21000 Novi Sad, e-mail: lookic@uns.ac.rs
Profesor dr Dušan Kovačević, dipl. inž. građ. Fakultet tehničkih nauka Univerziteta u Novom Sadu, Trg Dositeja Obradovića 6, 21000 Novi Sad, e-mail: dusan@uns.ac.rs

Vladimir Zivaljevic, MSc in Civil Engineering, University of Novi Sad, Faculty of Technical Sciences, Trg Dositeja Obradovica 6, 21000 Novi Sad, e-mail: zivaljevic.vladimir@uns.ac.rs
Vlastimir Radonjanin, Prof. PhD in Civil Engineering, University of Novi Sad, Faculty of Technical Sciences, Trg Dositeja Obradovica 6, 21000 Novi Sad, e-mail: radonv@uns.ac.rs
Ivan Lukic, Asistant prof. PhD in Civil Engineering, University of Novi Sad, Faculty of Technical Sciences, Trg Dositeja Obradovica 6, 21000 Novi Sad, e-mail: lookic@uns.ac.rs
Dusan Kovacevic, Prof. PhD in Civil Engineering, University of Novi Sad, Faculty of Technical Sciences, Trg Dositeja Obradovica 6, 21000 Novi Sad, e-mail: dusan@uns.ac.rs

mogu da dožive lom na nekoliko različitih načina: pucanje (prskanje), drobljenje i otpadanje betona, tečenje i izvlačenje zategnutih šipki armature, te tečenje i izvijanje pritisnutih šipki armature. Radi što bolje opisivanja i sagledavanja ponašanja armiranobetonskih konstrukcija pri lomu, neophodne su napredne numeričke simulacije zasnovane na mehanici kontinuuma. Ovom zahtevu u suprotnosti stoje računarske mogućnosti i vreme koje na raspolaganju imaju inženjeri, te je upotreba pojednostavljenih modela, kako konstrukcije, tako i ponašanja materijala, uobičajena u praksi.

Veliki broj istraživanja urađeno je u prethodnih nekoliko godina, kako u pogledu razvika novih, sveobuhvatnijih numeričkih modela materijala betona, tako i u pogledu eksperimentalnog ispitivanja lakoagregatnog betona. Numeričko modeliranje pojave plastičnosti betona, te razvika oštećenja moguće je sprovesti upotrebom CDP (concrete damage plasticity) modela materijala. Ovaj model materijala uvodi pretpostavku da su dva glavna mehanizma loma betona pojava prslina usled zatezanja i drobljenje usled pritiska. Ovaj model materijala predstavljen je u [4], a tokom prethodne decenije doživio je brojna unapređivanja u pogledu određivanja varijabli neophodnih za njegovo definisanje [2, 5, 9]. Neka od značajnijih eksperimentalnih ispitivanja lakoagregatnog betona data su u [7, 8, 10].

U ovom radu predstavljen je koncept CDP modela materijala i urađena je numerička simulacija ponašanja uzoraka od lakoagregatnog betona u slučajevima laboratorijskog ispitivanja. Razmatrane su dve konfiguracije ispitivanja: određivanje čvrstoće betona pri pritisku na beotnskoj kocki stranice 150 mm i određivanje statičkog modula elastičnosti betona na betonskom cilindru prečnika 150 mm i visine 300 mm. S ciljem obuhvata realnog stanja i ponašanja materijala, u ovom radu je korišćen CDP model materijala betona.

2 MODEL PONAŠANJA BETONA

Ponašanje materijala pri lomu usled napona pritiska i napona zatezanja može se opisati na različite načine. U slučaju zatezanja, dolazi do pojave prslina, što se na dijagramu napon-deformacija ogleda u naglom padu krutosti u materijalu, a potom i padu krutosti rasterećujuće grane dijagrama. U slučaju napona pritiska, dolazi do povećanja zapremine materijala, drobljenja i klizanja unutar materijala. U kombinovanim stanjima napona, lom obično zavisi od odnosa između glavnih napona [2].

Nelinearno ponašanje betona je u ovom radu opisano korišćenjem CDP modela, implementiranog u softver Abaqus[®]. Ovaj model nelinearnog ponašanja materijala prvenstveno je namenjen modeliranju problema u kojima je moguća pojava plastičnosti betona, međutim, njime je moguće modelirati i druge kvazi-krte materijale. Glavna pretpostavka jeste da su dva glavna mehanizma loma betona pojava prslina usled zatezanja i drobljenje usled pritiska [1]. Pretpostavka ponašanja materijala usled jednoosnog napona pritiska i zatezanja data je na slici 1.

concrete structures can suffer failure in several different ways: cracking, crushing and scraping the concrete, yielding and pulling the tensioned reinforcement bars, and yielding and buckling the compressed reinforcement bars. Advanced numerical simulations based on continuum mechanics are required to better describe and understand the behaviour of the reinforced concrete structures during the failure. This requirement fails to agree with the computational capabilities and the time available to the engineers. Therefore, the use of the simplified models, both of the structure and of the material behaviour, is common in practice.

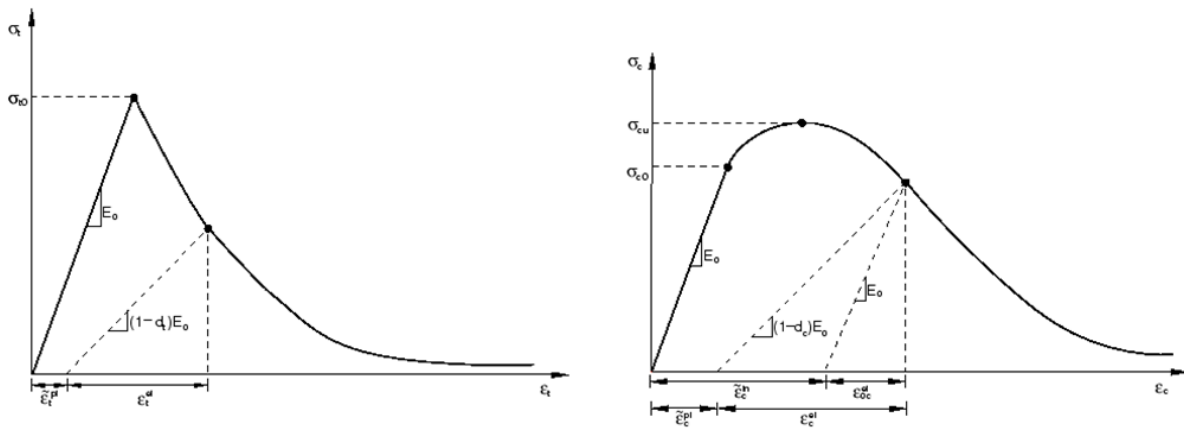
A great number of research activities has been done in the past few years, both with regard to the development of new, more comprehensive numerical concrete material models and the experimental testing of lightweight concrete. The numerical modelling of the concrete plasticity and the damage development can be performed using the CDP (concrete damage plasticity) material model. This material model introduces the assumption that the two main mechanisms of the concrete failure are cracking due to the tension and crushing due to the compression. This material model has been presented in [4]. It has undergone numerous improvements over the past decade while considering determination of the variables necessary to define it [2, 5, 9]. Some of the more significant experimental tests on lightweight concrete are given in [7, 8, 10].

In this paper, the concept of CDP material model is presented and numerical simulation of the behaviour of the lightweight concrete samples in the laboratory testing cases is done. Two test configurations were considered: the determination of the concrete compressive strength on a 150mm concrete cube and the determination of the concrete static modulus of elasticity on a concrete cylinder 150 mm in diameter and 300 mm in height. In order to capture the realistic behaviour of the material, the CDP model of the concrete was used in this paper.

2 CONCRETE BEHAVIOUR MODEL

The behaviour of the material at failure due to compressive and tensile stress can be described in various ways. In the case of tension, cracks occur, which is reflected in the stress-strain diagram in a sharp drop in the stiffness of the material, followed by a decrease in the stiffness of the load-bearing branch of the diagram. In the case of compression stress, an increase in material volume, crushing and slipping within the material occurs. In combined stress states, failure usually depends on the relation between the principal stresses [2].

The nonlinear behaviour of concrete is described in this paper using a CDP model, implemented in Abaqus[®] software. This model of non-linear behaviour of materials is primarily intended to model problems where the plasticity of concrete is possible, however, it is also possible to model other quasi-rigid materials. The main assumption is that the two main mechanisms of the concrete failure are cracking due to the tension and crushing due to the compression [1]. The assumption of the material behaviour due to the uniaxial tension and the tensile stress is given in Figure 1.



Slika 1. Odgovor betona na jednoosno zatezanje (levo) i pritisak (desno) [1]
 Figure 1. Concrete response to the uniaxial tension (left) and compression (right)[1]

Usled jednoosnog zatezanja, veza između napona i dilatacije je linearno-elastična sve dok se ne postigne vrednost čvrstoće betona pri zatezanju σ_{t0} . Dostizanje ove vrednosti napona tretira se kao početak formiranja mikroprrlina u betonu, koje se prikazuje padom napona, odnosno povećanjem dilatacija.

Usled jednoosnog pritiska, veza između napona i dilatacije je linearno-elastična sve dok se ne postigne vrednost napona tečenja σ_{c0} . Tokom plastifikacije, odgovor se karakteriše ojačanjem napona, koje je potom praćeno omekšanjem dilatacije nakon dostizanja čvrstoće betona pri pritisku σ_{cu} [1].

3 EKSPERIMENTALNO ISPITIVANJE

U ovom radu su korišćeni eksperimentalni podaci laboratorijskih ispitivanja predstavljenih u [7], [8] i [10]. Predmet ovog istraživanja su konstrukcijski lakoagregatni betoni, pri čemu je akcentat stavljen na analizu najznačajnijih fizičko-mehaničkih svojstava svežeg i očvrstlog betona. U tom istraživanju je predstavljeno pet različitih betonskih mešavina, pri čemu su u ovom radu korišćeni rezultati dobijeni od jedne mešavine, označene sa LLK-1.

Uzorci za koje je u ovom radu izvršeno poređenje eksperimentalnih i numeričkih rezultata spravljani su od lakog agregata na bazi ekspandirane gline „Leca-Laterlite“ (Italija). Upoređeni su rezultati ispitivanja čvrstoće betona na pritisak, kao i određivanja modula elastičnosti betona [7].

U Tabeli 1 date su količine komponentnih materijala korišćenih za spravljanje uzoraka za eksperimentalno ispitivanje i zapreminska masa betona za betonsku mešavinu LLK-1.

Due to the uniaxial tension, the stress-strain relation is linear-elastic until the tensile strength of σ_{t0} is reached. Reaching this stress value is treated as the beginning of the formation of micro cracks in concrete, which is represented by a decrease in stress, or by an increase in strains.

Due to uniaxial compression, the stress-strain relation is linear-elastic until the value of the yield stress σ_{c0} is reached. During the plastification, the response is characterized by the stress strengthening, which is then followed by softening the strain after reaching the concrete compressive strength σ_{cu} [1].

3 EXPERIMENTAL TESTING

In this paper, the experimental data of the laboratory tests presented in [7], [8] and [10] were used. The subject of this research was structural lightweight concrete, with the emphasis on the analysis of the most important physical and mechanical properties of fresh and hardened concrete. Five different concrete mixtures were presented in that study, while the results obtained from a single mixture, labelled as the LLK-1, were used in this paper.

Specimens for which the experimental and numerical results were compared in this paper were made from lightweight aggregate, which is based on the expanded clay "Leca-Laterlite" (Italy). The results of the concrete compressive strength tests as well as the determination of the modulus of elasticity of concrete were compared [7].

Table 1 lists the amounts of component materials used for the specimen mixtures for the experimental testing, as well as the density of the concrete for the LLK-1 concrete mixture.

Tabela 1. Karakteristike mešavine lakoagregatnog betona [7]
 Table 1. Properties of the lightweight concrete mixture [7]

Oznaka Label	Cement Cement [kg/m ³]	Voda / Water [kg/m ³]		Agregat / Aggregate [kg/m ³]		Zapreminska masa betona Concrete density [kg/m ³]
		m _v	m _{v,dod}	Rečni 0/4 River 0/4	Leca-laterlite 4/15 Leca-laterlite 4/15	
LLK-1	450	180	15.3	940	333	1902

3.1 Konfiguracija 1: Određivanje čvrstoće betona pri pritisku

Čvrstoća betona pri pritisku određena je prema standardu SRPS ISO 4012 na uzorcima oblika kocke ivice 150 mm, starosti 28 dana, kao srednja vrednost čvrstoća dobijenih na tri uzorka. Brzina nanošenja opterećenja iznosila je 0.6 ± 0.2 MPa/s. Ispitivanje čvrstoće pri pritisku prikazano je na slici 2. Vrednost čvrstoće pri pritisku lakoagregatnog betona starosti 28 dana određena eksperimentalnim putem iznosi $f_{cu,28} = 50.6$ MPa [8].



Slika 2. Određivanje čvrstoće pri pritisku [8]
Figure 2. Determination of the compressive strength [8]

3.1 Configuration 1: Determination of the concrete compressive strength

The compressive strength of the concrete was determined according to the standard SRPS ISO 4012 on cube shaped specimens with the dimension of 150mm, 28 days old, as the mean value of the strengths obtained on three different specimens. The loading rate was 0.6 ± 0.2 MPa/s. The compressive strength test is shown in Fig. 2. The compressive strength of the 28-days-old lightweight concrete, determined experimentally, is $f_{cu,28} = 50.6$ MPa [8].

3.2 Konfiguracija 2: Određivanje modula elastičnosti betona

Određivanje statičkog modula elastičnosti urađeno je prema standardu SRPS ISO 6784 na uzorcima oblika cilindra prečnika 150 mm i visine 300 mm, starosti između 28 i 35 dana. Ispitivanje je sprovedeno na tri cilindra, a reprezentativna vrednost modula elastičnosti dobijenih merenjem napona i deformacija na svakom uzorku. Brzina nanošenja opterećenja iznosila je 0.6 ± 0.2 MPa/s. Deformacije su registrovane pomoću ekstenzometra tačnosti 0.001 mm s mernom bazom 200 mm. Gornja granica opterećenja ($\sigma_a \approx 1/3 \cdot f_{c,28}$) definisana je na osnovu prethodno određene čvrstoće betona pri pritisku, dok je donja granica opterećenja definisana na način da mora biti ostvarena deformacija od 0.01 mm. Ispitivanje uzoraka je izvršeno u dva ciklusa (serije opterećenja) [7].

Nakon izvršenih ciklusa opterećenja i rasterećenja, modul elastičnosti je određen na osnovu izraza:

3.2 Configuration 2: Determination of the concrete modulus of elasticity

The determination of the static modulus of elasticity was done according to the standard SRPS ISO 6784, on specimens of cylinder shape with the dimensions of 150mm in diameter and 300mm in height, between 28 and 35 days old. The test was conducted on three different cylinders, and the representative value of the modulus of elasticity was determined as the mean value of the modulus of elasticity obtained by measuring the stresses and strains on each specimen. The loading rate was 0.6 ± 0.2 MPa/s. Deformations were recorded using an extensometer of the accuracy of 0.001mm with a measuring base of 200mm. The upper load limit ($\sigma_a \approx 1/3 \cdot f_{c,28}$) was defined based on the pre-determined concrete compressive strength, while the lower load limit is defined in the way that the deformation of 0.01mm must be achieved. Specimen testing was performed in two cycles (load series) [7].

After the load-unload cycles have been completed, the modulus of elasticity is determined using the expression:

$$E = \frac{2 \cdot \Delta\sigma}{\Delta\varepsilon_{long}} \quad (1)$$

gde su $\Delta\sigma = \sigma_a - \sigma_b$ razlika čitanja napona usled maksimalne sile na presi (σ_a – napon usled maksimalne sile P_a na presi, σ_b – napon usled sile P_b koja izaziva nultu dilataciju), $\Delta\varepsilon_{long}$ registrovana dilatacija koja odgovara naponu $\Delta\sigma$, određena prema sledećem izrazu:

$$\Delta\varepsilon_{long} = \frac{(\Delta l_{long,a} - \Delta l_{long,b})}{200} \quad (2)$$

gde je $\Delta l_{long,a} - \Delta l_{long,b}$ izraženo u mm razlika izduženja usled napona σ_a i σ_b , a 200 mm je merna baza deformetra.

Ispitivanje modula elastičnosti prikazano je na slici 3. Vrednost modula elastičnosti lakoagregatnog betona određena eksperimentalnim putem iznosi $E = 23.21$ GPa [7].

where $\Delta\sigma = \sigma_a - \sigma_b$ is the difference in the stress readings due to the maximal force on the press (σ_a - stress due to maximal force P_a on the press, σ_b - stress due to force P_b that causes zero strain), $\Delta\varepsilon_{long}$ is registered strain corresponding to the stress $\Delta\sigma$, determined by the following expression:

where $\Delta l_{long,a} - \Delta l_{long,b}$ is expressed in mm as the difference in elongation due to the stresses σ_a and σ_b , and 200 mm is the measuring base of the deformer.

Experimental testing of the modulus of the elasticity is shown in Figure 3. The value of the modulus of elasticity of lightweight concrete determined experimentally is $E = 23.21$ GPa [7].



Slika 3. Određivanje statičkog modula elastičnosti [10]
Figure 3. Determination of the static modulus of elasticity [10]

4 NUMERIČKI MODEL I

Numeričke analize sprovedene su u softveru Abaqus® [1], baziranom na metodi konačnih elemenata. Sprovedene su numeričke analize na dve različite konfiguracije modela: na modelu cilindra dimenzija $d/L = 150/300$ mm i na modelu kocke stranice 150 mm. Prilikom modeliranja, korišćeni su 3D konačni elementi oblika heksaedra, prosečne veličine 10 mm.

MKE model kocke korišćen je c ciljem upoređenja sa eksperimentalnim rezultatima ispitivanja čvrstoće betona pri pritisku. Model se sastoji od betonske kocke dimenzija stranica 150 mm i dve čelične ploče dimenzija $170 \times 170 \times 40$ mm. MKE model cilindra je korišćen radi upoređenja sa eksperimentalnim rezultatima određivanja modula elastičnosti betona. Model se sastoji od

4 NUMERICAL MODEL

Numerical analyses were performed in Abaqus® [1] software, based on the finite element method. Numerical analyses were performed on two different model configurations: on the cylinder model with dimensions $d/L = 150/300$ mm and on the 150mm cube model. 3D finite element hexahedrons, average size of 10mm, were used for the modelling.

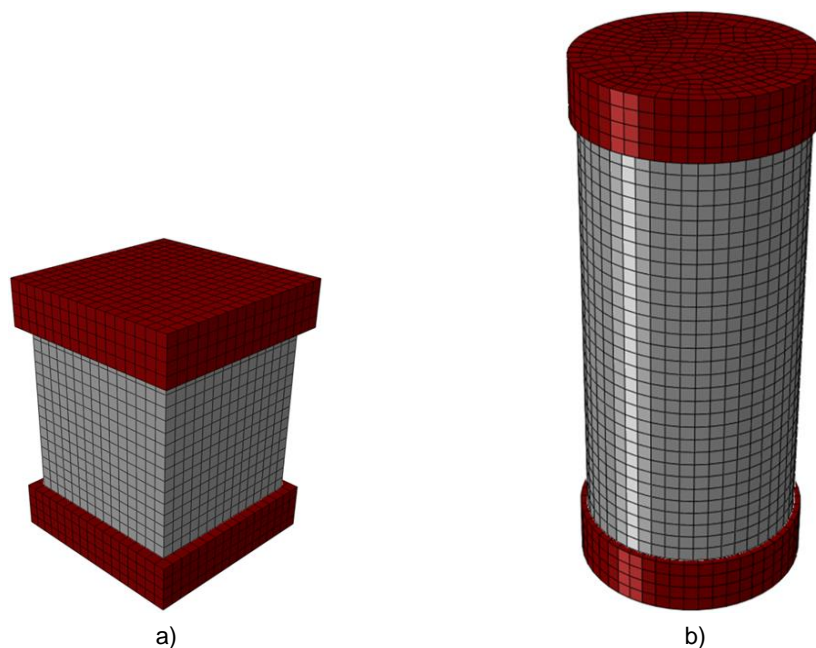
The FEM model of the cube was used in order to compare with the experimental results of the concrete compressive strength tests. The model consists of the 150mm cube and two $170 \times 170 \times 40$ mm steel plates. The FEM cylinder model was used for comparison with the experimental results of the determination of the concrete modulus of elasticity. The model consists of the concrete

betonskog cilindra dimenzija $d/L = 150/300$ mm i, kao u prethodnom slučaju, dve čelične ploče dimenzija $d/L = 160/40$ mm.

Čelične ploče, koje se nalaze sa gornje i donje strane betonskih uzoraka korišćene su u modelima radi što vernijeg prikaza realnog stanja, gde se kocka u hidrauličkoj presi oslanja s donje strane na čeličnu ploču, dok se opterećenje aplicira sa gornje strane, takođe preko čelične ploče. Ovim je omogućeno realnije modeliranje kontaktnih uslova između uzoraka i podloge. Debljina čeličnih ploča od 40 mm obezbeđuje dovoljnu krutost da njihove deformacije budu višestruko manje od deformacije betonskog uzorka.

U oba slučaja je model oslonjen površinski preko donje površine donje čelične ploče, na način da su sprečena pomeranja u sva tri pravca. Trodimenzionalni MKE modeli betonske kocke i cilindra prikazani su na slici 4.

cylinder with dimensions $d/L = 150/300$ mm and, as in the previous case, two steel plates with dimensions $d/L=160/40$ mm. Steel plates, located on the top and bottom of the concrete specimens, were used to achieve the real situation, where the cube in the hydraulic press is supported on the bottom on the steel plate, while the load is applied on the upper side, also via steel plate. This allows more realistic modelling of the contact conditions between the specimens and the pedestal. The steel plates thickness of 40mm provides sufficient rigidity for their deformation that should be several times lesser than the deformation of the concrete specimen. In both cases, the model rests over the lower surface of the lower steel plate, in the way that displacements in all three directions are prevented. Three-dimensional FEM models of concrete cube and cylinder are shown in Figure 4.



Slika 4. 3D prikaz modela: a) betonska kocka i b) betonski cilindar
Figure 4. 3D view of the model: a) concrete cube and b) concrete cylinder

4.1 Model ponašanja materijala

U modelu su korišćena dva tipa modela materijala: linearno-elastični model i elasto-plastični model (CDP model). Linearno-elastični model materijala korišćen je za potrebe modeliranja čeličnih ploča u obe konfiracije. Ovakva pretpostavka ponašanja materijala je opravdana iz više razloga. Prvo, vrednost modula elastičnosti čelika (210 GPa) više je od devet puta veća od vrednosti modula elastičnosti razmatranog lakoagregatnog betona (23.21 GPa). Drugo, vrednosti napona dostignute u modelu višestruko su manje od granice proporcionalnosti čelika, stoga, čelik ni u jednom trenutku neće ući u plastičnu fazu rada.

CDP model materijala je korišćen za potrebe modeliranja betonskog cilindra i kocke. Ovaj model uvodi pretpostavku o nelinearnom ponašanju materijala. Veza napon-dilatacija lakoagregatnog betona pri pritisku je definisana prema [6] izrazom:

4.1 Material model

Two types of material models were used in the model: the linear-elastic model and the elasto-plastic model (CDP model). A linear-elastic material model was used for modelling steel plates in both configurations. This assumption of material behaviour is justified for several reasons. Firstly, the value of the modulus of elasticity of steel (210 GPa) is more than nine times higher than the value of modulus of elasticity of lightweight aggregate concrete (23.21 GPa). Secondly, the stress values reached in the model are several times lesser than the steel proportionality limit. Therefore, the steel will not enter the plastic phase of the operation at any time.

The CDP material model was used for the purpose of modelling the concrete cylinder and cube. This model introduces the assumption of nonlinear material behaviour. The stress-strain relationship of lightweight

concrete due to the compression is defined according to [6]:

$$\sigma = \frac{E_0 \varepsilon}{1 + \left(\frac{E_0}{E_s} - 2\right) \cdot \frac{\varepsilon}{\varepsilon_{cu}} + \left(\frac{\varepsilon}{\varepsilon_{cu}}\right)^\alpha} \quad (3)$$

gde su E_0 inicijalni modul elastičnosti, E_s sekantni modul elastičnosti koji odgovara maksimalnom naponu i odgovarajućoj dilataciji, ε_{cu} dilatacija koja odgovara maksimalnom naponu, a α parametar koji kontroliše oblik krive, čija je vrednost usvojena prema [6] i iznosi 1.5.

Ovde je pretpostavljeno da veza napon-dilatacija postaje nelinearna nakon dostizanja dilatacije od $5.5 \cdot 10^{-4}$, što odgovara naponu od 12.65 MPa.

Veza napon-dilatacija betona pri zatezanju usvojena je kao linearna do dostizanja vrednosti čvrstoće betona na zatezanje, nakon čega nastupa lom. Čvrstoća lakoagregatnog betona na zatezanje definisana je prema [3] izrazom:

$$f_t = 0.81 \cdot \left[\left(\frac{\rho_c}{\rho_0} \right)^{1.5} \cdot f'_c \right]^{0.35} \quad (4)$$

gde su ρ_c zapreminska masa lakoagregatnog betona, ρ_0 referentna vrednost zapreminske mase koja iznosi 2200 kg/m³, f'_c čvrstoća betona pri pritisku određena na cilindru $d/L = 150/300$ mm.

Nakon što se u izraz (4) uvrste vrednosti zapreminske mase analiziranog betona (1902 kg/m³), referentna vrednost zapreminske mase (2200 kg/m³) i čvrstoća betona pri pritisku (39.7 MPa; vrednost dobijena množenjem čvrstoće betona pri pritisku određena na kocki dimenzija 150 mm i koeficijenta 0.79 koji predstavlja odnos čvrstoće pri pritisku cilindra ($d/L = 150/300$ mm) i kocke ($a = 150$ mm)), dobija se vrednost čvrstoće betona pri zatezanju od 2.72 MPa.

4.2 Konačni elementi

Za modeliranje problema u Abaqus[®] dostupni su 1D, 2D, 3D i drugi, specijalni, konačni elementi. U ovom radu korišćeni su trodimenzionalni (zapreminski; solid) KE. U zavisnosti od tipa i reda 3D elementa, softver nudi mogućnosti izbora od tetraedarnog elementa prvog reda sa 4 čvorova do heksaedarnog elementa drugog reda sa 27 čvorova. Čvorovi trodimenzionalnih elemenata imaju 3 stepena slobode, koja se odnose na tri moguće translacije u prostoru.

U ovom radu su korišćeni C3D8R konačni elementi (3D heksaedarni KE prvog reda sa 8 čvorova). Ovaj tip elementa koristi redukovanu integraciju za formiranje matrice krutosti, pri čemu je broj integracionih tačaka 1 [1].

4.3 Modeliranje kontakta

Stav da usled jednoosnog pritiska uzorak ne trpi nikakva ograničenja u smislu poprečnog deformisanja ne važi u zoni oslanjanja uzorka, već samo u zoni koja se može aproksimirati srednjom trećinom visine uzorka. U zonama oslanjanja, usled trenja koje se javlja na kon-

where E_0 is the initial modulus of elasticity, E_s is the secant modulus of elasticity corresponding to the maximum stress and the corresponding strain, ε_{cu} is the strain corresponding to the maximum stress, and α is the parameter controlling the shape of the curve, whose value is adopted according to [6] and equals to 1.5.

Here, it is assumed that the stress-strain relationship becomes non-linear after reaching a strain of $5.5 \cdot 10^{-4}$, which corresponds to the stress of 12.65 MPa.

The tension stress-strain relationship of the concrete is adopted as linear until the tensile strength of the concrete is reached, followed by failure. Tensile strength of lightweight concrete is defined according to [3]:

where ρ_c is the volume mass of lightweight concrete, ρ_0 is the reference mass density of 2200 kg/m³, f'_c is the tensile strength of the concrete determined on the cylinder $d/L = 150/300$ mm.

The value of the concrete tensile strength of 2.72 MPa is obtained when the values of the bulk mass of the analyzed concrete (1902 kg/m³), the reference value of the density (2200 kg/m³) and the concrete compressive strength (39.7 MPa; the value obtained by multiplying the concrete strength at compression determined by the 150mm cube and coefficient 0.79 representing the ratio of the compressive strength of the cylinder ($d/L = 150/300$ mm) and the cube ($a = 150$ mm)) are incorporated in the expression (4).

4.2 Finite elements

1D, 2D, 3D and other special, finite elements are available for modelling in Abaqus[®]. Three-dimensional (solid) FEs were used in this paper. Depending on the type and order of the 3D element, the software offers choices from a 4-node tetrahedral element to a 27-node hexahedral element. Nodes of the three-dimensional elements have 3 degrees of freedom, which refer to three possible translations in space.

In this paper, C3D8R finite elements (3D first order hexahedral KE with 8 nodes) were used. This type of element uses reduced integration to form a stiffness matrix, with the number of integration points being 1 [1].

4.3 Contact modelling

The premise that due to the uniaxial compression the specimen fails to suffer any restrictions since transverse deformation does not apply in the area of support of the specimen, but only in the zone that can be approximated by the middle third of the height of the specimen. In the support zones, due to the friction occurring at the

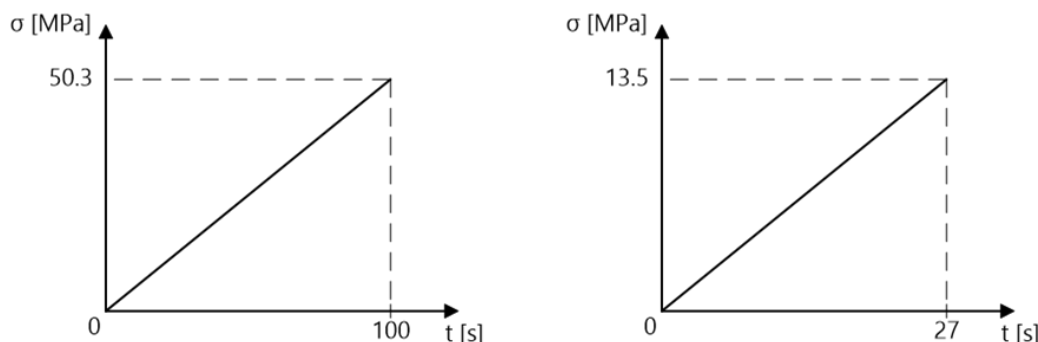
taktima uzorak-ploča, dolazi do određenog ograničavanja bočnih deformacija uzoraka. Stoga, naponsko stanje će u tim zonama biti znatno složenije u odnosu na uslove aksijalnog pritiska.

Radi zadovoljenja ovog stava, kontakt između uzoraka (kocke; cilindra) i čeličnih ploča modeliran je koristeći tangencijalne i normalne komponente. Tangencijalnoj komponenti (trenje na spoju uzorak-ploča) dodeljena je vrednost koeficijenta trenja od 0.57, što predstavlja uobičajenu vrednost koeficijenta trenja između betona i čelika. Normalna komponenta je modelirana na način da se, kada su površine u kontaktu, može preneti bilo koji kontaktni pritisak između njih, pri čemu dolazi do razdvajanja kontaktnih površina ako kontaktni pritisak dostigne nultu vrednost. Drugim rečima, zatezanje na kontaktnoj površini nije dozvoljeno.

4.4 Definisane opterećenja

Opterećenje je u oba slučaja (ispitivanje na kocki i ispitivanje na cilindru) definisano kao jednakopodeljeno površinsko i deluje na gornjoj površini gornje čelične ploče.

Vremenske funkcije opterećenja za obe konfiguracije ispitivanja date su na slici 5. Nanošenjem opterećenja u intervalima od 100 s i 27 s aproksimirano je realno stanje u kojem se opterećenje koje izaziva napone u presecima kocke i cilindra u iznosu od 50.3 MPa i 13.5 MPa nanosi brzinom od 0.6 ± 0.2 MPa/s.



Slika 5. Vremenska funkcija opterećenja betonske kocke (levo) i betonskog cilindra (desno)
Figure 5. Time function of the load of concrete cube (left) and concrete cylinder (right)

5 ANALIZA REZULTATA NUMERIČKOG MODELA

Sprovedene su nelinearne statičke analize za dve konfiguracije numeričkih modela. Za iterativno rešavanje sistema jednačina korišćena je Njutnova metoda, pri čemu je maksimalan broj inkremenata bio 100.

Rezultati nelinearne statičke analize dati su samo za deo numeričkog modela koji obuhvata betonske uzorke, budući da su čelične ploče u numeričkom modelu prisutne radi što vernijeg prikaza kontaktnih uslova u zoni kontakta sa uzorkom. Zbog svoje debljine i činjenice da imaju višestruko veći modul elastičnosti, kao i grancu tečenja, čelične ploče u svakom trenutku ostaju u elastičnoj fazi rada, te u ovom radu neće biti predmet razmatranja.

specimen-plate contacts, there is some limitation of the lateral deformations of the specimens. Therefore, the stress state in these zones will be much more complex than the axial compression conditions.

The contact between specimens (cubes; cylinders) and steel plates was modelled using tangential and normal components to meet this argument. Coefficient of friction of 0.57 was assigned to the tangential component (friction at the specimen-steel plate surface), which is the common value of the friction coefficient between the concrete and steel. The normal component is modelled in the way that, when the surfaces are in contact, any contact compression between them can be transferred, whereby the contact surfaces are separated if the contact compression reaches zero. In other words, tension on the contact surface in normal direction is not allowed.

4.4 Load definition

The load is defined in both cases (cube test and cylinder test) as uniformly distributed surface load and acts on the upper surface of the upper steel plate.

The time load functions for both test configurations are given in Figure 5. Applying a load at 100 and 27 s intervals approximates the real state in which the load that causes stresses in the cube and cylinder sections of 50.3 MPa and 13.5 MPa, respectively, is applied at the rate of 0.6 ± 0.2 MPa/s.

5 ANALYSIS OF THE RESULTS OF THE NUMERICAL MODEL

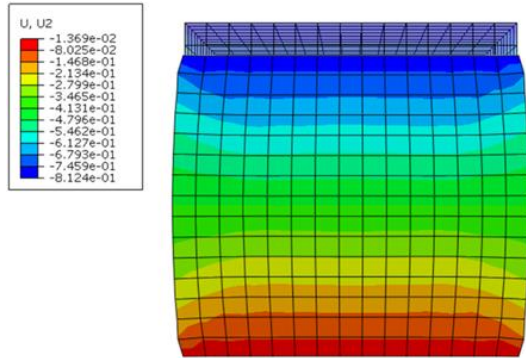
Nonlinear static analyses were performed for the two configurations of numerical models. Newton's method was used to iteratively solve the system of equations, with the maximum number of increments being 100.

The results of the nonlinear static analysis are given only for the part of the numerical model that includes concrete specimens, since the steel plates in the numerical model are present for the most accurate representation of the contact conditions in the contact zone with the specimen. Due to their thickness and the fact that their modulus of elasticity is several times larger, as well as the yield strength, steel plates remain in the elastic phase during the analysis, and will not be considered in this paper.

5.1 Konfiguracija 1

Rezultati modela kocke prikazuju pomeranja, napone i odgovarajuće dilatacije uzorka, kao i napone smicanja na kontaktu između uzorka i čelične ploče.

Na slici 6 prikazan je deformisan oblik uzorka u pogledu sa strane s vrednostima vertikalnog pomeranja, dok je na slici 7 prikazano bočno pomeranje uzorka u X pravcu.

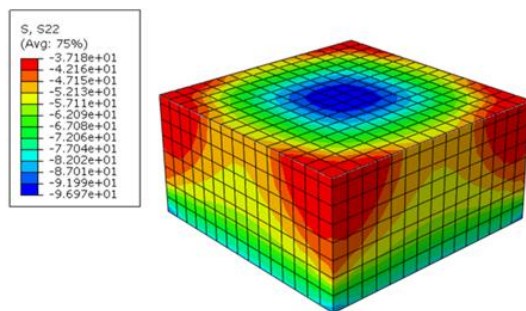


Slika 6. Vertikalno pomeranje – deformisana i nedeformisana kontura [mm]

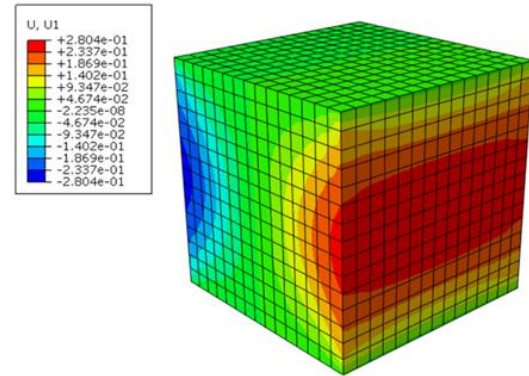
Figure 6. Vertical displacement - deformed and undeformed contour [mm]

Uočljivo je da se uzorak deformiše na način koji odgovara realnom stanju: budući da usled jednoosnog pritiska uzorak ne trpi nikakva ograničenja u smislu poprečnog deformisanja, on se slobodno deformiše u poprečnom pravcu u zoni srednje trećine uzorka. Približavanjem osloncima poprečna deformacija se smanjuje usled trenja koje se javlja na kontaktima uzorak-ploča. Maksimalno vertikalno pomeranje uzorka iznosi: $U_2 = 0.8124 \text{ mm} - 0.0137 \text{ mm} = 0.7987 \text{ mm}$.

Na slici 8 prikazani su naponi i odgovarajuće dilatacije u podužnom pravcu kocke (po visini).



a)

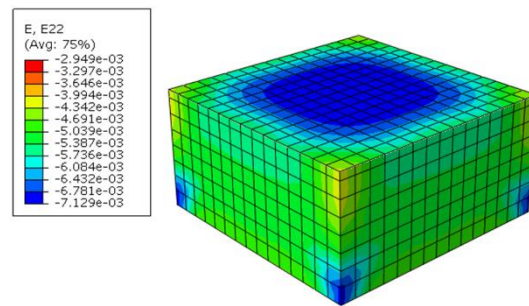


Slika 7. Bočno pomeranje u X pravcu [mm]

Figure 7. Lateral displacement in the X direction [mm]

It is noticeable that the specimen deforms in the way that corresponds to the real state: since, due to uniaxial compression, the specimen does not suffer any restrictions in terms of transverse deformation. It freely deforms in the transverse direction in the zone of the middle third of the specimen. When approaching the supports, the transverse deformation is reduced due to the friction that occurs on the specimen-plate contacts. The maximum vertical displacement of the specimen is: $U_2 = 0.8124 \text{ mm} - 0.0137 \text{ mm} = 0.7987 \text{ mm}$.

Figure 8 shows the stresses and corresponding strains in the longitudinal direction of the cube (in height).



b)

Slika 8. Polovina uzorka (horizontalni presek): a) napon S22 [MPa] i b) dilatacija E22
Figure 8. Half of the specimen (horizontal section): a) stress S22 [MPa] and b) strain E22

Slike 9 i 10 daju prikaz napona i odgovarajućih dilatacija u preostala dva ortogonalna pravca u

Figures 9 and 10 show the stresses and corresponding strains in the remaining two orthogonal

poprečnom preseku (po visini) kocke. Ovde se uočava jasno izražena granica između zategnutog i pritisnutog i dela betonske kocke, koji zauzima prostorni X-oblik. Ovakav oblik loma posledica je sila trenja na kontaktu sa čeličnim pločama, koje deluju tako da „utežu” beton. Utegnuti deo betona je oblika klina u donjem i gornjem delu kocke, koji deluje na način da istiskuje okolni zategnuti beton nakon dostizanja čvrstoće betona na zatezanje i formiranja prvih prslina.

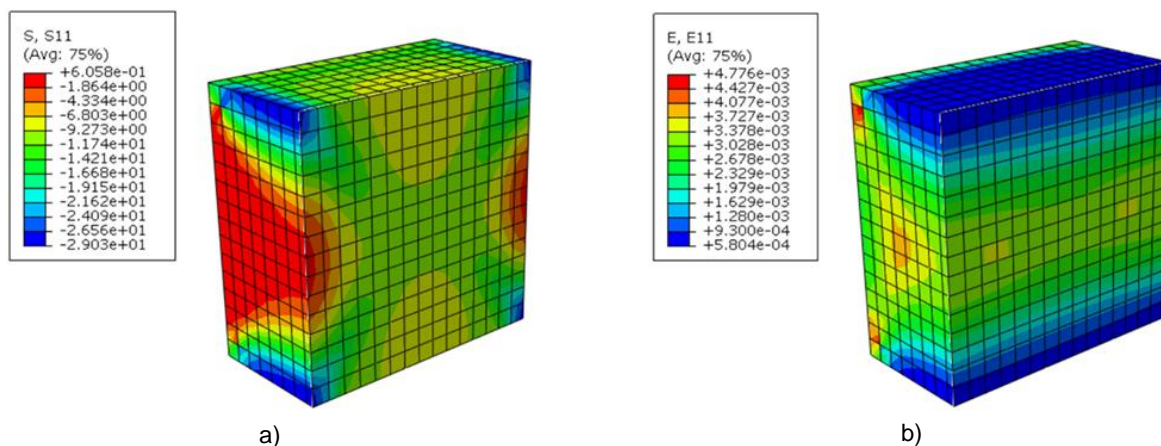
Veće vrednosti napona u unutrašnjosti kocke posledica su „utegnutosti” betona, odnosno činjenice da beton bliži spoljašnjosti sprečava bočne deformacije betona u unutrašnjosti kocke.

Slika dilatacija prati sliku napona. Maksimalne dilatacije na spoljašnjoj strani imaju vrednosti $3.150 \cdot 10^{-3}$ i $-5.547 \cdot 10^{-3}$ a u unutrašnjosti $3.494 \cdot 10^{-3}$ i $-7.160 \cdot 10^{-3}$.

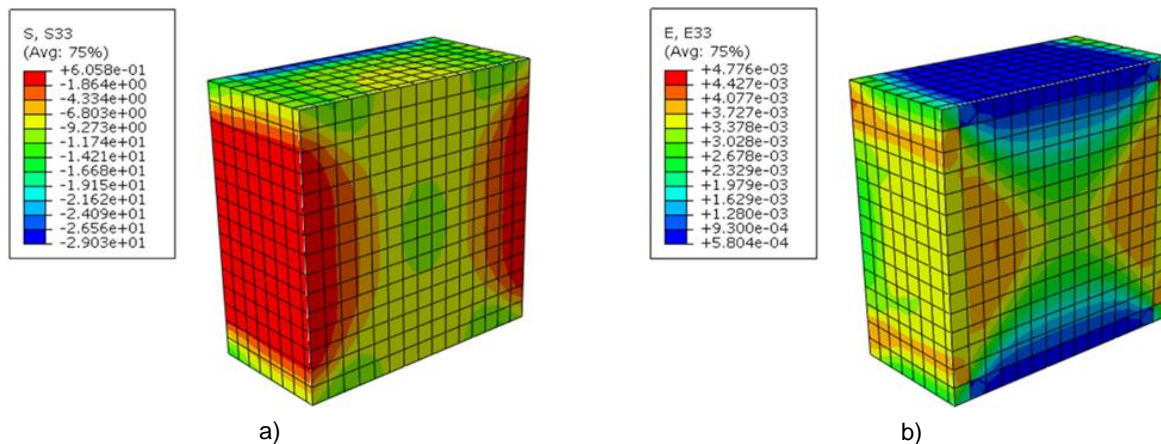
directions in the cross-section (vertical section) of the cube. Here, a clear distinction is made between the tensiled and the compressed sections of the concrete cube, which occupies a spatial X-shape. This type of failure occurs due to the friction forces on contact with the steel plates, which confine the concrete. The confined part of the concrete is a wedge-shaped part in the lower and upper parts of the cube, which acts in such a way to squeeze out the surrounding tensiled concrete after reaching the tensile strength of the concrete and formation of the first cracks.

Higher values of stress inside the cube are due to the confinement of the concrete, i.e. the fact that the concrete closer to the outside prevents lateral deformation of the concrete inside the cube.

The strain pattern follows the stress pattern. The maximal strains on the outside are $3.150 \cdot 10^{-3}$ and $-5.547 \cdot 10^{-3}$ and on the inside are $3.494 \cdot 10^{-3}$ and $-7.160 \cdot 10^{-3}$.



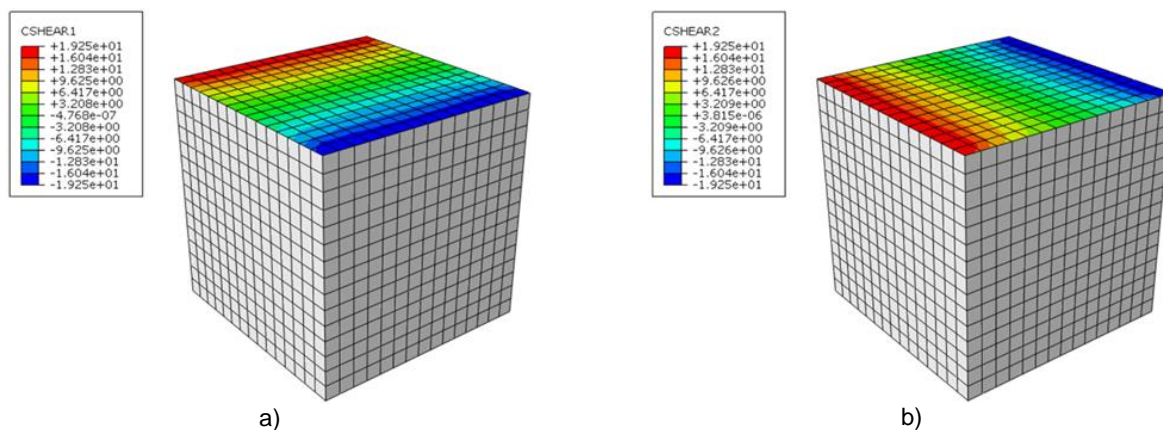
Slika 9. Polovina uzorka (vertikalni presek): a) napon S11 [MPa] i b) dilatacija E11
Figure 9. Half of the specimen (vertical section): a) stress S11 [MPa] and b) strain E11



Slika 10. Polovina uzorka (vertikalni presek): a) napon S33 [MPa] i b) dilatacija E33
Figure 10. Half of the specimen (vertical section): a) stress S33 [MPa] and b) strain E33

Na slici 11 prikazani su naponi u ravni kontakta kocke i čelične ploče s gornje strane

Figure 11 shows the stresses in the contact surface between the cube and the steel plate on the upper side.



Slika 11. Napon smicanja [MPa] na kontaktu između betonske kocke i čelične ploče:
 a) u X pravcu i b) u Y pravcu
 Figure 11. Shear stress [MPa] on contact between concrete cube and steel plate:
 a) in the X direction and b) in the Y direction

5.2 Konfiguracija 2

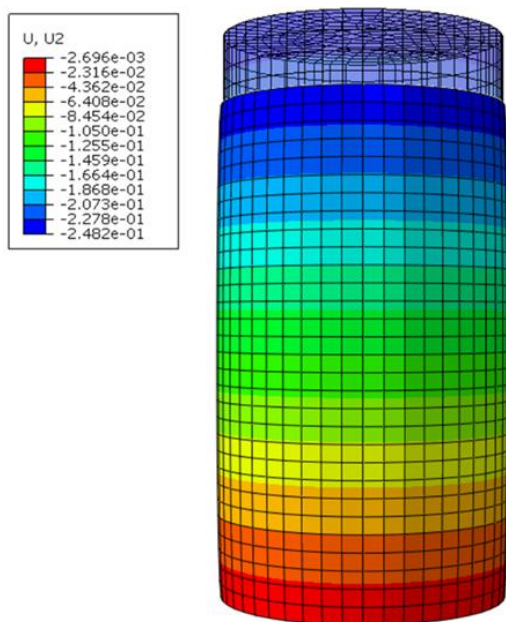
Rezultati modela cilindra prikazuju pomeranja uzorka u vertikalnom i bočnom pravcu, napone u pravcu poduže ose cilindra i odgovarajuće dilatacije, dilatacije u poprečnim pravcima kao i napone smicanja na kontaktu između uzorka i čelične ploče.

Na slici 12 prikazan je deformisan oblik uzorka u pogledu sa strane s vrednostima vertikalnog pomeranja, dok je na slici 13 prikazano bočno pomeranje uzorka u X pravcu.

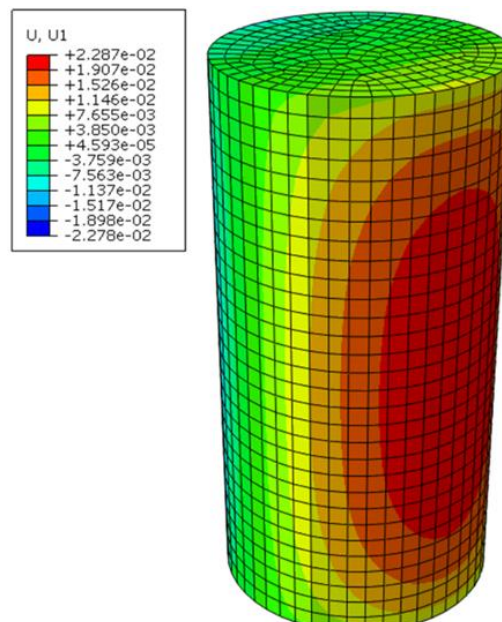
5.2 Configuration 2

The results of the cylinder model show the displacements of the specimen in the vertical and lateral directions, the stresses in the longitudinal direction of the cylinder axis and the corresponding strains, the strains in the transverse directions, and the shear stresses at the contact between the specimen and the steel plate.

Figure 12 shows the deformed shape of the specimen in the side view with the values of the vertical displacement, while Figure 13 shows the lateral displacement of the specimen in the X direction



Slika 12. Vertikalno pomeranje – deformisana i nedeformisana kontura [mm]
 Figure 12. Vertical displacement - deformed and undeformed contour [mm]



Slika 13. Bočno pomeranje U1 [mm]
 Figure 13. Lateral displacement U1 [mm]

Može se zapaziti sličnost u pogledu oblika deformacije uzorka cilindra i kocke: slobodna poprečna defor-

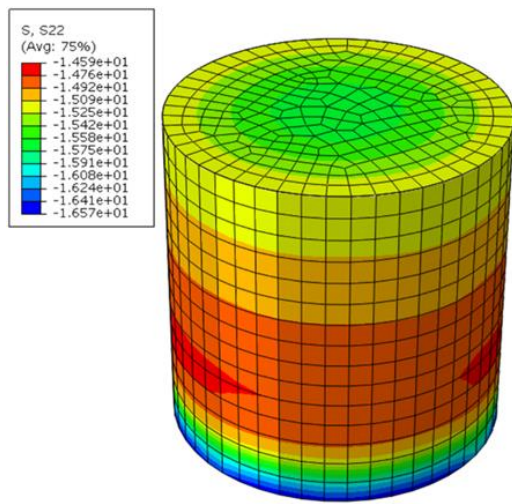
The similarity may be observed with respect to the deformation patterns of the cylinder and cube speci-

macija cilindra usled jednoosnog pritiska u zoni srednje trećine uzorka. Približavanjem osloncima poprečna deformacija smanjuje se usled trenja koje se javlja na kontaktima uzorak-ploča. Maksimalno vertikalno pomeranje uzorka iznosi: $U_2 = 0.2482 \text{ mm} - 0.0027 \text{ mm} = 0.2455 \text{ mm}$.

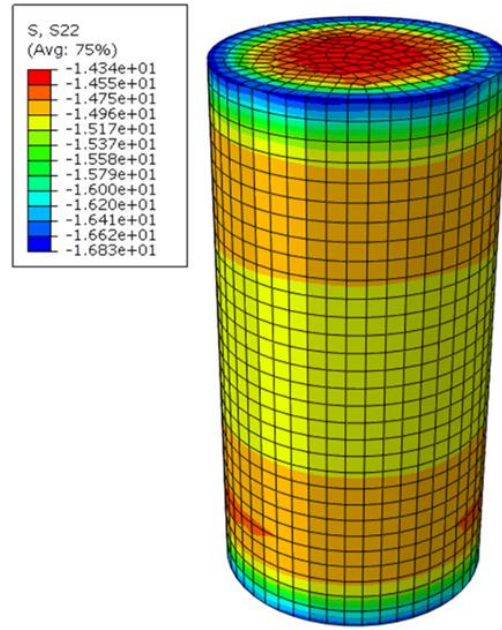
Na slici 14 dati su slika i vrednosti napona u podužnom pravcu cilindra, na jednoj polovini uzorka i na celom uzorku. Slike 15 i 16 daju prikaz slike i vrednosti podužnih i poprečnih dilatacija uzorka.

mens: free transverse deformation of the cylinder due to uniaxial compression in the mid-third zone of the specimen. When approaching the supports, the transverse deformation is reduced due to the friction that occurs on the specimen-plate contacts. The maximum vertical displacement of the specimen is: $U_2 = 0.2482 \text{ mm} - 0.0027 \text{ mm} = 0.2455 \text{ mm}$.

Figure 14 shows the pattern and the values of the stress in the longitudinal direction of the cylinder, on the one half of the specimen and on the entire specimen. Figures 15 and 16 show the pattern and values of the longitudinal and transverse strains of the specimen.

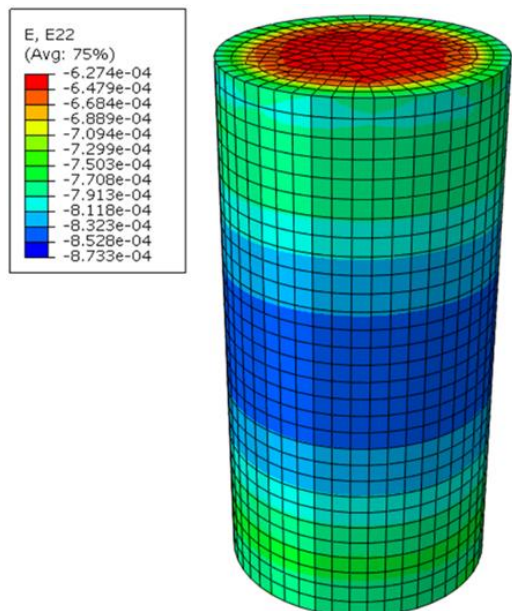


a)

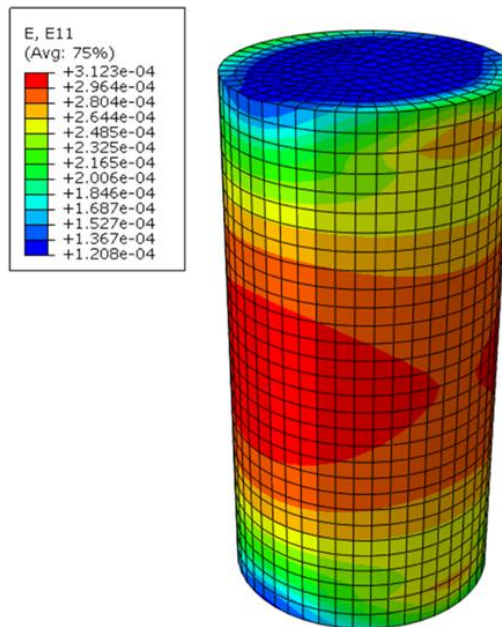


b)

Slika 14. Napon S22: a) polovina uzorka i b) ceo uzorak
Figure 14. Stress S22: a) half of the specimen and b) whole specimen



Slika 15. Dilatacija E22
Figure 15. Strain E22



Slika 16. Dilatacija E11
Figure 16. Strain E11

Maksimalan napon na spoljašnjoj strani cilindra iznosi 15.09 MPa, a u unutrašnjosti cilindra 15.91 MPa. Vrednosti napona pritiska u unutrašnjosti cilindra veće su u odnosu na spoljašnje delove zbog istog razloga opisanog u prethodnoj konfiguraciji.

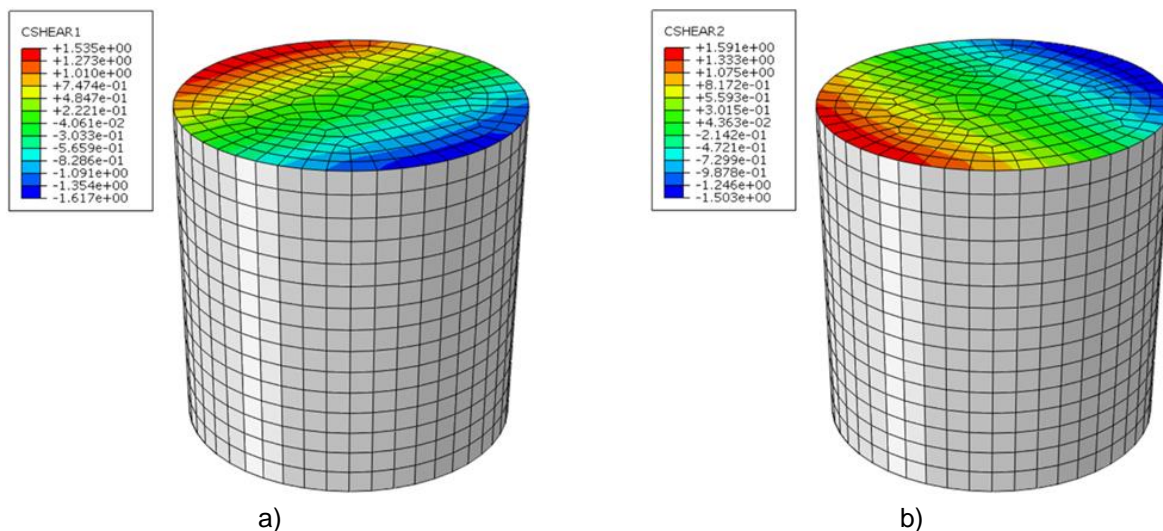
I ovde, kao i u prethodnoj konfiguraciji, slika dilatacija prati sliku napona. Maksimalna dilatacija na spoljašnjoj strani cilindra iznosi $8.336 \cdot 10^{-4}$, a u unutrašnjosti $8.733 \cdot 10^{-4}$.

Na slici 17 prikazani su naponi u ravni kontakta cilindra i čelične ploče s gornje strane.

The maximal stress on the outside of the cylinder is 15.09 MPa and 15.91 MPa on the inside of the cylinder. The compression values inside the cylinder are higher than the outer parts for the same reason described in the previous configuration.

Here, as in the previous configuration, the strain pattern follows one of the stress. The maximum strain on the outside of the cylinder is $8.336 \cdot 10^{-4}$ and $8.733 \cdot 10^{-4}$ on the inside.

Figure 17 shows the stresses in the contact surface between the cylinder and the steel plate on the upper side.



Slika 17. Napon smicanja [MPa] na kontaktu između betonskog cilindra i čelične ploče (polovina uzorka): a) u X pravcu i b) u Y pravcu

Figure 17. Shear stress [MPa] at the contact between the concrete cylinder and the steel plate (half of the specimen): a) in the X direction and b) in the Y direction

5.3 Rekapitulacija rezultata

U Tabeli 2 prikazani su najznačajniji rezultati laboratorijskih ispitivanja i numeričkih analiza.

5.3 Result summary

Table 2 shows the most significant results of the experimental testing and the numerical analyses.

Tabela 2. Rekapitulacija rezultata numeričkih analiza
Table 2. Recapitulation of numerical analysis results

	Konfiguracija 1 / Configuration 1		Konfiguracija 2 / Configuration 2	
	Laboratorijski uzorak <i>Experimental specimen</i>	Numerički model <i>Numerical model</i>	Laboratorijski uzorak <i>Experimental specimen</i>	Numerički model <i>Numerical model</i>
Maksimalno vertikalno pomeranje U_2 [mm] <i>Maximum vertical displacement U_2 [mm]</i>	/	0.7987	0.218	0.245
Dilatacija na spoljašnjosti uzorka / <i>Strain on the outside of the specimen</i>	/	$3.150 \cdot 10^{-3}$ $-5.547 \cdot 10^{-3}$	$1.10 \cdot 10^{-3}$	$8.336 \cdot 10^{-4}$
Maksimalan napon [MPa] <i>Maximum stress [MPa]</i>	-50.6	-51.29 (spoljašnja strana uzorka) <i>-51.29 (on the outer side of the specimen)</i>	/	-15.14 (spoljašnja strana uzorka) <i>-15.14 (on the outer side of the specimen)</i>

Maksimalan napon [MPa] Maximum stress [MPa]	-50.6	-96.97 (unutrašnja strana uzorka) -96.97 (in the inside of the specimen)	/	-16.12 (unutrašnja strana uzorka) -16.12 (in the inside of the specimen)
--	-------	---	---	---

6 ZAKLJUČAK

Eksperimentalni podaci laboratorijskih ispitivanja predstavljenih u [7], [8] i [10] poslužili su kao osnova za formiranje MKE modela ponašanja lakoagregatnog betona. Eksperimentom su određeni čvrstoća betona pri pritisku i modul elastičnosti betona starosti 28 dana za nekoliko različitih mešavina, dok je numeričkom analizom obuhvaćena jedna mešavina (LLK-1). Ponašanje betona kao materijala obuhvaćeno je tzv. concrete damage plasticity (CDP) modelom. Sprovedena je statička nelinearna (inkrementalno-iterativna) analiza za dve konfiguracije modela, po jedna za ispitivanje čvrstoće betona pri pritisku i određivanje modula elastičnosti betona. Prva konfiguracija modela sadrži kocku dimenzija 150 x 150 x 150 mm, a druga cilindar dimenzija $d/L = 150/300$ mm. Potom su analizirani rezultati proračuna i izvučeni su sledeći zaključci:

- Ponašanje betonske kocke u MKE analizi blisko je ponašanju kocke tokom laboratorijskog ispitivanja. Naime, kao i u eksperimentu, i u numeričkom modelu je jasno izražen oblik, tj. mehanizam loma uzorka. Ovaj oblik zauzima prostorni X-oblik, budući da se usled sila trenja na kontaktu sa čeličnim pločama obrazuje utegnuti deo betona oblika klina koji deluje na način da istiskuje okolni zategnuti beton nakon dostizanja čvrstoće betona na zatezanje i formiranja prvih prslina. Pritisnuti beton ovde je već pomenutog X-oblika, dok se u betonu bližem spoljašnjim stranama javlja zatezanje, pa je jasno uočljiva i granica između zona ova dva naponska stanja. Upravo se na ovoj granici javljaju prsline koje će narušiti integritet uzorka i diktirati oblik loma.

- Rezultati numeričkog modela u celokupnom pogledu ukazuju na poklapanje sa eksperimentalnim rezultatima. Međutim, neophodna su dalja, finija podešavanja MKE modela, pre svega modela ponašanja betona, radi potpune kompatibilnosti sa eksperimentalnim podacima.

- Ponašanje betonskog cilindra u MKE analizi, kao i u slučaju betonske kocke, blisko je ponašanju cilindra tokom laboratorijskog ispitivanja. Skraćenje cilindra u MKE modelu u iznosu od 0.245 mm veoma je blisko prosečnom skraćenju cilindra u eksperimentu, koje iznosi 0.218 mm, pri istom nivou opterećenja.

- Deformacija cilindra u MKE modelu približno odgovara realnom stanju, gde usled jednoosnog pritiska u zoni srednje trećine uzora, uzorak ne trpi nikakva ograničenja u smislu poprečnog deformisanja, te se on slobodno deformiše u poprečnom pravcu. U zoni kontakta sa čeličnim pločama, poprečna deformacija smanjuje se usled trenja koje se javlja na kontaktima uzorak-ploča.

- Takođe, dilatacija na spoljašnjoj strani cilindra, u srednjoj trećini visine, u MKE modelu ima vrednost od $0.85 \cdot 10^{-3}$, dok je u toj istoj zoni u eksperimentu registrovana dilatacija od $1.10 \cdot 10^{-3}$.

- Veće vrednosti napona u unutrašnjosti cilindra (15.91 MPa) u odnosu na vrednosti napona na

6 CONCLUSIONS

The experimental data from the laboratory tests presented in [7], [8] and [10] served as the basis for the formation of the FEM model of the behaviour of the lightweight concrete. The experiment determined the compressive strength of the concrete and the modulus of elasticity of concrete at 28 days of age for several different mixtures, while numerical analysis included one mixture (LLK-1). The behaviour of concrete as a material was accounted by the concrete damage plasticity (CDP) model. The static nonlinear (incremental-iterative) analysis was conducted for two model configurations, one for the determination of the compressive strength of concrete and the other for the determination of the modulus of elasticity of concrete. The first configuration of the model consists of the cube measuring 150x150x150 mm and the second one of the cylinder $d/L = 150/300$ mm. The results of the numerical analyses were analyzed and the following conclusions were drawn:

- Concrete cube behaviour in FEM analysis is close to cube behaviour during laboratory testing. Namely, as in the experiment, the failure mechanism pattern is clearly expressed in the numerical model as well. This shape takes the spatial X-shape, since due to the friction forces on the contact with the steel plates, a wedge-shaped portion of concrete is formed, which acts to squeeze out the surrounding tensiled concrete after reaching the tensile strength and forming the first cracks. The compressed concrete has aforementioned X-shape, while in the concrete closer to the outside the tension occurs, so that the boundary between the zones of these two stress states is clearly visible. It is at this border that cracks appear that will impair the integrity of the specimen and dictate the shape of the failure.

- The results of the numerical model in the overall view indicate a congruence with the experimental results. However, further fine-tuning of the FEM model, especially the concrete behaviour model, is required in order to be fully compatible with the experimental data.

- The behaviour of the concrete cylinder in the FEM analysis is, as in the case of the concrete cube, close to the behaviour of the cylinder during laboratory testing. The 0.245 mm cylinder shortening in the FEM model is very close to the average cylinder shortening in the experiment, which is amounted to 0.218 mm, at the same load level.

- The deformation of the cylinder in the FEM model approximates the real state, where due to uniaxial compression in the middle third zone of the specimen, the specimen fails to suffer any restrictions in terms of transverse deformation, and it deforms freely in the transverse direction. In the contact zone with the steel plates, the transverse deformation is reduced due to the friction that occurs on the specimen-plate contact surface.

- In addition, the strain on the outside of the cylinder,

spoljašnjoj strani cilindra (15.09 MPa) u MKE modelu su posledica „utegnutosti“ betona, odnosno činjenice da beton bliži spoljašnjosti sprečava bočne deformacije betona u unutrašnjosti cilindra. Takođe, razlozi za veće vrednosti napona u MKE modelu u odnosu na eksperiment mogu se tražiti u činjenici da je prilikom eksperimenta napon određen kao količnik ukupne sile i površine poprečnog preseka cilindra, dok je u MKE analizi cilindar posmatran kao trodimenzionalno telo, s mogućnošću obuhvatanja u obzir triaksonalnog stanja pritiska.

ZAHVALNOST

U radu je prikazan deo istraživanja koje je pomoglo Ministarstvo prosvete, nauke i tehnološkog razvoja Republike Srbije u okviru tehnološkog projekta TR 36017 pod nazivom: „Istraživanje mogućnosti primene otpadnih i recikliranih materijala u betonskim kompozitima, sa ocenom uticaja na životnu sredinu, u cilju promocije održivog građevinarstva u Srbiji“.

7 LITERATURA

- [1] Abaqus Analysis User's Guide, 2016
- [2] Alfarah B., López-Almansa F., Oller S.: New methodology for calculating damage variables evolution in Plastic Damage Model for RC structures, *Engineering Structures* 132, 2017, 70-86.
- [3] Choi S., Yang K., Sim J., Choi B.: Direct tensile strength of lightweight concrete with different specimen depths and aggregate sizes, *Construction and Building Materials* 63, 2014, 132-141.
- [4] Cicekli U., Vojiadjis G., Al-Rub R.: A plasticity and anisotropic damage model for plain concrete, *International Journal of Plasticity* 23, 2007, 1874-1900.
- [5] Grassi P., Xenos D., Nystrom U., Rempling R., Gylltoft K.: CDPM2: A damage-plasticity approach to modelling the failure of concrete, *International Journal of Solids and Structures* 50, 2013, 3805-3816.
- [6] Han B., Xiang T.: Axial compressive stress-strain relation and Poisson effect of structural lightweight aggregate concrete, *Construction and Building Materials* 146, 2017, 338-343.
- [7] Malešev M., Radonjanin V., Lukić I., Bulatović V.: The effect of aggregate, type and quantity of cement on modulus of elasticity of lightweight aggregate concrete, *Arabian Journal for Science and Engineering* 39, 2014, 705-711.

in the middle third of the height, has a value of $0.85 \cdot 10^{-3}$ in the FEM model, while a strain of $1.10 \cdot 10^{-3}$ was registered in the same zone in the experiment.

Higher values of stress inside the cylinder (15.91 MPa) compared to the stress values on the outside of the cylinder (15.09 MPa) in the FEM model are due to the confinement of the concrete, i.e. the fact that the concrete closer to the outside prevents lateral deformation of the concrete inside the cylinder. In addition, the reasons for higher stress values in the FEM model compared to the experiment can be found in the fact that in the experiment the stress was determined as a quotient of the total force and the cross-sectional area of the cylinder, while in the FEM analysis the cylinder was considered as a three-dimensional body, with the possibility of consideration of the triaxial compression state.

ACKNOWLEDGEMENTS

The paper has been prepared within the scientific research project TR 36017 "Utilization of by-products and recycled waste materials in concrete composites in the scope of sustainable construction development in Serbia: investigation and environmental assessment of possible applications ", which is funded by the Ministry of Science of Serbia.

- [8] Malešev M., Radonjanin V., Lukić I., Bulatović V.: Basic properties and possibilities of use of structural lightweight aggregate concrete with aggregate from industrial waste materials - Part 1, 12th International Scientific Conference iNDiS 2012, 28-30 November 2012, Novi Sad, Serbia, 634-645.
- [9] Poliotti M., Bairan J.M.: A new concrete plastic-damage model with an evolutive dilatancy parameter, *Engineering structures* 189, 2019, 541-549.
- [10] Radonjanin V., Malešev M., Lukić I., Bulatović V.: Basic properties and possibilities of use of structural lightweight aggregate concrete with aggregate from industrial waste materials - Part 2, 12th International Scientific Conference iNDiS 2012, 28-30 November 2012, Novi Sad, Serbia, 646-657.
- [11] Wang X., Zhanga M., Jivkov P.A.: Computational technology for analysis of 3D meso-structure effects on damage and failure of concrete, *International Journal of Solids and Structures* 80, 2016, 310-333.

REZIME

NUMERIČKA SIMULACIJA PONAŠANJA UZORAKA OD LAKOAGREGATNOG BETONA U SLUČAJEVIMA LABORATORIJSKOG ISPITIVANJA

Vladimir ŽIVALJEVIĆ
Vlastimir RADONJANIN
Ivan LUKIĆ
Dušan KOVAČEVIĆ

U ovom radu prikazano je numeričko modeliranje eksperimentalnog određivanja čvrstoće lakoagregatnog betona pri pritisku i statičkog modula elastičnosti primenom metode konačnih elemenata (MKE). U okviru teorijskog pregleda predstavljen je i opisan CDP (concrete damage plasticity) model ponašanja betona. Numeričko modeliranje i nelinearni statički (inkrementalno-iterativni) proračuni rađeni su za dve različite konfiguracije primenom softvera Abaqus®. Prva konfiguracija modela obuhvata eksperimentalno određivanje čvrstoće betona pri pritisku betonske kocke, a druga određivanje statičkog modula elastičnosti na betonskom cilindru. Trodimenzionalnim MKE modelima uzete su u obzir i čelične ploče, koje se nalaze s gornje i donje strane uzorka i služe za oslanjanje, odnosno apliciranje opterećenja, čime su na realan način obuhvaćeni kontaktni uslovi betonskih uzoraka sa opremom za ispitivanje.

Ključne reči: concrete damage plasticity model, lakoagregatni beton, numerička simulacija, čvrstoća pri pritisku, modul elastičnosti

ABSTRACT

NUMERICAL SIMULATION OF THE BEHAVIOUR OF THE LIGHTWEIGHT CONCRETE SPECIMEN IN THE LABORATORY TESTING

Vladimir ZIVALJEVIC
Vlastimir RADONJANIN
Ivan LUKIC
Dusan KOVACEVIC

This paper presents the numerical modelling of the experimental determination of the compressive strength and the static modulus of elasticity of the lightweight concrete using the finite element method (FEM). In the theoretical review, a concrete damage plasticity (CDP) model of the concrete behaviour is described. Numerical modelling and nonlinear static (incremental-iterative) analyses were performed for two different configurations using the Abaqus® software. The first configuration of the model considers the experimental determination of the concrete compressive strength of the concrete cube, and the second one the determination of the static modulus of elasticity on the concrete cylinder. Steel plates in the three-dimensional FEM models located on the upper and lower sides of the specimens, which serve as the support or for the load application, thus capturing the contact conditions of concrete specimens with testing equipment more realistically, have also been taken into account.

Key words: concrete damage plasticity model, lightweight concrete, numerical simulation, compressive strength, modulus of elasticity

UPUTSTVO AUTORIMA*

Prihvatanje radova i vrste priloga

U časopisu Materijali i konstrukcije štampaće se neobjavljeni radovi ili članci i konferencijska saopštenja sa određenim dopunama, iz oblasti građevinarstva i srodnih disciplina (geodezija i arhitektura). Vrste priloga autora i saradnika koji će se štampati su: originalni naučni radovi, prethodna saopštenja, pregledni radovi, stručni radovi, prikazi objekata i iskustava (studija slučaja), kao i diskusije povodom objavljenih radova.

Originalni naučni rad je primarni izvor naučnih informacija i novih ideja i saznanja kao rezultat izvornih istraživanja uz primenu adekvatnih naučnih metoda. Dobijeni rezultati se izlažu sažeto, ali tako da poznavalac problema može proceniti rezultate eksperimentalnih ili teorijsko numeričkih analiza, tako da se istraživanje može ponoviti i pri tome dobiti iste ili rezultate u okvirima dopuštenih odstupanja, kako se to u radu navodi.

Prethodno saopštenje sadrži prva kratka obaveštenja o rezultatima istraživanja ali bez detaljnih objašnjenja, tj. kraće je od originalnog naučnog rada.

Pregledni rad je naučni rad koji prikazuje stanje nauke u određenoj oblasti kao plod analize, kritike i komentara i zaključaka publikovanih radova o kojima se daju svi neophodni podaci pregledno i kritički uključujući i sopstvene radove. Navode se sve bibliografske jedinice korišćene u obradi tematike, kao i radovi koji mogu doprineti rezultatima daljih istraživanja. Ukoliko su bibliografski podaci metodski sistematizovani, ali ne i analizirani i raspravljani, takvi pregledni radovi se klasifikuju kao stručni radovi.

Stručni rad predstavlja koristan prilog u kome se iznose poznate spoznaje koje doprinose širenju znanja i prilagođavanja rezultata izvornih istraživanja potrebama teorije i prakse.

Ostali prilogi su prikazi objekata, tj. njihove konstrukcije i iskustava-primeri u građenju i primeni različitih materijala (studije slučaja).

Da bi se ubrzao postupak prihvatanja radova za publikovanje, potrebno je da autori uvažavaju Uputstva za pripremu radova koja su navedena u daljem tekstu.

Uputstva za pripremu rukopisa

Rukopis otkucati jednostrano na listovima A-4 sa marginama od 31 mm (gore i dole) a 20 mm (levo i desno), u Wordu fontom Arial sa 12 pt. Potrebno je uz jednu kopiju svih delova rada i priloga, dostaviti i elektronsku verziju na navedene E-mail adrese, ili na CD-u. Autor je obavezan da čuva jednu kopiju rukopisa kod sebe.

Od broja 1/2010, prema odluci Upravnog odbora Društva i Redakcionog odbora, radovi sa pozitivnim recenzijama i prihvaćeni za štampu, publikovaće se na srpskom i engleskom jeziku, a za inostrane autore na engleskom (izuzev autora sa govornog područja srpskog i hrvatskog jezika).

Svaka stranica treba da bude numerisana, a optimalni obim članka na jednom jeziku, je oko 16 stranica (30000 slovnih mesta) uključujući slike, fotografije, tabele i popis literature. Za radove većeg obima potrebna je saglasnost Redakcionog odbora.

* Uputstvo autorima je modifikovano i treba ga, u pripremi radova, slediti.

GUIDELINES TO AUTHORS

Acceptance and types of contributions

The Building Materials and Structures journal will publish unpublished papers, articles and conference reports with modifications in the field of Civil Engineering and similar areas (Geodesy and Architecture). The following types of contributions will be published: original scientific papers, preliminary reports, review papers, professional papers, objects describe / presentations and experiences (case studies), as well as discussions on published papers.

Original scientific paper is the primary source of scientific information and new ideas and insights as a result of original research using appropriate scientific methods. The achieved results are presented briefly, but in a way to enable proficient readers to assess the results of experimental or theoretical numerical analyses, so that the research can be repeated and yield with the same or results within the limits of tolerable deviations, as stated in the paper.

Preliminary report contains the first short notifications on the results of research but without detailed explanation, i.e. it is shorter than the original scientific paper.

Review paper is a scientific work that presents the state of science in a particular area as a result of analysis, review and comments, and conclusions of published papers, on which the necessary data are presented clearly and critically, including the own papers. Any reference units used in the analysis of the topic are indicated, as well as papers that may contribute to the results of further research. If the reference data are methodically systematized, but not analyzed and discussed, such review papers are classified as technical papers.

Technical paper is a useful contribution which outlines the known insights that contribute to the dissemination of knowledge and adaptation of the results of original research to the needs of theory and practice.

Other contributions are presentations of objects, i.e. their structures and experiences (examples) in the construction and application of various materials (case studies).

In order to speed up the acceptance of papers for publication, authors need to take into account the Instructions for the preparation of papers which can be found in the text below.

Instructions for writing manuscripts

The manuscript should be typed one-sided on A-4 sheets with margins of 31 mm (top and bottom) and 20 mm (left and right) in Word, font Arial 12 pt. The entire paper should be submitted also in electronic format to e-mail address provided here, or on CD. The author is obliged to keep one copy of the manuscript.

As of issue 1/2010, in line with the decision of the **Management Board of the Society and the Board of Editors, papers with positive reviews, accepted for publication, will be published in Serbian and English, and in English for foreign authors (except for authors coming from the Serbian and Croatian speaking area).**

Each page should be numbered, and the optimal length of the paper in one language is about 16 pages (30.000 characters) including pictures, images, tables and references. Larger scale works require the approval of the Board of Editors.

Naslov rada treba sa što manje reči (poželjno osam, a najviše do jedanaeset) da opiše sadržaj članka. U naslovu ne koristiti skraćenice ni formule. U radu se iza naslova daju ime i prezime autora, a titule i zvanja, kao i ime institucije u podnožnoj napomeni. Autor za kontakt daje telefon, adresu elektronske pošte i poštansku adresu.

Uz sažetak (rezime) od oko 150-250 na srpskom i engleskom jeziku daju se ključne reči (do sedam). To je jezgrovit prikaz celog članka i čitaocima omogućuje uvid u njegove bitne elemente.

Rukopis se deli na poglavlja i potpoglavlja uz numeraciju, po hijerarhiji, arapskim brojevima. Svaki rad ima uvod, sadržinu rada sa rezultatima, analizom i zaključcima. Na kraju rada se daje popis literature.

Kod svih dimenzionalnih veličina obavezna je primena međunarodnih SI mernih jedinica.

Formule i jednačine treba pisati pažljivo vodeći računa o indeksima i eksponentima. Autori uz izraze u tekstu definišu simbole redom kako se pojavljuju, ali se može dati i posebna lista simbola u prilogu.

Prilozi (tabele, grafikoni, sheme i fotografije) rade se u crno-beloj tehnici, u formatu koji obezbeđuje da pri smanjenju na razmere za štampu, po širini jedan do dva stupca (8 cm ili 16,5 cm), a po visini najviše 24,5 cm, ostanu jasni i čitljivi, tj. da veličine slova i brojeva budu najmanje 1,5 mm. Originalni crteži treba da budu kvalitetni i u potpunosti pripremljeni za presnimavanje. Mogu biti i dobre, oštre i kontrastne fotokopije. Koristiti fotografije, u crno-beloj tehnici, na kvalitetnoj hartiji sa oštrim konturama, koje omogućuju jasnu reprodukciju.

U popisu literature na kraju rada daju se samo oni radovi koji se pominju u tekstu. Citirane radove treba prikazati po abecednom redu prezimena prvog autora. Literaturu u tekstu označiti arapskim brojevima u uglastim zagradama, kako se navodi i u Popisu citirane literature, napr [1]. Svaki citat u tekstu mora se naći u Popisu citirane literature i obrnuto svaki podatak iz Popisa se mora citirati u tekstu.

U Popisu literature se navode prezime i inicijali imena autora, zatim potpuni naslov citiranog članka, iza toga sledi ime časopisa, godina izdavanja i početna i završna stranica (od - do). Za knjige iza naslova upisuje se ime urednika (ako ih ima), broj izdanja, prva i poslednja stranica poglavlja ili dela knjige, ime izdavača i mesto objavljivanja, ako je navedeno više gradova navodi se samo prvi po redu. Kada autor citirane podatke ne uzima iz izvornog rada, već ih je pronašao u drugom delu, uz citat se dodaje «citirano prema...».

Autori su odgovorni za izneseni sadržaj i moraju sami obezbediti eventualno potrebne saglasnosti za objavljivanje nekih podataka i priloga koji se koriste u radu.

Ukoliko rad bude prihvaćen za štampu, autori su dužni da, po uputstvu Redakcije, unesu sve ispravke i dopune u tekstu i prilozima.

Rukopisi i prilozi objavljenih radova se ne vraćaju. Sva eventualna objašnjenja i uputstva mogu se dobiti od Redakcionog odbora.

Radovi se mogu slati i na e-mail: folic@uns.ac.rs ili miram@uns.ac.rs

Veb sajt Društva i časopisa: www.dimk.rs

The title should describe the content of the paper using a few words (preferably eight, and up to eleven). Abbreviations and formulas should be omitted in the title. The name and surname of the author should be provided after the title of the paper, while authors' title and position, as well as affiliation in the footnote. The author should provide his/her phone number, e-mail address and mailing address.

The abstract (summary) of about 150-250 words in Serbian and English should be followed by key words (up to seven). This is a concise presentation of the entire article and provides the readers with insight into the essential elements of the paper.

The manuscript is divided into chapters and sub-chapters, which are hierarchically numbered with Arabic numerals. The paper consists of introduction and content with results, analysis and conclusions. The paper ends with the list of references. All dimensional units must be presented in international SI measurement units. The formulas and equations should be written carefully taking into account the indexes and exponents. Symbols in formulas should be defined in the order they appear, or alternatively, symbols may be explained in a specific list in the appendix. Illustrations (tables, charts, diagrams and photos) should be in black and white, in a format that enables them to remain clear and legible when downscaled for printing: one to two columns (8 cm or 16.5 cm) in height, and maximum of 24.5 cm high, i.e. the size of the letters and numbers should be at least 1.5 mm. Original drawings should be of high quality and fully prepared for copying. They also can be high-quality, sharp and contrasting photocopies. Photos should be in black and white, on quality paper with sharp contours, which enable clear reproduction.

The list of references provided at the end of the paper should contain only papers mentioned in the text. The cited papers should be presented in alphabetical order of the authors' first name. References in the text should be numbered with Arabic numerals in square brackets, as provided in the list of references, e.g. [1]. Each citation in the text must be contained in the list of references and vice versa, each entry from the list of references must be cited in the text.

Entries in the list of references contain the author's last name and initials of his first name, followed by the full title of the cited article, the name of the journal, year of publication and the initial and final pages cited (from - to). If the doi code exists it is necessary to enter it in the references. For books, the title should be followed by the name of the editor (if any), the number of issue, the first and last pages of the book's chapter or part, the name of the publisher and the place of publication, if there are several cities, only the first in the order should be provided. When the cited information is not taken from the original work, but found in some other source, the citation should be added, "cited after ..."

Authors are responsible for the content presented and must themselves provide any necessary consent for specific information and illustrations used in the work to be published.

If the manuscript is accepted for publication, the authors shall implement all the corrections and improvements to the text and illustrations as instructed by the Editor.

Writings and illustrations contained in published papers will not be returned. All explanations and instructions can be obtained from the Board of Editors.

Contributions can be submitted to the following e-mails: folic@uns.ac.rs or miram@uns.ac.rs

Website of the Society and the journal: www.dimk.rs

Izdavanje časopisa "Građevinski materijali i konstrukcije" finansijski su pomogli:



**REPUBLIKA SRBIJA
MINISTARSTVO PROSVETE, NAUKE I
TEHNOLOŠKOG RAZVOJA**



**UNIVERZITET U BEOGRADU
GRAĐEVINSKI FAKULTET**



**DEPARTMAN ZA GRAĐEVINARSTVO I
GEODEZIJU
FAKULTET TEHNIČKIH NAUKA NOVI SAD**



INSTITUT IMS AD, BEOGRAD



doka

Oplatna tehnika.

Vaš pouzdan partner

za brzu, bezbednu i ekonomičnu gradnju!

Doka Serb je srpski ogranak austrijske kompanije **Doka GmbH**, jednog od svetskih lidera na polju inovacija, proizvodnje i distribucije oplatnih sistema za sve oblasti građevinarstva. Delatnost kompanije Doka Serb jeste isporuka oplatnih sistema i komponentni za primenu u visokogradnji i niskogradnji, pružanje usluga konsaltinga, izrade tehničkih planova i asistencije na gradilištu.

Panelna oplata za ploče Dokadek 30 – Evolucija u sistemima oplata za ploče

Dokadek 30 je ručna oplata lake čelične konstrukcije, bez nosača sa plastificiranim ramovima, koji su prekriveni kompozitnim drveno-plastičnim panelom površine do 3 m².

Izuzetno brzo, bezbedno i lako postavljanje oplata

- Mali broj delova sistema i pregledna logistika uz samo dve veličine panela (2,44 x 1,22 m i 2,44 x 0,81 m)
- Dovoljan 2-člani tim za jednostavnu i brzu montažu elemenata sa tla bez merdevina i bez kрана
- Sistemski određen položaj i broj podupirača i panela, unapred definisan redosled postupaka
- Prilagođavanje svim osnovama zahvaljujući optimalnom uklapanju sa Dokaflex-om
- Specijalni dizajn sprečava odizanje panela pod uticajem vetra
- Horizontalno premeštanje do 12 m² Dokadek 30 pomoću DekDrive

Više informacija o sistemu naći ćete na našem sajtu www.doka.rs

Doka Serb d.o.o. | Svetogorska 4, 22310 Šimanovci | Srbija | T +381 22 400 100
F +381 22 400 124 | serb@doka.com | www.doka.rs



UZ MAPEI SVE JE OK



Kada birate, birajte tehnološki napredna rešenja, stručnost i **Mapei proizvode** najvišeg kvaliteta.
Za izgradnju novih, sanaciju i rekonstrukciju postojećih ili konzervaciju istorijskih građevina.
Napravite razliku, odaberite Mapei – vašeg partnera u izgradnji.

Više na: mapei.rs i mapei.com

 **MAPEI**[®]
GRAĐEVINSKI LEPKOVI • HIDROIZOLACIONI SISTEMI
HEMIJSKI PROIZVODI ZA GRAĐEVINARSTVO



MATEST "IT TECH" KONTROLNA JEDINICA



JEDNA TEHNOLOGIJA MNOGO REŠENJA

IT Touch Technology je Matestov najnoviji koncept koji ima za cilj da ponudi inovativna i user-friendly tehnologiju za kontrolu i upravljanje najmodernijom opremom u domenu testiranja građevinskih materijala

Ova tehnologija je srž Matestove kontrolne jedinice, software baziran na Windows platformi i touch screen sistem koji je modularan, fleksibilan i obavlja mnoge opcije

- IT TECH pokriva
- | INOVATIVNOST
- | INTERNET KONEKCIJA
- | INTERFEJS SA IKONICAMA
- | INDUSTRIJALNA TEHNOLOGIJA

SISTEM JEDNOG RAZMIŠLJANJA JEDNOM SHVATIŠ - SVE TESTIRAŠ



NAPREDNA TEHNOLOGIJA ISPITIVANJA ASFALTA

- | GYROTRONIC - Gyrotory Compactor
- | ARC - Electromechanical Asphalt Roller Compactor
- | ASC - Asphalt Shear Box Compactor
- | SMARTRACKER™ - Multiwheels Hamburg Wheel Tracker, DRY + WET test environment
- | SOFTMATIC - Automatic Digital Ring & Ball Apparatus
- | Ductilometers with data acquisition system

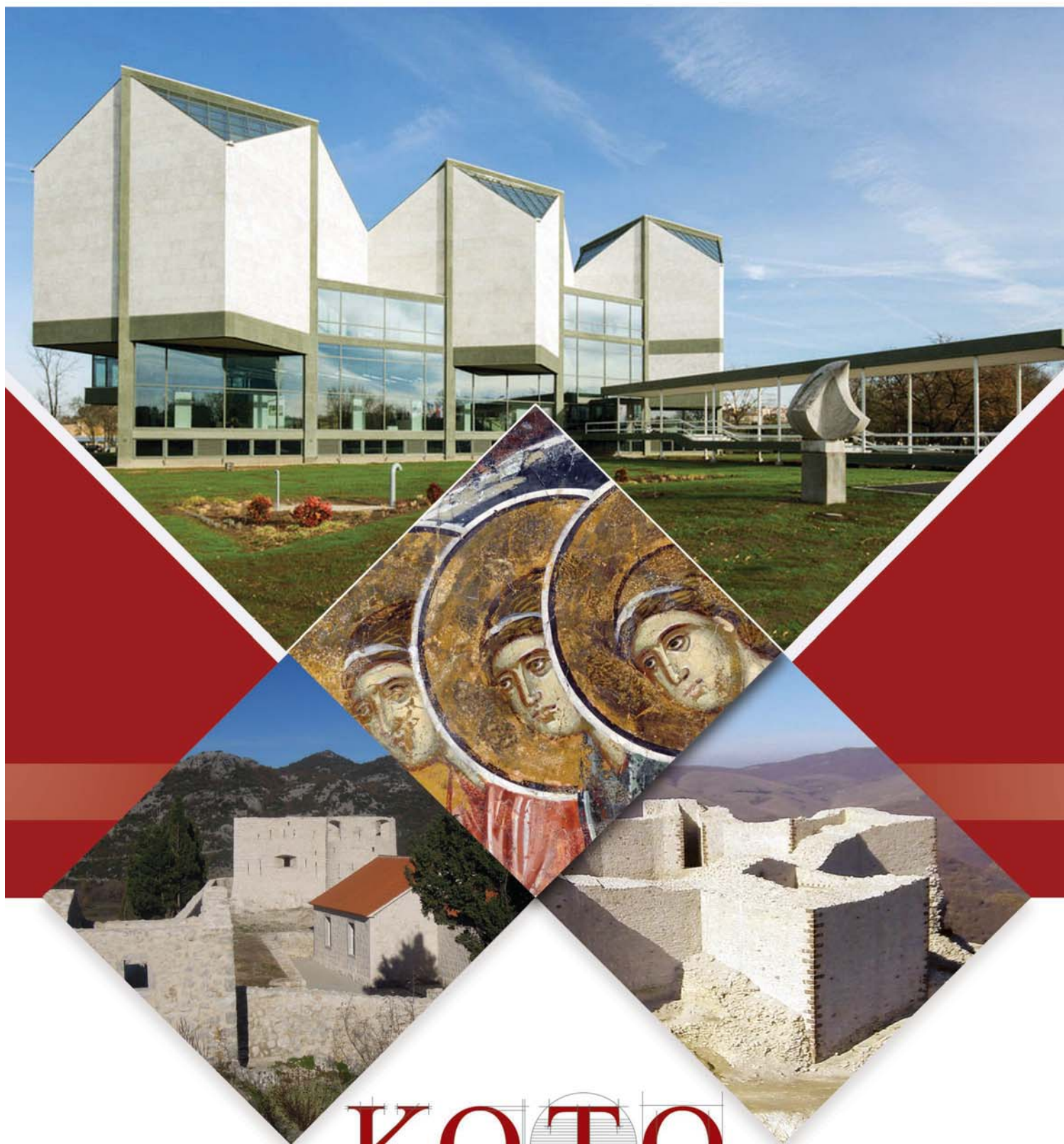
MULTIFUNKCIONALNI RAMOVI ZA TESTIRANJE

- | CBR/Marshall digital machines
- | Universal multispeed load frames
- | UNITRONIC 50kN or 200kN Universal multipurpose compression/flexural and tensile frames

OPREMA ZA GEOMEHANIČKO ISPITIVANJE

- | EDOTRONIC - Automatic Consolidation Apparatus
- | SHEARLAB - AUTOSHEARLAB - SHEARTRONIC
- Direct / Residual shear testing systems
- | Triaxial Load Frame 50kN

MIXMATIC - Automatic Programmable Mortar Mixer



KOTO

www.koto.rs | office@koto.rs | 011 309 7410 | Vojvode Stepe br. 466, Beograd



**Građevinska hemija
za profesionalce**



TKK DODACI ZA BETONE I MALTERE I ZAŠTITNI PREMAZI

CEMENTOL

dodaci za proizvodnju trajnog i kvalitetnog betona

SILIFOB

vodootporne i druge zaštite mineralnih i drugih
građevinskih materijala

TEKAMAL

vodonepropusni cementni premazi



www.tkk.rs

TKK d.o.o., Ugrinovačka 206, 11080 Zemun

Tel: +381 11 316 91 10, M: +381 641 549 007, office@tkk.rs



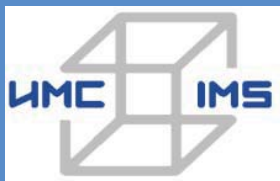
INSTITUT IMS a.d.

Institut za ispitivanje materijala IMS, sa tradicijom od 1929. godine, predstavlja najstariju naučno-istraživačku instituciju u Srbiji. Osnovna ideja prilikom osnivanja bila je potreba za jedinstvenom institucijom koja bi se osim istraživanja bavila i kontrolom građevinske industrije.

Delatnost Instituta IMS obuhvata laboratorijska ispitivanja građevinskih materijala, sertifikaciju proizvoda, nadzor nad izvođenjem radova i ispitivanje različitih tipova konstrukcija, izradu projektne dokumentacije, kao i naučno - istraživački rad u svim oblastima građevinarstva.

Poslovni centri Instituta IMS :

- Centar za puteve i geotehniku
- Centar za materijale
- Centar za metale i energetiku
- Centar za konstrukcije i prednaprezanje



INSTITUT IMS a.d.

Bulevar vojvode Mišića 43

11 000 Beograd

Tel: 011-2651-949

Faks: 011-3692-772

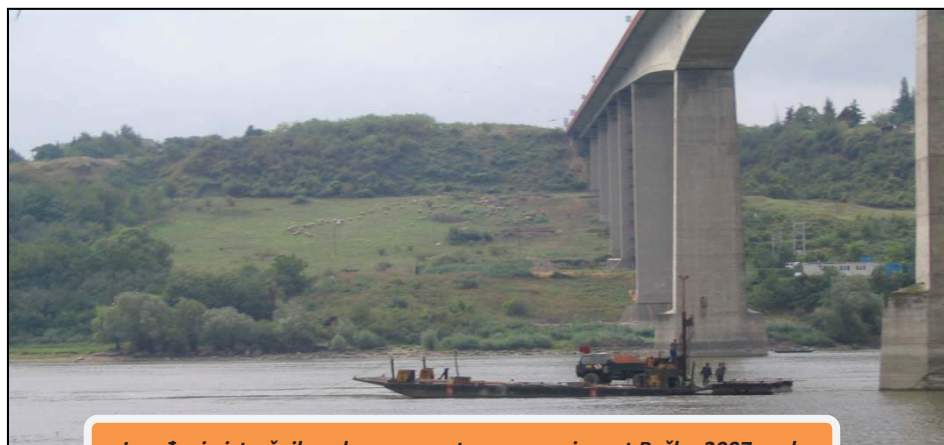
office@institutims.rs

www.institutims.rs

Institut IMS sertifikovao je sistem kvaliteta prema zahtevima standarda SRPS ISO 9001:2001. Svoju kompetentnost je potvrdio najvećim obimom akreditacije kod Akreditacionog tela Srbije (ATS) i Sertifikacionog tela.

Kadrovsku strukturu Instituta IMS čine doktori nauka, diplomirani inženjeri sa licencama Inženjerske komore Srbije i stručni tehnički kadar. Inženjeri Instituta IMS aktivno učestvuju na naučno-stručnim skupovima u zemlji i inostranstvu.

Institut IMS kontinuirano unapređuje kvalitet poslovanja na svim nivoima, kako u okviru terenskih i laboratorijskih ispitivanja, tako i na izradi projektno-tehničke dokumentacije s ciljem uspešne realizacije postavljenih zadataka.



Izvođenje istražnih radova sa pontona za novi most Beška, 2007.god.

Geotehnička istraživanja i ispitivanja – in situ

Od terenskih istražnih radova izdvajamo izvođenje istražnih bušotina (IB), standardnih penetracionih opita (SPT), statičkih penetracionih opita (CPT i CPTU), opita dilatometarskom sondom (DMT i SDMT), ispitivanja vodopropustljivosti tla različitim terenskim metodama (VDP), ugradnja pijezometara i dr.

Terenske metode ispitivanja šipova zauzimaju značajno mesto u našoj delatnosti, a na tržištu se izdvajamo kao lideri u toj oblasti u protekloj deceniji.

Ispitivanje šipova

SLT metoda (Static load test) ispitivanje nosivosti šipova statičkim opterećenjem;

DLT metoda (Dynamic load test) ispitivanje nosivosti šipova dinamičkim opterećenjem;

PDA metoda (Pile driving analysis) omogućava praćenje i optimizaciju procesa pobijanja prefabrikovanih betonskih i čeličnih šipova u tlo;

PIT (SIT) metoda (Pile(Sonic) integrity testing) koristi se za ispitivanje integriteta izvedenih šipova (dužine, prekida, suženja ili proširenja).



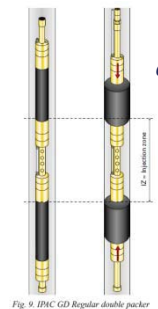
DLT-dinamičko ispitivanje šipova



CPT/CPTU opiti



Aktivno klizište



oprema za ispitivanje vodopropusnosti stena pod pritiskom do 10 bar-a metodom LIŽONA

Laboratorija za puteve i geotehniku

Laboratorija za puteve i geotehniku akreditovana je kod Akreditacionog tela Srbije – ATS prema SRPS ISO/IEC 17025:2006. U njoj se vrše ispitivanja tla (identifikaciono–klasifikaciona ispitivanja, fizičko–mehanička modelska ispitivanja), kamenog agregata i brašna, bitumena i bitumenskih emulzija, asfaltnih mešavina. U okviru laboratorijskih ispitivanja na terenu vrši se kontrola kvaliteta ugrađenog materijala i izvedenih radova (prethodna, tekuća, kontrolna ispitivanja i izvođenja opita in situ).

Projektovanje puteva i sanacija klizišta

U okviru projektovanja značajno mesto u radu zauzimaju geotehnička istraživanja terena i projekti sanacije klizišta - nestabilnih kosina useka i nasipa puteva i prirodno nestabilnih padina . Značajna su i projekovanja svih vrsta fundiranja specijalnih geotehničkih konstrukcija. Ističe se i iskustvo u oblasti putarstva, na projektovanju novih, rehabilitacija i rekonstrukcija postojećih puteva svih rangova sa pratećim objektima i dimenzionisanjem kolovoznih konstrukcija.

Nadzor

Naši inženjeri imaju veliko iskustvo u kontroli i proveru kvaliteta izvođenja svih vrsta radova, kontroli građevinske dokumentacije i praćenju radova u skladu sa njom, kao i rešavanju novonastalih situacija tokom izvođenja radova.

ZAŠTITNI PREMAZI ZA BETONE

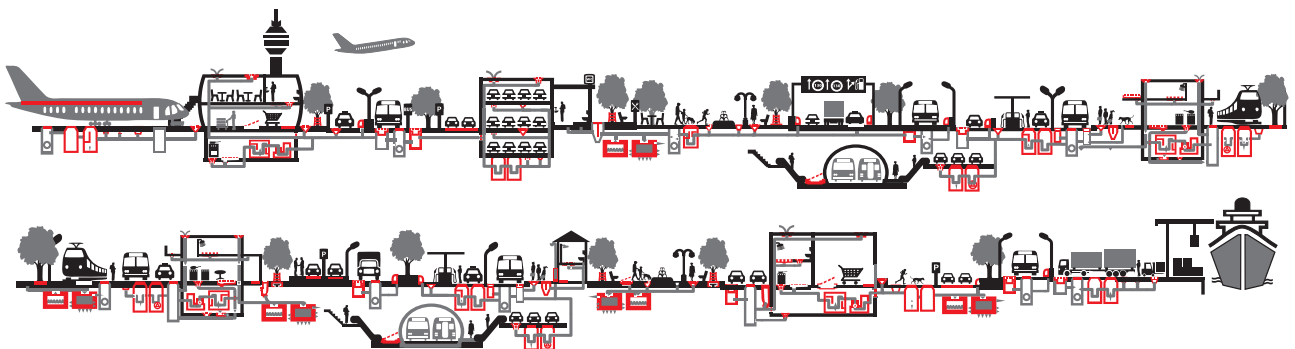
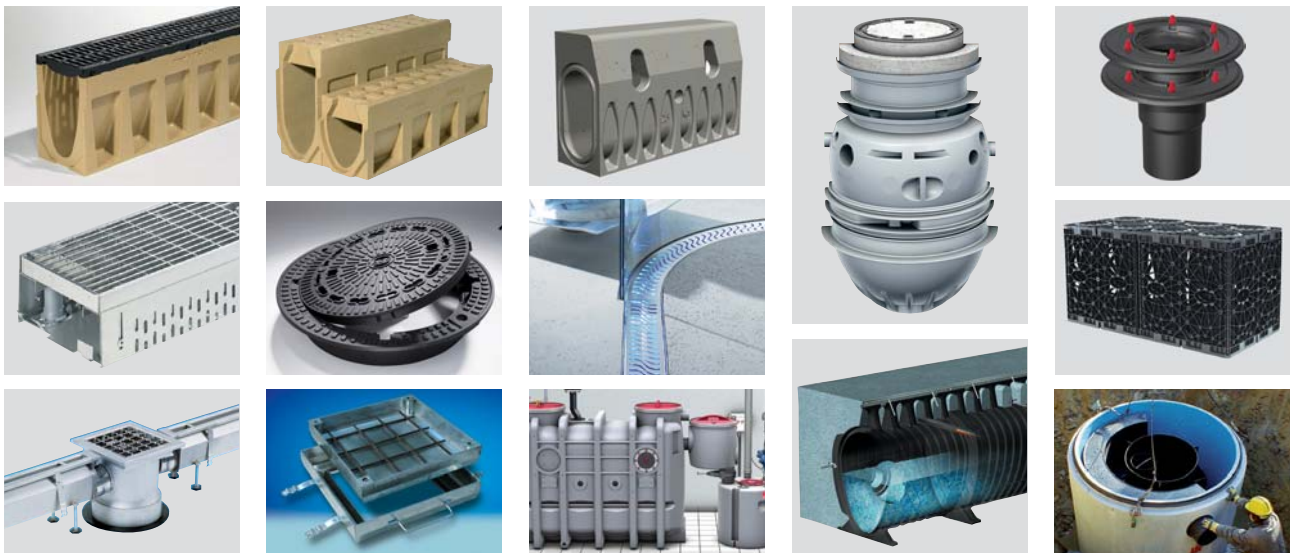


PROIZVODNI PROGRAM

- | | | |
|--------------------------------|---|-------------------------------|
| Aditivi za betone i maltere | ● | Zaštitni premazi |
| Smese za zalivanje | ● | Protivpožarni materijali |
| Reparacija betona | ● | Građevinska lepila |
| Industrijski i sportski podovi | ● | Smese za izravnavanje |
| Kitovi | ● | Dekorativni premazi i malteri |
| Hidroizolacije | ● | Proizvodi za građevinarstvo |

www.ading.rs

ACO. The future of drainage.



aco.rs

NAPREDNA SIKA REŠENJA U OBLASTI STRUKTURALNIH OJAČANJA

Kompanija Sika pruža trajnu dodatnu vrednost vlasnicima građevinskih objekata, njihovim konsultantima i izvođačima, kao i tehničku podršku tokom svih faza projekta,

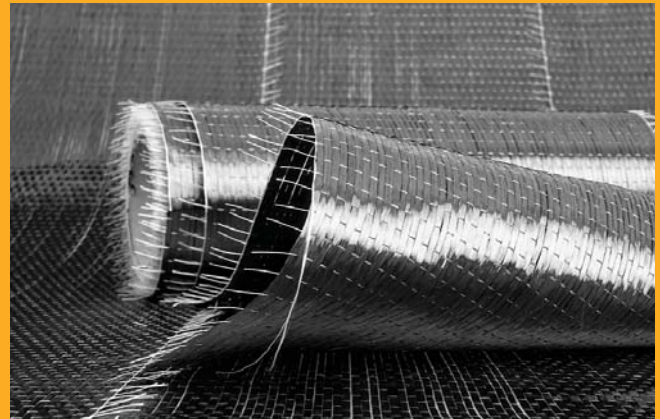
od ispitivanja uslova i razvoja inicijalnog koncepta ojačanja pa sve do uspešnog završetka i primopredaje projekta

SIKA - VAŠ PARTNER NA GRADILIŠTU



- Globalni lider na tržištu građevine i građevinske hemije
- Najbolja tehnička ekspertiza i praksa za sanaciju betona i strukturalna ojačanja
- Odlična reputacija kod vodećih izvođača i ugovarača posla

SIKA VREDNOSTI I INOVACIJE U GRAĐEVINI



- Integrisani proizvodi i sistemi visokih performansi koji mogu da povećaju i poboljšaju kapacitet, efikasnost, trajnost i estetiku zgrada i drugih objekata – u korist naših klijenata i boljeg održivog razvoja
- Sika mreža obučenih i iskusnih građevinskih stručnjaka

JEDINSTVENA SIKA REŠENJA U ZAHTEVNIM USLOVIMA



- Rešenja za gotovo sve uslove apliciranja
- Kontrolisano vreme rada, vreme sazrevanja i očvršćavanja za različite vremenske uslove
- Posebna rešenja završnih ojačanja za korišćenje kod betona slabije jačine i drugih podloga

POTVRĐENI SIKA SISTEMI I TEHNIKE APLICIRANJA



- Preko 40 godina iskustva u strukturalnim ojačanjima, sistemima i tehnikama
- Proizvodi i sistemi sa brojnim testovima i procenama kako internim tako i eksternim
- Najviši međunarodni standardi proizvodnje i kontrole kvaliteta

PUT INŽENJERING



Put inženjering d.o.o punih 25 godina radi kao specijalizovano preduzeće za izgradnju infrastrukture u niskogradnji i visokogradnji, kao i proizvodnjom kamenog agregata i betona. Preduzeće se bavi i transportom, uslugama građevinske mehanizacije i specijalne opreme.

Koristeći inovativne tehnike i kvalitetan građevinski materijal iz sopstvenih resursa, spremni smo da odgovorimo na mnoge zahteve naših klijenata iz oblasti niskogradnje.



Osnovna prednost prefabrikovane konstrukcije jeste brzina kojom konstrukcija može biti projektovana, proizvedena, transportovana i namontirana.



Izvodimo hidrograđevinske radove u izgradnji kanalizacionih mreža za odvođenje atmosferskih, otpadnih i upotrebljenih voda, izvođenjem hidrograđevinskih radova u okviru regulacije rečnih tokova, kao i izvođenjem hidrotehničkih objekata.



Površinski kop udaljen je 35 km od Niša. Savremene drobilice, postrojenje za separaciju i sejalice efikasno usitnjavaju i razdvajaju kamene agregate po veličinama. Tehnički kapacitet trenutne primarne drobilice je 300 t/h.



Za spravljanje betona koristimo drobljeni krečnjački agregat sa našeg kamenoloma, deklariranih frakcija, kontrolisane vlažnosti. Kompletan proces proizvodnje i kontrole kvaliteta vršimo prema važećim standardima.



Obradu armature vršimo brzo, stručno i kvalitetno, sa kompjuterskom preciznošću i dimenzijama po projektu.



Naša kompanija u oblasti visokogradnje primenjuje sistem prefabrikovanih betonskih elemenata koji u odnosu na klasičnu gradnju ima brojne prednosti.



Prednapregnute šuplje ploče su konstruktivni elementi visokog kvaliteta, proizvedeni u fabrički kontrolisanim uslovima.



Izrađujemo betonske "New Jersey profile" koji se u svetu koriste za preusmeravanje saobraćaja i zaštitu pešaka u toku izgradnje puta, kao i Betonblock sistem betonskih blokova.



Uslugu transporta vršimo automikserima, kapaciteta bubnja od 7 m³ do 10 m³ betonske mase. Za ugradnju betona posedujemo auto-pumpu za beton, radnog učinka 150 m³/h, sa dužinom strele od 36 m.



Kao generalni izvođač radova, vršimo koordinaciju svih učesnika na projektu, planiranje, praćenje i nabavku materijala, kontrolu kvaliteta izvedenih radova, poštujući zadate vremenske rokove i finansijski okvir investitora.



Osnovi princip našeg poslovanja zasniva se na individualnom pristupu svakom klijentu i pronalaženje najoptimalnijeg rešenja za njegove transportne i logističke potrebe.



Usluge građevinske mehanizacijom vršimo tehnički ispravnim mašinama, sa potrebnim sertifikatima kako za rukovoce građevinskim mašinama tako i za same mašine.



Raspoložemo opremom i mašinama za sve zemljane radove, kipere i dampere za rad u teškim terenskim uslovima, automiksere i pumpe za beton, autodizalice, podizne platforme.



Sakupljanje i privremeno skladištenje otpada vršimo našim specijalizovanim vozilima i deponujemo na našu lokaciju sa odgovarajućom dozvolom. Kapacitet mašine je 250 t/h građevinskog neopasnog otpada.



NIŠ

Knjaževačka bb, 18000 Niš - Srbija
+381 18 215 355
office@putinzenjering.com

BEOGRAD

Jugoslovenska 2a, 11250 Beograd - Železnik
+381 11 25 81 111
beograd@putinzenjering.com



Najlepši krov u komšiluku



Continental Plus Natura je premium crep u natur segmentu! Dobro poznatog oblika, trajan i veoma otporan, a povrh svega pristupačan, naprosto oduzima dah svima. Čak i vašim komšijama!

Continental Plus Natura crep potražite kod ovlašćenih Tondach partnera.

VODOGRADNJA

D.O.O.



ISKOP I PRERADA PESKA
PROIZVODNJA
I ISPORUKA BETONA
ISPORUKA I UGRADNJA
ASFALTA



"MEĐARCI"

***18255 Pukovac, tel.018/813-622 separacija
mob. 062/2000-99, 063/475-350***

VODOGRADNJA

E-mail: doovodogradnja@gmail.com



Ваш партнер
за сигурну будућност

www.grading.rs

**Имате локацију за изградњу
у Београду или Крагујевцу?**

**Контактирајте
нас!**



тим стручњака



25 година искуства



више стотина објеката



PERI sistemi oplata i skela Rešenja za infrastrukturne projekte

Optimizacija procesa, sigurnost i efikasnost izvršenja.

Već 50 godina PERI je pouzdan partner u oblasti sistema oplata i skela I to u svim fazama projekta, od planiranja do završetka radova. PERI sisteme karakteriše maksimalna jednostavnost montaže i rukovanja kao i maksimalna fleksibilnost prilikom međusobnog kombinovanja kod specijalnih objekata, inovativni dizajn, odlična mehanička svojstva i praktični detalji izrađeni prema visokim standardima kvaliteta koji su idealni za teške uslove rada na gradilištu.

Saznajte više o PERI sistemima i rešenjima na našem sajtu.



Oplate
Skele
Inženjering

www.peri.rs